NOTE TO USERS

This reproduction is the best copy available.

uOttawa

L'Université canadienne
Canada's university

FACULTÉ DES ÉTUDES SUPÉRIEURES ET POSTDOCTORALES

uOttawa

L'Université canadienne
Canada's university

FACULTY OF GRADUATE AND POSTDOCTORAL STUDIES

Tahir Rana

AUTEUR DE LA THÈSE / AUTHOR OF THESIS

M.Sc. (Chemistry)

GRADE / DEGREE

Department of Chemistry

FACULTÉ, ÉCOLE, DÉPARTEMENT / FACULTY, SCHOOL, DEPARTMENT

Synthesis of C-Linked Antifreeze Glycoprotein Building Block Containting an Internal Olefin

TITRE DE LA THÈSE / TITLE OF THESIS

R. Ben

DIRECTEUR (DIRECTRICE) DE LA THÈSE / THESIS SUPERVISOR

CO-DIRECTEUR (CO-DIRECTRICE) DE LA THÈSE / THESIS CO-SUPERVISOR

EXAMINATEURS (EXAMINATRICES) DE LA THÈSE / THESIS EXAMINERS

W. Ogilvie

T. Durst

Gary W. Slater

Le Doyen de la Faculté des études supérieures et postdoctorales / Dean of the Faculty of Graduate and Postdoctoral Studies

Synthesis of a *C*-Linked Antifreeze Glycoprotein Building Block Containing an Internal Olefin

By
Tahir Rana

Thesis submitted to the
Faculty of Graduate and Postdoctoral Studies
University of Ottawa
In partial fulfillment of the requirements
For the M.Sc. degree in Chemistry

Department of Chemistry
Faculty of Science
University of Ottawa

Candidate

Tahir Rana

Supervisor

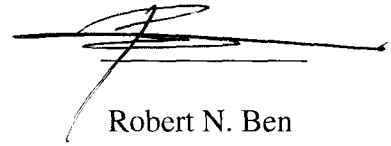

Robert N. Ben

Your file Votre référence
ISBN: 978-0-494-58215-2
Our file Notre référence
ISBN: 978-0-494-58215-2

Abstract

Antifreeze glycoproteins (AFGPs) are polypeptide compounds found in the blood of Antarctic notothenioids and northern cod. These substances inhibit the growth and proliferation of ice in fish inhabiting sub-zero conditions. The structure of AFGPs, and the mechanism of ice growth inhibition at the molecular level have been a source of intense debate. Work in our laboratory involves the synthesis of AFGP analogues in an effort to discern the mechanism of ice growth inhibition and enhance antifreeze attributes for potential therapeutic applications.

We have previously synthesized *C*-linked AFGP analogues possessing antifreeze properties (TH, RI and DIS). One such analogue, $[OGG]_4[Gal]$, has exhibited recrystallization inhibition (RI) activity comparable to native AFGPs. An important structural feature of $[OGG]_4[Gal]$ is the presence of an amide bond. We report herein the synthesis of a *C*-linked AFGP building block with an internal olefin as an amide isostere, in an effort to elucidate the function of the amide bond in the recrystallization inhibition activity of $[OGG]_4[Gal]$.

Acknowledgements

I would like to thank my supervisor Robert Ben for his patience, guidance, encouragement and support over the past two years. I would also like to thank Liz and Jenn for their help in preparing my seminar, Roger for taking the time to answer my questions, Pawel for his valuable advice and Wendy for proof reading this thesis.

I would like to thank Jackie, Sandra, Gloria, Taline, Dr. Michael Souweha, Dr. Mathieu Leclere and Taz for their assistance and insightful discussions; chemistry and life in general. A special thanks for my 'bay buddy' John Trant, who was always willing to help. I am also grateful to the NMR and Mass Spectrometry Facilities at the University of Ottawa.

Finally, I would like to thank my family for their love and support.

Table of Contents

List of Figures

List of Graphs

List of Schemes

List of Tables

List of Abbreviations

$[OGG]_4[Gal]$	(Ornithine, glycine, glycine)$_4$ (galactose)
AFPs	Antifreeze proteins
AFGPs	Antifreeze glycoproteins
Ala	Alanine
Asn	Asparagine
Asx	Asparagine/ aspartic acid
Bn	Benzyl
Boc	*tert*-Butyloxycarbonyl
CD	Circular Dichroism
CDI	1,1-Carbonyldiimidazole
DCM	Dichloromethane
DIPEA	Diisopropylethylamine
DIS	Dynamic ice shaping
DMAP	Dimethylaminopyridine
DMF	*N, N*-Dimethyl formamide
DMSO	Dimethyl sulfoxide
DPPA	Diphenylphosphorylazide
ESI	Electrospray ionization
Fmoc	9-Fluorenylmethoxycarbonyl
Fmoc-OSu	Fmoc-succinimide
Gly	Glycine

HBTU	2-(1H-Benzotriazole-1-yl)-1,1,3,3-tetramethyluronium hexafluorophosphate
Hz	Hertz
J	Coupling constant
kDa	Kilo Dalton
Lys	Lysine
M^+	Molecular Ion
MLGS	Mean largest grain size
MS	Mass spectrometry
MTT	Methylthiazolediphenyl-tetrazolium bromide
Orn	Ornithine
PBS	Phosphate buffered saline
ppm	Parts per million
RI	Recrystallization inhibition
Ser	Serine
SPS	Solid phase synthesis
SAR	Structure-activity relationship
TBDMS	*tert*-Butyldimethylsilyl
TH	Thermal hysteresis
Thr	Threonine
TMSOTf	Trimethylsilyltrifluoromethane sulfonate

Chapter 1

Introduction to Biological Antifreezes

1.1 Overview of Biological Antifreezes

Biological antifreezes are naturally occurring polypeptide compounds found in a variety of organisms. These substances are essential for the survival of organisms inhabiting sub-zero environments. Biological antifreezes have been shown to inhibit ice crystal growth and the recrystallization of ice which would otherwise prove fatal.[1,2,3]

In contrast to homeotherms (warm-blooded birds and mammals), poikilotherms (cold-blooded fish, amphibians and reptiles) regulate their body temperature according to their ambient environment. The internal temperature of poikilotherms in sub-zero conditions often matches that of their surroundings. This raises an interesting question regarding fish that inhabit Arctic and Antarctic waters, which often reach -1.8 °C; why don't they freeze? The apparent paradox was resolved by Scholander and colleagues[4] who discovered that certain poikilotherms, Teleost fish for example, are able to survive at extreme temperatures (-1.8 °C) due to the unusually low freezing temperature of their blood.

The water temperature in McMurdo Sound Antarctica averages -1.87 °C throughout the year.[5] The freezing point depression of seawater (1.87 °C) has been attributed to the colligative effect. Colligative properties of solutions are dependent upon the concentration of solutes rather than their composition. Despite the frigid seawater, Teleost fish such as *Pathogenia hansoni*, *Pathogenia bernacchii* and *Pathogenia borchgrevinki* are able to survive in this habitat. DeVries and coworkers have determined that the freezing point of blood in Teleost fish is approximately -2.1 °C.[5] The 0.23 °C difference between seawater and blood serum freezing point is sufficient to ensure that

fish do not freeze in ice laden water. Curiously, dialyzable solutes such as sodium chloride, urea, and free amino acids in the blood of *Pathogenia borchgrevinki* account for only 70 % of the observed freezing-point depression. DeVries and coworkers discovered that biological antifreezes, antifreeze glycoproteins (AFGPs), were responsible for the remaining 30 % of the observed freezing-point depression.[5,6,7] DeVries determined that the manner in which AFGPs depress the freezing point of Teleost blood is not colligative. AFGPs are present in the blood of fish at low molar concentrations, and consequently their ability to influence the freezing point in a colligative manner is negligible. In fact, AFGPs in Teleost blood are able to depress the freezing point only 0.002 °C according to the colligative property alone.[3] In contrast, the observed freezing point depression attributed to AFGPs in Teleost fish is 0.65 °C. Thus, the mechanism by which antifreeze glycoproteins inhibit the growth of ice is different than that of colligatively acting substances.

A comparison of the freezing points of aqueous solutions of AFGP3-5, sodium chloride, chicken lysozyme (a protein) and galactose (a carbohydrate) are illustrated on the following page.

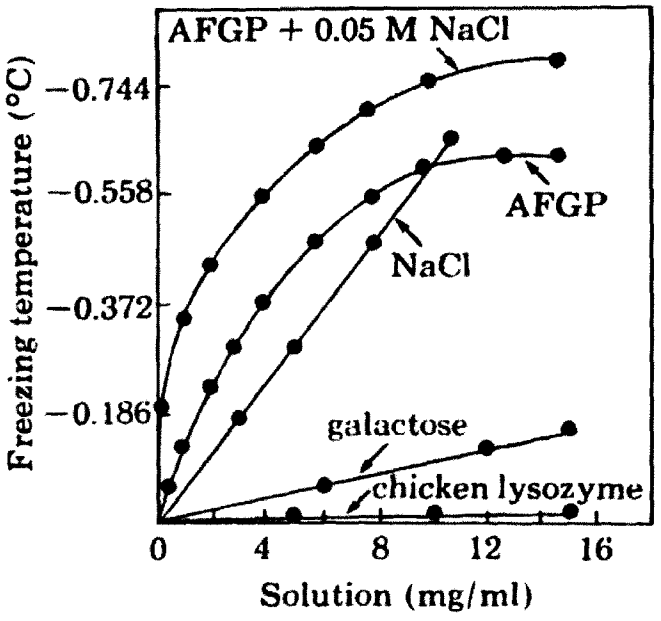

Graph 1.1: Freezing temperatures of solutions of NaCl, galactose, lysozyme, AFGP3-5, and a mixture of AFGP + NaCl as a function of solute concentration (in mg/mL).[3]

According to **Graph 1.1**, at low concentrations AFGPs exhibit a greater ability to reduce the freezing point of aqueous solutions than sodium chloride and structurally similar components (i.e. galactose and lysozyme). It is important to note that due to the size of AFGPs (AFGP3-5 range from 10.5-21.5 kDa), the effective molar concentration of AFGPs is 500x lower than that of sodium chloride. As a result, AFGPs are more active per mole of compound than sodium chloride. Furthermore, the activity of AFGPs can not be explained solely by reference to their constituent parts (carbohydrate and peptide moieties). For example, antifreeze glycoproteins exhibit greater freezing point depression than galactose and lysozyme. Finally, the parallel nature of the plots of AFGP and AFGP + sodium chloride indicate that the effect of the salt is strictly additive; implying that sodium chloride does not interact with the glycoproteins in a manner which influences the freezing point-depressing behaviour of AFGPs.

1.2 Classification of Biological Antifreezes

Biological antifreezes are divided into two categories based upon their structures; carbohydrate containing antifreeze glycoproteins (AFGPs) and antifreeze proteins(AFPs).

1.2.1 Antifreeze Proteins (AFPs)

Antifreeze proteins are non-homologous biopolymers. They can be divided into five subtypes based upon their structural variability. AFP Types I-IV are native to fish, while Type V AFPs are insect biological antifreezes.

Characteristic	Type I AFP	Type II AFP	Type III AFP	Type IV AFP	Type V AFP
Mass (kDa)	3.3 – 4.5	11.0-24.0	6.5-14.0	12.0	8.4-12.5
Properties	alanine rich, single α-helix	globular, random coil, cysteine rich	globular, β-sandwich 3° structure	glutamine rich, α-helical bundles	threonine and cysteine rich, disulfide bridges
Structure					
Source	Sculpin and right-eyed flounder 	sea raven, smelt, atlantic herring 	wolfish, eel pout and ocean pout 	longhorn sculpin 	yellow meal worm beetle 

Table 1.2.1 Characteristics of antifreeze proteins (adapted from Haymet[8]).

Type I AFPs were originally discovered by DeVries[9, 10] and are the most documented antifreeze protein. These proteins vary in size from 3.3 – 4.5 kDa. They consist of repeating amino acid sequences characterized by an alanine rich amphiphilic α-helix. Hew[11] has shown that the α-helix possesses a hydrophilic face with threonine hydroxyl functionalities oriented parallel to the longitudinal axis of the helix (refer to **Figure 1.2.1**). It has been hypothesized that the hydrophilic face is involved in the binding of the protein to ice.[1, 3, 12]

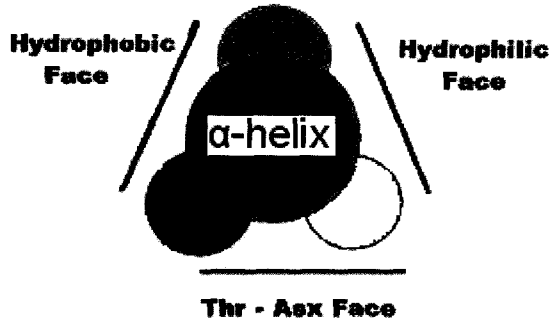

Figure 1.2.1 Cross-section of Type I AFP depicting the three faces of the α-helix; the threonine-aspartic acid/asparagine face, the hydrophobic face (consisting of alanine), and the hydrophilic face (comprised of threonine) which has been associated with ice binding.

Type II AFPs have been found in sea raven, smelt and herring.[3, 13] These cysteine and alanine rich globular proteins range from 11.0 to 24.0 kDa. The secondary structure of Type II AFPs is mainly random coil; however, other elements of the secondary structure include α-helices and β-pleated sheets.[3] Sonnichsen[14] has postulated that disulfide bridges between proximal cysteine residues are essential for antifreeze activity.

Type III AFPs have been isolated from ocean pout by Hew *et al.*[15] and are globular in structure. These proteins vary in size from 6.5-14.0 kDa and the primary structure is not dominated by any particular amino acid.[3] The secondary structure of Type III AFPs consist of β-sheets arranged orthogonally, resulting in the formation of a 'β-sandwich' tertiary structure.[3]

Type IV AFPs were first isolated by Deng and coworkers[16] from longhorn sculpin. These antifreezes are approximately 12 kDa and are characterized by a glutamine rich primary structure. The tertiary structure of Type IV AFPs consist of a bundle of 4 α-helices (refer to **Table 1.2**).[16,17]

Insect AFPs have been isolated and characterized by Graham[18] from the yellow meal-worm beetle *Tenebrio molitor.* These AFPs consist of 12 amino acid repeats with a cysteine moiety positioned at intervals no farther than 6 residues. These proteins vary in molecular weight from 8.4 kDa to 12.5 kDa.[18]

1.2.2 Antifreeze Glycoproteins (AFGPs)

AFGPs were first isolated and characterized by DeVries[5] from the blood serum of Antarctic notothenioids *Pathogenia borchgrevinki, hansoni*, and *bernacchii.* Antifreeze glycoproteins have also been identified in Arctic and north Atlantic cod.[19] Unlike AFPs which are structurally diverse, AFGPs are structurally homologous. Each AFGP consists of a peptide backbone composed of alanine-alanine-threonine (Ala-Ala-Thr) repeats, with slight sequence variation, and a β-D-galactosyl-(1→3)-α-*N*-acetyl-D-galactosamine disaccharide fused to the threonine hydroxyl[3, 8] (**Figure 1.2.2**).

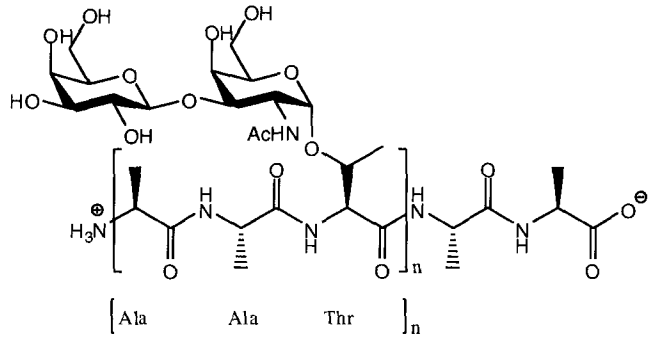

Figure 1.2.2 Structure of a typical AFGP. The repeating unit (n) can vary from 4-55. AFGP8 is the smallest glycopeptide with n=4.

Notothenioid glycoproteins have been further divided into 8 classes (AFGP1-8) based upon their mobility in electrophoretic media (which is proportional to molecular weight).[8] These proteins range in size from 2.6 kDa (n=4) to 33.7 kDa (n=50). On the basis of molecular weight, AFGP1-5 are classified as *large* while AFGP6-8 are classified as *small* (**Table 1.2.2**).[8]

Antifreeze	Molecular Weight (kDa)
AFGP1	33.7
AFGP2	28.8
AFGP3	21.5
AFGP4	15.5
AFGP5	10.5
AFGP6	5.0
AFGP7	3.8
AFGP8	**2.6**

Table 1.2.2 Classification of AFGPs based on molecular weight.[6]

In addition to variations in molecular weight, the amino acid composition can differ in *small* AFGPs since proline is often substituted for alanine (**Figure 1.2.3**).

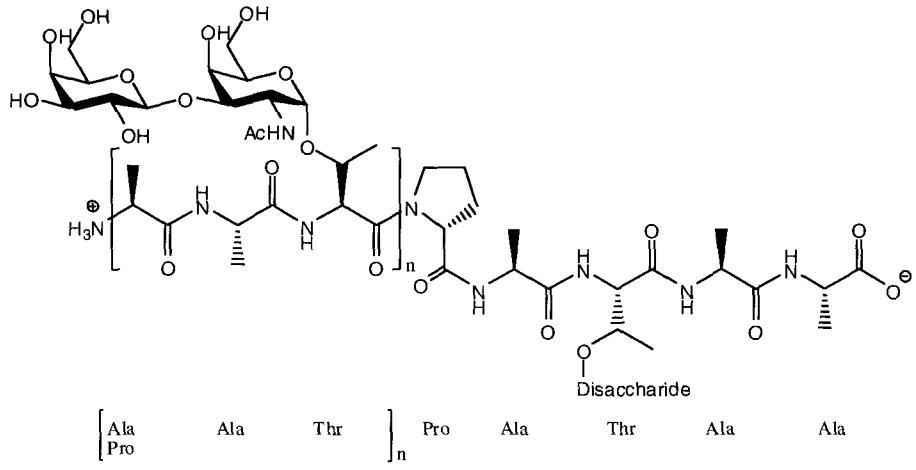

Figure 1.2.3 Structure of AFGP6-8 with minor sequence variation. The first repeating unit may consist of proline instead of alanine and the *C*-terminus is characterized by a Pro-Ala-Ala-Thr-Ala-Ala motif.

Although notothenioid AFGPs possess simple primary structures, their amino acid composition can vary slightly and their size can vary considerably.

Arctic and North Atlantic cod AFGPs are remarkably similar to their unrelated notothenioid counterparts. One notable variation in these species is replacement of threonine with arginine, and the resulting absence of a sugar moiety at this position (refer to **Figure 1.2.4**). However, the lack of a sugar residue at this location is under dispute, since the absence may be an artifact of isolation.

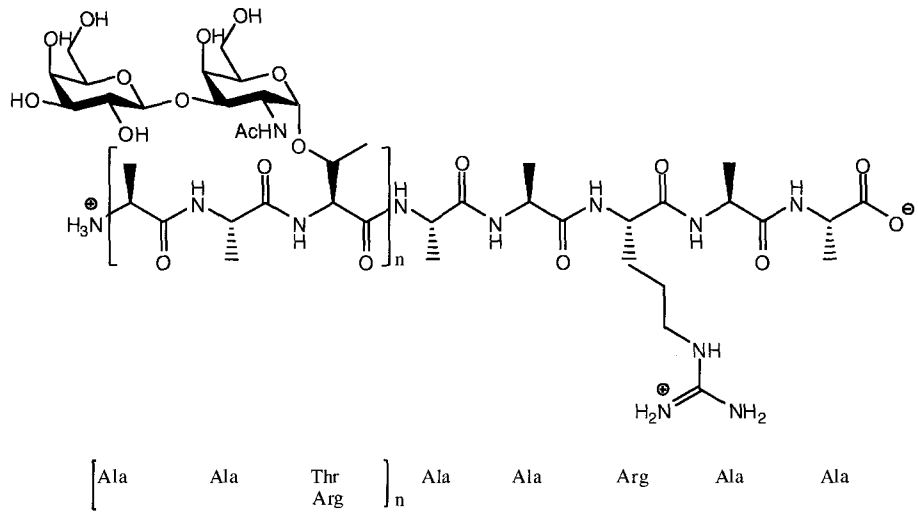

Figure 1.2.4 Structure of Arctic and North Atlantic cod AFGPs. In this example threonine may be replaced with arginine.

Isolation of AFGPs from the rock cod *Gadus ogac* by Fletcher and co-workers[20] indicate that multiple isoforms of AFGPs can exist within a particular class. For example, AFGP6 was found to contain 14 different isoforms. A protein isoform is any of several different forms of the same protein arising from single nucleotide polymorphisms (SNPs). As a result, the notation AFGPx should not always be interpreted to refer to a single compound.

Fletcher and colleagues[20] have shown that larger AFGPs are more active than their smaller counterparts.

AFGP8 has been a synthetic target of numerous groups due to its small size, and consequential ease of preparation. In addition, synthetic analogues for structure activity studies are predicated upon AFGP8.

1.3 In Vivo Localization of Biological Antifreezes

Biological antifreezes have been traditionally isolated from the blood of vertebrates; however, they have also been found in tissue. AFGPs have been discovered in the blood, peritoneal, pericardial and extradural fluid of Antarctic notothenioid fish.[27] Secreted fluids such as urine contain low concentrations of AFGP6-8. It has been postulated that biological antifreezes are secreted by the liver and reach fluid compartments via passive distribution. AFGPs have been identified in the interstitial fluid of all fish tissues except the brain. Some researchers[28] have suggested that AFGPs can be synthesized in the epidermis of fish. Hew has shown contrary to long held belief that AFGPs are not confined solely to extra-cellular media, but can also accumulate in cells.

1.4 Antifreeze Properties

1.4.1 Thermal Hysteresis (TH)

A characteristic property of biological antifreezes is the ability to depress the freezing point of aqueous solution without significantly affecting the melting point. This property is referred to as thermal hysteresis (TH) and is used to detect and quantify antifreeze activity. In contrast to colligatively acting solutes such as sodium chloride, which depress the freezing and melting points to the same extent, biological antifreezes do not depress the freezing and melting points to the same extent. The difference between melting temperature (T_m) and freezing temperature (T_f) is known as the thermal hysteretic gap (TH gap) (**Figure 1.4.1**).

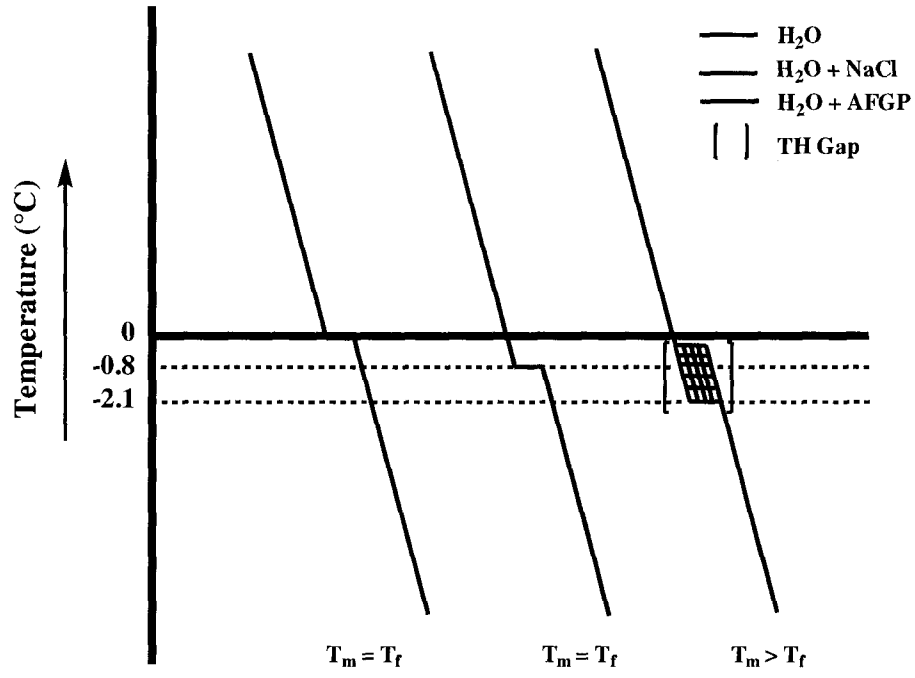

Figure 1.4.1 A schematic representation of thermal hysteresis. For reference, the profile of water is provided ($T_m = T_f = 0°C$).

The magnitude of the TH gap is dependent upon the nature and concentration of the biological antifreeze employed. Large AFGPs (AFGP1-4) have been shown to exhibit greater TH activity than smaller sized AFGPs (AFGP6-8).[29] Due to structural differences, direct TH comparisons between AFGPs and AFPs are tenuous; however, in terms of molecular mass, Type I winter flounder AFPs exhibit greater activity than similar sized glycoproteins.[30] With respect to concentration dependence, biological antifreezes exhibit an asymptotic concentration at which activity is saturated (i.e. increases in solution concentration of the protein beyond the saturation level will not increase TH activity appreciably, refer to **Figure 1.1**).

1.4.2 Dynamic Ice Shaping

The growth of ice crystals is inhibited in the TH gap. This is due to the adsorption of antifreezes on specific faces of the nascent ice crystal.[31] The result of antifreeze adsorption is the formation of alternative crystal structures. This generation of ice crystals with variable morphology is referred to as dynamic ice shaping.

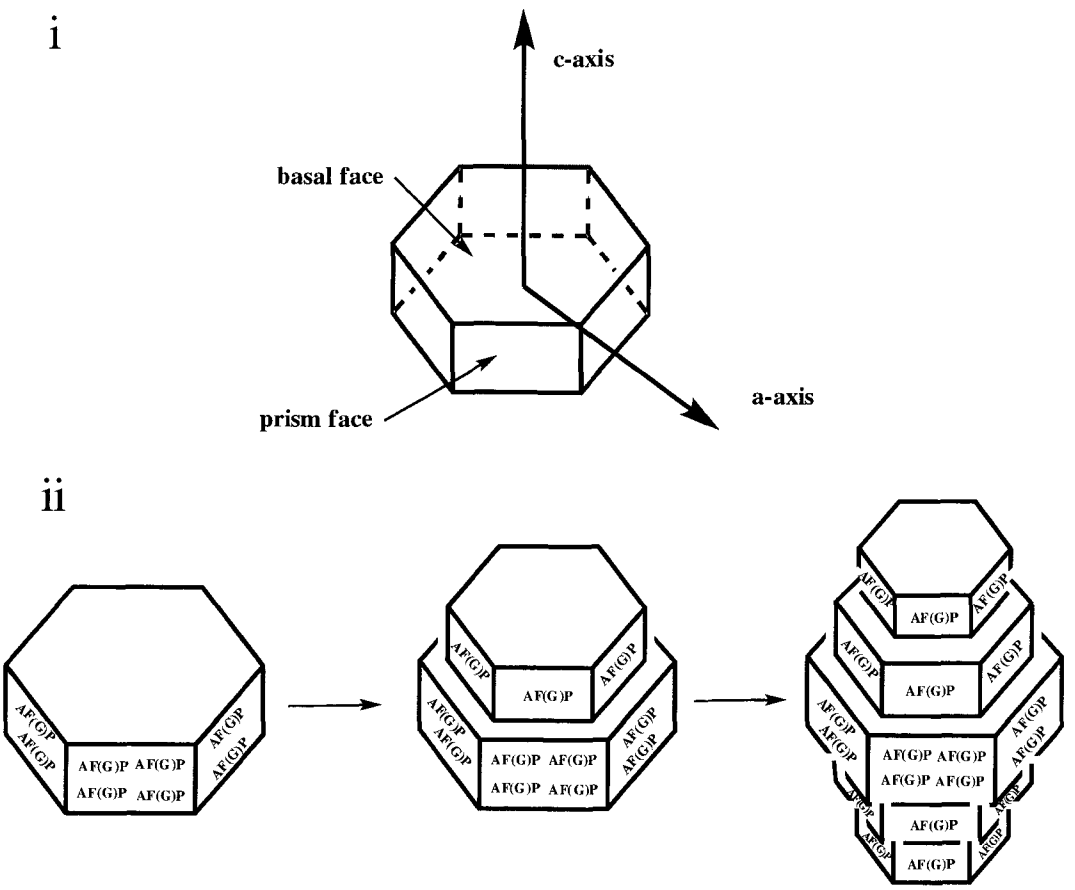

Figure 1.4.2 i) Hexagonal structure of an ice Ih lattice unit and **ii)** Dynamic ice-shaping, resulting in the formation of a hexagonal bipyramidal crystal.

In the absence of antifreezes, ice crystals grow perpendicular to the c-axis, enlarging the basal plane.[31, 32] In contrast, in the presence of biological antifreezes ice

grows parallel to the c-axis (**Figure 1.4.2**).[33] DeVries[34, 35, 36, 37] has shown that antifreezes can selectively adsorb to the prism faces preventing growth along the a-axes. As a result, in the presence of biological antifreezes crystal growth occurs along the c-axis forming a hexagonal bipyramidal structure (**Figure 1.4.2**).

Within the TH gap, biological antifreezes retard the growth of ice and alter the morphology of ice crystals to hexagonal bipyridmidal. At temperatures below the TH gap, ice crystal growth has been described as "explosive," resulting in the formation of ice spicules. While spiculation may be attractive for procedures such as cryosurgery, the shape and rapid growth of ice crystals is detrimental for cryopreservation.

i) 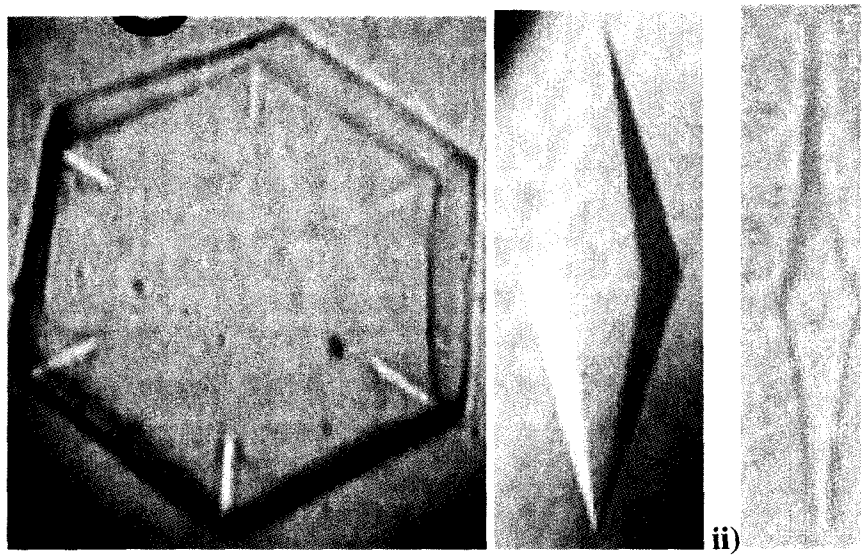 **ii)**

Figure 1.4.3 i) Ice crystals grown with AFP within the TH gap showing bipyramidal morphology (left; birds eye view, right; profile).[38, 39] **ii)** Ice crystal grown with AFP below the TH gap, showing spiculation.[38]

1.4.3 Recrystallization Inhibition

In addition to thermal hysteresis (TH) and dynamic ice shaping (DIS), recrystallization inhibition is an important property of biological antifreezes. When a frozen sample is maintained below its melting point or warmed slightly above its melting point, ice grains permeating the sample will change in shape and size. This phenomenon is referred to as ice recrystallization. In this process, smaller grains are incorporated into larger grains to yield a sample with a larger mean grain size and fewer grains. It has been postulated that the migration of the grain boundary is driven by an effort to minimize the overall grain boundary energy via an increase in grain size.[3]

There are two ways by which recrystallization can be inhibited; changing the boundary energy, or diminishing the diffusion of water. With regards to changing the interface energy, AFGPs are able to bind to the surface of crystals at the ice/water interface and prevent ice boundary migration. Furthermore, biological antifreezes are able to achieve this at very low concentrations.[40,41] Knight[42] has shown that even peptides devoid of antifreeze activity are able to display RI activity by decreasing the diffusion of water. This occurs due to the extrusion of solutes from the ice lattice during freezing, resulting in a highly concentrated inter-boundary region which inhibits the necessary diffusion of water to the growing crystal.

It should be noted that thermal hysteresis and recrystallization inhibition are not linked to one another, i.e. they are decoupled.[43]

1.4.4 Membrane Stabilization

The ability of AFGPs to maintain cell membrane integrity at low physiological temperatures is an important attribute. In the absence of antifreeze glycoproteins, liposome membranes leak as they are cooled/warmed through the thermotropic phase transition.[44, 45] The thermotropic phase transition is the change from a liquid state to a crystalline state. In this transitionary stage both crystalline and liquid states coexist, resulting in increased membrane permeability. In the absence of AFGPs, Hayes[46] has reported the leakage of trapped markers during the transition. No leakage was observed in the presence of AFGPs. Fletcher[47] has proposed that AFGPs prevent disruption of the cell membrane by inserting into the lipid bilayer and stabilizing it.

1.5 Mechanism of Ice Inhibition

At The Macroscopic Level:

Currently there are two mechanisms which have been theorized to explain the macroscopic mechanism of ice inhibition, a nucleation inhibition model and an adsorption-inhibition model. The nucleation inhibition paradigm suggests that antifreezes prevent the formation of a nucleus of critical size by blocking interfacial sites and/or increasing the interfacial energy.[3, 48]

The adsorption-inhibition model advocated by Knight and DeVries[49, 50] suggests that antifreezes bind to the growing ice surface preventing additional water molecules from adding to where the antifreeze has adsorbed. This results in ice growth between antifreeze adsorption sites only. The shape of the ice front becomes spherical and since

the water-ice interfacial energy increases with curvature of the ice front, growth becomes thermodynamically unfavourable ($\Delta G = +$). This is known as the Kelvin Effect.[51]

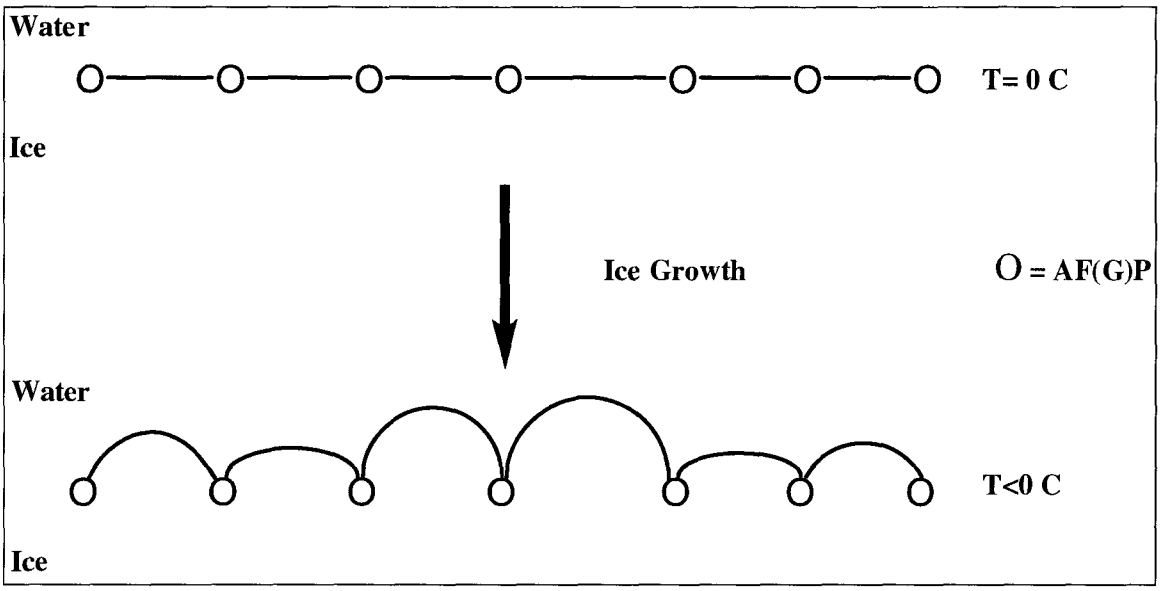

Figure 1.5.1 Adsorption-inhibition model.

The exact mode of antifreeze binding in the adsorption-inhibition model is still under debate. Knight and DeVries[50] suggest that antifreeze binding is irreversible. Their assertion is predicated upon the unlikelihood of the 24 hydrogen bonds formed per AFGP8 molecule from being broken in concert. Kuroda[52] has suggested that this model is incorrect, and adsorption may be reversible. Wen and Laursen[53] have attempted to reconcile these conflicting views suggesting that antifreeze binding is concentration dependent. At low concentrations reversible adsorption occurs; however, at elevated glycoprotein concentrations, intermolecular interactions (van der Waals forces) between antifreezes dominate, resulting in greater binding affinity.

At The Molecular Level:

The mechanism of antifreeze interaction with the ice-water interface is a subject of controversy. Hydrogen bonding between the disaccharide moiety of the glycoprotein and the ice surface has been postulated to account for ice binding. Proponents[54] of this theory advocate that antifreezes such as AFGP8 are capable of forming 24 Hydrogen bonds with the ice lattice per molecule. This figure is derived from the observation that only two carbohydrate hydroxyls are appropriately aligned to interact with the ice surface per repeating unit (n=4), and each hydroxyl forms 3 hydrogen bonds.[54]

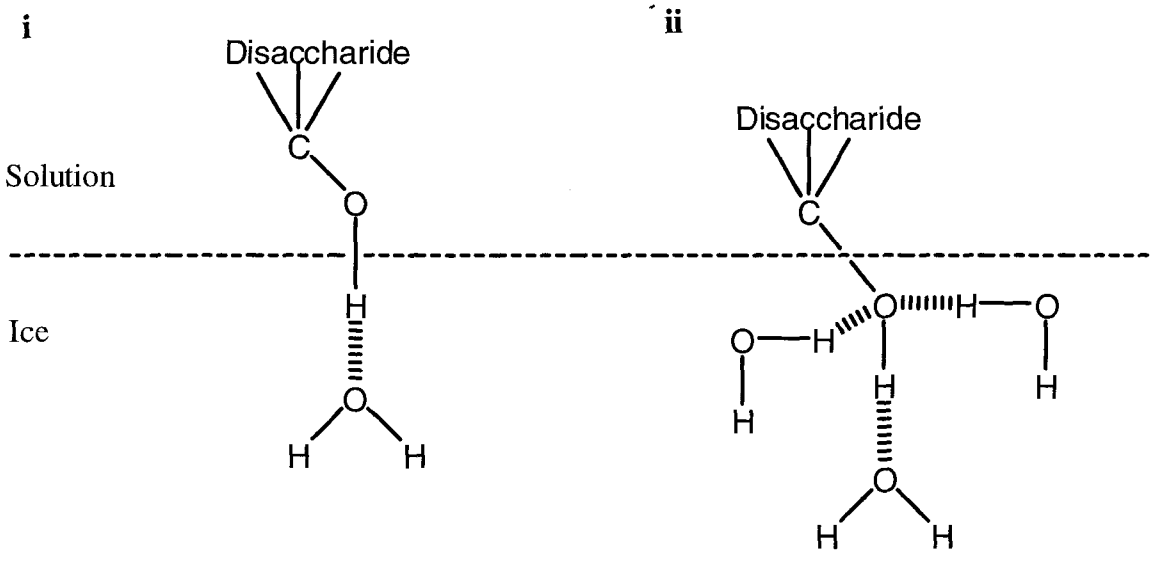

Figure 1.5.2 i) Early model hypothesizing 1 hydrogen-bond per aligned hydroxyl. **ii)** Revised model, hypothesizing 3 hydrogen-bonds per aligned hydroxyl.

The hydrogen bonding hypothesis is an extension of a similar supposition proposed for AFP1. According to this model, the hydroxyl groups of the L-threonine

residues and the carboxyl group of the aspartates form hydrogen-bonds with the oxygen atoms on the pyramidal faces of the ice lattice[55] (**Figure 1.5.3**).

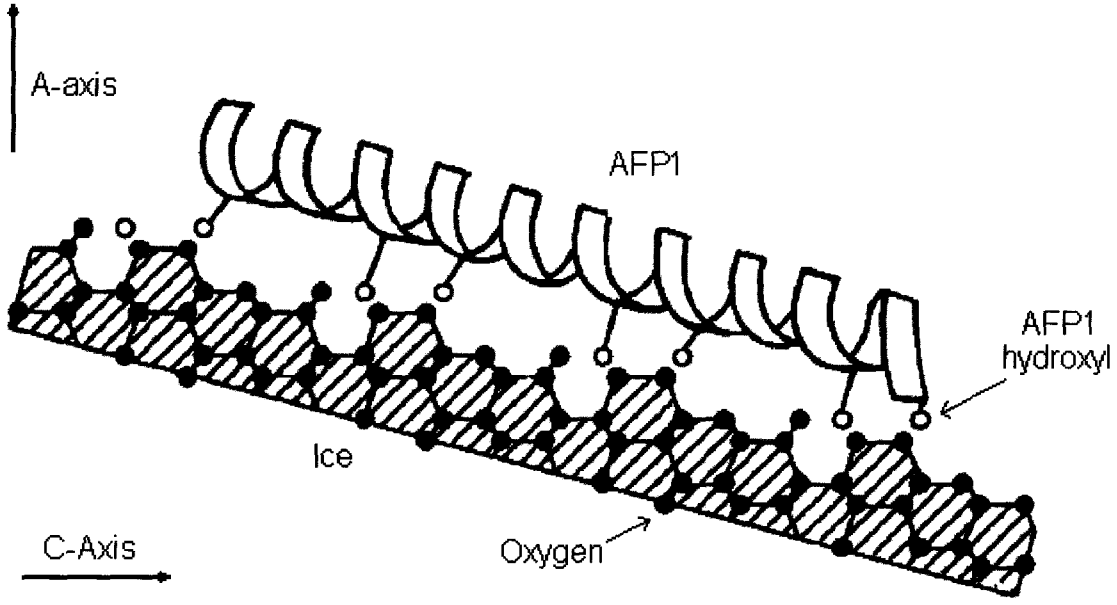

Figure 1.5.3 Interaction of AFP1 with ice lattice.[55]

Furthermore, structure activity studies have indicated that hydrophobic interactions may be just as important as hydrophilic interactions. Replacement of L-threonine residues on AFP1 with L-serine and L-valine indicate that hydrophobic methyl groups may play a larger role than previously thought.[56, 57] L-Serine mutants were devoid of antifreeze activity, while L-valine mutants showed comparable activity to native AFP1. The only difference between L-valine, L-threonine and L-serine AFPs which can possibly account for the variation in activity is the presence of β-methyl moieties in L-valine and L-threonine AFPs and the absence of β-methyl functionalities in L-serine mutants.

1.6 Conformational Analysis

Determining the conformation adopted by biological antifreezes is essential for elucidating how they function. The conformation adopted by AFGPs in solution has an important role in how the glycoprotein interacts with the ice lattice. In contrast to the well defined structure of AFPs, the secondary structure of AFGPs has not been definitively addressed.

DeVries has reported that AFGPs possess minimal α-helix content.[6] Early circular dichroism (CD) studies suggest that the secondary structure of AFGPs in solution is random coil.[58, 59] In contrast, Morris[60] has suggested that AFGPs form an extended 3-fold left-handed helix. This supposition was made on the basis that sugar residues align on only one side of the helix, affording a stable hydrogen-bonding face capable of interacting with the ice lattice. Rao[61] has hypothesized that the helical arrangement represents an energy minima.

Feeney[62] has indicated that AFGP conformation is temperature dependent. At low temperatures AFGP8 has been reported to adopt a rod-like conformation, reminiscent of a three fold polyproline type II helix. At higher temperatures, a flexible coil structure has been observed. Using CD, Ben[63] has indicated that at room temperature random coil is the predominant conformation with minor α-helix and β-sheet contributions. These results suggest that AFGPs are highly flexible, and are capable of adopting various conformations depending on the conditions.

1.7 Structure Activity Relationships

Detailed structure-activity relationship studies have been conducted on AFPs and AFGPs.[64, 65, 66, 67] Early structure-activity work performed by Feeney[68] on native AFGPs has shown a correlation between TH activity and length of the polypeptide. Small glycopeptides obtained via subtilisin hydrolysis of AFGP8 exhibited no discernable antifreeze activity. These penta-Ala-Ala-Thr-Ala-Ala peptides were devoid of any TH activity. This is not surprising considering earlier data shows that larger AFGPs(1-4) are more active than smaller AFGPs.

Sugar residues on AFGP8 have proven essential for TH activity. Cleavage of the base labile glycosidic bond with 0.5M NaOH results in β-elimination of the disaccharide moiety and loss of activity.[64] In addition to highlighting the importance of the sugar residue, racemization was also observed, indicating the significance of the amino acid side chain.

Periodate oxidation of the terminal galactosyl hydroxyls resulted in a loss of TH activity (**Figure 1.7**).[65] Furthermore, acetylation of the sugar hydroxyls inactivated the glycoprotein as well.[65] These results suggest that certain hydroxyl groups are essential for TH activity. Oxidation of the disaccharide C6 hydroxyls with galactose oxidase did not impact activity.[66] This suggests that the C6 hydroxyls are not essential for TH. However, generation of C6 carboxylates and bisulfite adducts (**Figure 1.7**) has shown that a negative charge on the carbohydrate is not amenable for activity.[70, 71] Formation of borate esters at C3 and C4, or C4 and C6 of the terminal galactose moiety also exhibited a lack of TH, indicating that the functional groups on the sugar are important.

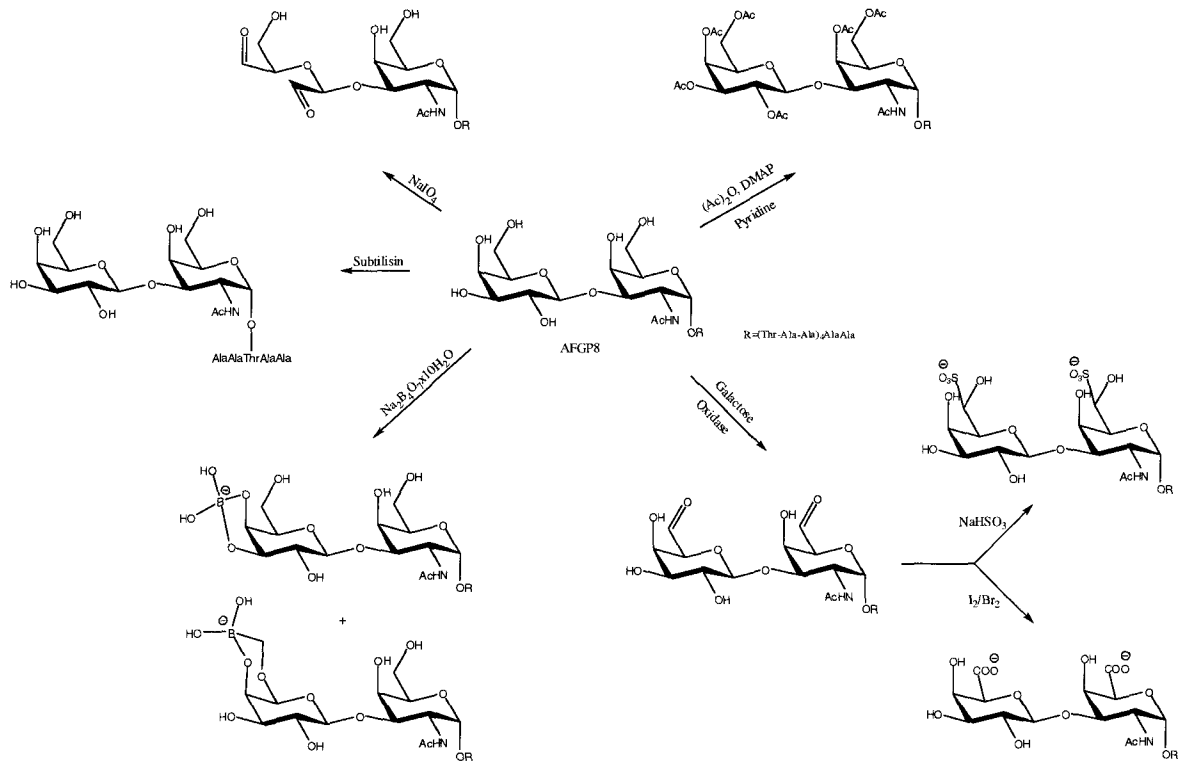

Figure 1.7 Early structure-function studies on AFGP8.

Recent SAR work by Nishimura[72, 73, 74] has confirmed previous assumptions and led to the development of additional hypotheses. The independent synthesis and testing of a series of AFGP8 analogues by Nishimura has confirmed the necessity of hydrophobic functionalities such as *N*-acetyl and β-methyl groups (**Table 1.7;** Entries 2 & 3). Furthermore, Nishimura has shown that the α-glycosidic-peptide linkage is essential for TH activity (**Table 1.7**; Entry 4). In addition, the configuration of sugar hydroxyls was also found to be crucial, since lactose analogues were devoid of activity (**Table 1.7**; Entry 5). Curiously, the galactosamine monosaccharide exhibited comparable activity to AFGP8 (**Table 1.7**; Entry 6), suggesting that disaccharide and terminal galactose moieties are not essential for TH activity.

Entry	Analogue	TH Activity
1 (AFGP 8)	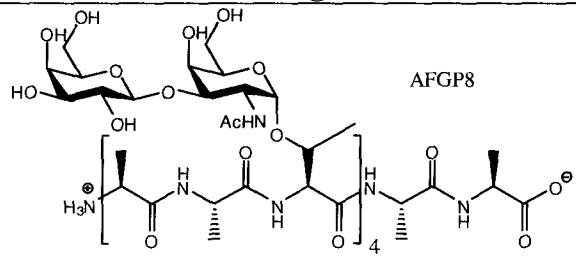	Yes
2	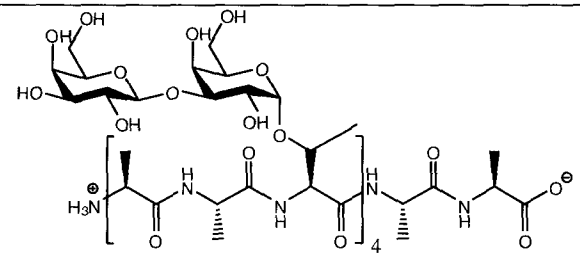	No
3	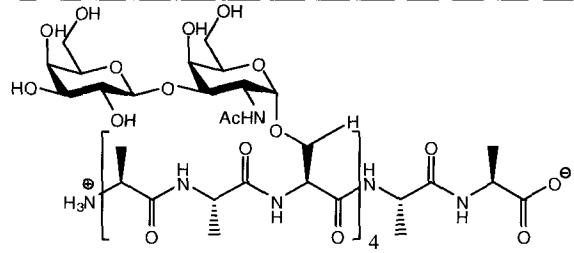	No
4	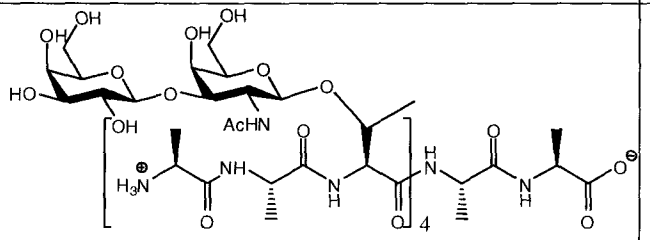	No
5	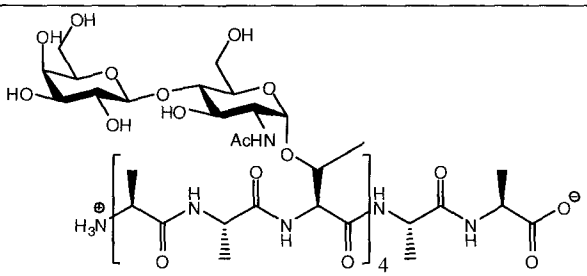	No
6	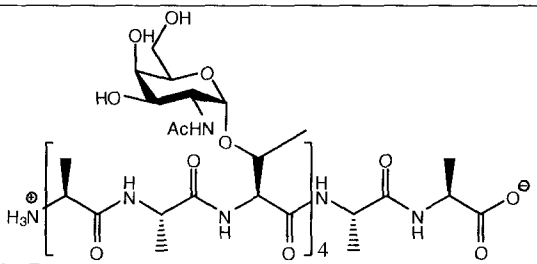	Yes

Table 1.7 Nishimura's SAR results.

1.8 Applications of Biological Antifreezes

The properties of biological antifreezes make them valuable tools for a variety of applications, ranging from cryopreservation, to ice cream.

The preservation of perishable foods such as frozen meats and ice cream is important to the frozen food industry. The concern regarding frozen foods is the loss of texture and the detrimental effect on taste. This is due to the formation of large ice crystals via improper storage and multiple freezing-thawing cycles. The ability of AFPs and AFGPs to inhibit ice recrystallization and therefore prevent the loss of ice cream texture make them valuable tools in the ice cream industry. Recently, Goff and Regand[75] have shown that AFPs from cold-acclimated winter wheat extract (AWWE) can be successful in improving ice cream texture, making the frozen dessert more palatable. Furthermore, the American Food and Drug Administration has recently approved the use of biological antifreezes in food products.[76] Isolation of AFPs from ocean pout, and large scale cloning in yeast cell lines has been accomplished by Unilever. These AFPs have been incorporated in Breyer's Light ice cream bars with great success.

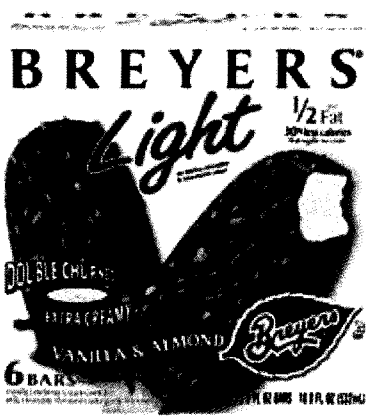

Figure 1.8 Breyer's Light ice cream bars containing Type III AFPs from ocean pout.

Payne and colleagues[77] have also shown that AFGPs administered to lamb prior to slaughter, followed by storage at -20 °C for 2-16 weeks, results in meat samples with smaller ice crystals and decreased drip (water retention). These examples illustrate the utility of biological antifreezes in the burgeoning frozen food industry.

The application of antifreezes to cryosurgery is an area of significant interest. Cryosurgery is a procedure which employs subzero temperatures to destroy specific tissues. The destruction of cancer cells via cryosurgery has the benefits of being minimally invasive and cost effective.[78, 79] *In vivo* tumor treatment with AFP1 by Rubinsky[80, 81] was found to be extremely effective (mortality rate of 100 %). This is due to the dynamic ice shaping (DIS) properties of biological antifreezes which result in the formation of membrane damaging ice spicules. In contrast, cryosurgery without these chemical adjuvants is problematic due to the survival of cancerous tissue.

The formation of intracellular and/or extracellular ice is a problem for cryopreservation. While intracellular ice formation results in mechanical damage to organelles and is almost always lethal, accumulation of extracellular ice can result in mechanical damage to the cell membrane, and cellular dehydration. Cellular dehydration is due to the formation of ice crystals outside the cell, resulting in an expulsion of solutes from the ice lattice and an increase in extracellular solute concentration. This results in an osmotic imbalance, with the cell hyperosmotic relative to the extracellular fluid. The subsequent movement of water out of the cell to the extracellular fluid results in dehydration. Permeable cryoprotectants such as DMSO can alleviate the osmotic imbalance, but are incapable of inhibiting extracellular ice formation. A possible solution

to this challenge is a procedure called *vitrification*. Vitrification is a fast-cooling technique and can be coupled with high concentrations of cryoprotectants to convert a sample into a glass like amorphous solid. A drawback of this technique is the toxicity associated with conventional cryoprotectants. One way to overcome these challenges is to use biological antifreezes. Seren[82] has shown that AFGPs regulate the osmotic pressure and inhibit the growth of ice during vitrification of pig oocytes.

Biological antifreezes are also useful for the hypothermic storage of organs. The ability of AFGPs to stabilize the cellular membrane through the thermotropic transition makes them ideal for conventional storage protocols.

References:

---

1. Fletcher, G.L., Hew, L.H., and Davies, P. *Annual Rev. Physiol.* **2001**. 63, 359-390.

2. Zongchao, J. and Davies, P. *Trends in Biochem. Sci.* **2002**. 27(2), 101-106.

3. Yeh, Y. and Feeney, R.E. *Chem. Rev.* **1996**. 96(2), 601-618

4. Scholander, F., van Dam, L., Kanwisher, J.W., Hammel and Gordon, M.S. *Comp. Physiol.* **1957**. 49, 5-24.

5. DeVries, A.L., and Wohlschlag, *Science.* **1969**. 163(3871), 1073-1075.

6. DeVries, A.L., Komatsu, S.K. and Feeney, R.E. *J. Bio. Chem.* **1970**. 245(11), 2901-2908.

7. DeVries, A.L., Vandenheede, J., and Feeney, R.E. *J. Bio. Chem.* **1971**. 246(2), 305-308.

8. Harding, M.M., Anderberg, P.I., and Haymet, A.D.J. *Eur. J. Biochem.* **2003**. 270, 1381-1392.

9. Duman, J.G. and DeVries, A.L. *Nature.* **1974**. 247, 237-238.

10. Duman, J.G. and DeVries, A.L. *Comp. Biochem. Physiol.* **1976**. 54B, 375-380.

11. Yang, D.S.C., Sax, M., Chakrabartty, A. and Hew, C.L. *Nature.* **1988**. 333, 232-237.

12. Davies, P.L., and Hew, C.L. *The. FASEB J.* **1990.** 4, 2460-2468.

13. Jia, Z.C., Deluca, C.I., and Davies, P.L. *Protein Sc.* **1995.** 4, 1236–1238.

14. Sonnichsen, F. D.; Sykes, B. D.; Davies, P. L. *Protein Sci.* **1995**, 4, 460.

15. Hew, C.L., Slaughter, D., Joshi, S.B., Fletcher, G.L. and Ananthanarayanan, V. S. *J. Comp. Physiol.* **1984**, 155B, 81.

16. Deng, G.J., Andrews, D.W. and Laursen, R.A. *FEBS Lett.* **1997**. 402, 17–20.

17. Deng, G. J. and Laursen, R. A. *Biochim. Biophys. Acta.* **1998.** 1388, 305–314.

18. Graham, L.A., Liou, Y-C., Walker, V. K. and Davies, P.L. *Nature.* **1997.** 388(21), 727-279.

19. O'Grady, S.M., Schrag, J.D., Raymond, J.A. and DeVries, A.L. *J. Exp. Zool.* **1982**. 224, 177-185.

20. Wu,Y., Banoub, J., Goddard, S.V., Kao, M.H. and Fletcher, G.L. *Comp. Biochem. Physiol. B.* **2001.** 128, 265–273.

21. Tomimatsu, Y., Scherer, J.R., Yeh, Y. and Feeney, R.E. *J. Biol. Chem.* **1976**. 251, 2290.

22. Bush, C.A., Feeney, R.E., Osuga, D.T., Ralapati, S. and Yeh., Y. *Int. J. Peptide Protein Res.* **1981**. 17, 125-129.

23. Bush, C.A., Ralapati, S., Matson, G.M., Yamasaki, R.B., Osuga, D.T., Yeh, Y. and Feeney, R.E. *Arch. Biochem. Biophys.* **1984**. 232, 624.

24. Bush, C.A. and Feeney, R. E. *Int. J. Peptide Protein Res.* **1986**, 28, 386-397.

25. Franks, F., and Morris, E. R. *Biochim. Biophys. Acta.* **1978.** 540, 348-356.

26. Bouvet, V.R., Lorello, G.R., and Ben, R.N. *Biomacromolecules.* **2006**. 7(2), 565-571.

27. Ahlgren, J.A., Cheng, C.C., Schrag, J.D. and DeVries, A.L. *J. Exp. Biol.* **1988**. 137, 549-563.

28. Valerio, P.F., Kao, M.H. and Fletcher, G.L. *J. Exp. Biol.* **1992**. 164, 135-151.

29. Knight, C.A., DeVries, A.L. and Oolman, L.D. *Nature*. **1984**. 308, 295–296.

30. Kao, M.H., Fletcher, G.L., Wang, N.C., and Hew, C.L. *Can. J. Zool.* **1986**. 64, 578–582.

31. Yang, D.S.C., Sax, M., Chakrabartty, A. and Hew, C.L. *Nature*. **1988**. 333, 232-237.

32. Fletcher, N.H. *The Chemical Physics of Ice.* **1970**. Cambridge University Press.

33. Feeney, R.E., Burcham, T.S. and Yeh, Y. *Ann. Rev. Biophys, biophys. Chem.* **1986.** 15, 59-78.

34. Raymond, J.A. and DeVries, A.L. *Proc. Nat. Acad. Sci. U.S.A.* **1977**. 74, 2589-2593.

35. Knight, C.A., DeVries, A.L. and Oolman, L.D. *Nature*. **1984**. 308, 295-296.

36. Knight, C.A., Cheng, C.C., and DeVries, A.L. *J. Biophys.* **1991**. 59, 409-418.

37. Knight, C.A., Driggers, E., and DeVries, A.L. *J. Biophys.* **1993**. 64, 252-259.

38. Wathen, B., Kuiper, M.J., Walker, V.K. and Jia, Z. *Can. J. Phys*. **2003**. 81, 39-45.

39. Haymet, A.D.J., Ward, L.G. and Harding, M.M. *FEBS Lett.* **2001**. 491, 285-288.

40. Knight, C.A., DeVries, A.L. and Oolman, L.D. *Nature*. **1984**. 308, 295-296.

41. Knight, C.A., Hallet, J. and DeVries, A.L. *Cryobiology.* **1988.** 25, 55-60.

42. Knight, C.A., Wen, D.-Y. and Laursen, R.A. *Cryobiology.* **1995**, 32, 23-34.

43. Sidebottom, C., Buckley, S., Twigg, S., Telford, J., Warrall, D., Hubbard, R., Lillford, P., Holt, C., McArthur, A. Jarman, C., and Pudney, S.P. *Nature.* **2000**, 406, 256-258

44. Quinn, P.J. *Cryobiology.* **1985.** 22, 128.

45. Clerc, S.G. and Thompson, T.E. *J. Biophys.* **1995.** 68, 2323.

46. Hayes, L., Feeney, R.E., Crowe, L.M., Crowe, J.H., Oliver, A.E. *Proc. Natl. Acad. Sci.* USA. **1996.** 93, 6835.

47. Wu, Y., and Fletcher, G.L. *Biochim. Biophys. Acta.* **2000.** 1524, 11.

48. Wilson, P. W., Leader, J. P. *Biophys. J.* **1995**, 68, 2098.

49. Raymond, J.A. and DeVries, A. L. *Cryobiology.* **1972**. 9, 541.

50. Knight, C.A., Driggers, E. and DeVries, A.L. *Biophys. J.* **1993**. 64, 252.

51. Wilson, P.W. *Cryoletters.* **1993.** 14, 31-36.

52. Kuroda, T. *Proc. 4th Topical Conference on Crystal Growth Mechanisms.* **1991**. Hokkaido Press, Japan, p 157.

53. Wen, D. and Laursen, R.A. *J. Biophys..* **1992.** 63, 1659.

54. Knight, C.A., Driggers, E. and DeVries, A.L. *J. Biophys.* **1993**. 64, 252.

55. Wen, D. and Laursen, R.A. *J. Biophys.* **1992**. 63, 1659.

56. Haymet, A.D.J., Ward, L.G. and Harding, M. *J. Am. Chem. Soc.* **1999.** 121, 941-948.

57. Chao, H., Houston, M.E. Jr., Hodges, R.S., Kay, C.M. Sykes, B.D., Loewen, M.C., Davies, P.L. and Sonnichsen, F.D. *Biochemistry.* **1997.** 36, 14652-14660.

58. Bush C.A., Feeney, R.E., Osuga, D.T., Ralapati, S., and Yeh, Y. *Int. J. Pept. Protein Res.* **1981.** 17, 125-129.

59. Rao, B.N. and Bush, C.A. *Biopolymers.* **1987.** 26, 1227-1244.

60. Franks, F., and Morris, E.R. *Biochim. Biophys. Acta.* **1978.** 540. 348-356.

61. Rao, B.N. and Bush, C.A. *Biopolymers.* **1987.** 26, 1227-1244.

62. Bush, C.A. and Feeney, R. E. *Int. J. Peptide Protein Res.* **1986**, 28, 386-397.

63. Bouvet, V.R., Lorello, G.R., and Ben, R.N. *Biomacromolecules.* **2006**. 7(2), 565-571.

64. Komatsu, S.K., DeVries, A.L., and Feeney, R.E. *J. Biol. Chem.* **1970.** 245, 2909-2913.

65. DeVries, A.L., Komatsu, S.K. and Feeney, R.E. *J. Biol. Chem.* **1970.** 245, 2901-2908.

66. Geoghegan, K.F., Osuga, D. T., Ahmed, A.I., Yeh, Y. and Feeney. R.E. *J. Biol. Chem.* **1980.** 255, 663-667.

67. Osuga, D.T., Yeh, Y. and Feeney, R.E. *J. Carbohydr. Chem.* **1994**. 13, 347-361.

68. Yeh, Y. and Feeney, R.E. *Adv. Protein Chem.* **1978**. 32, 191-282.

69. Ahmed, A.I., Yeh, Y., Osuga, D.T. and Feeney, R.E. *J. Biol. Chem.* **1976.** 251, 3033-3036.

70. DeVries, A.L. *Science.* **1971.** 171, 1152-1155.

71. Vandenheede, J.R., Ahmed, A.I., and Feeney, R.E. *J. Biol. Chem.* **1972.** 247, 7885-7889.

72. Tachibana, Y., Fletcher, G.L., Fujitani, N., Tsuda, S., Monde, K. and Nishimura, S. *Angew. Chem. Int. Ed.* **2004**. 43, 856-862.

73. Tsuda, T. and Nishimura, S. *Chem. Commun.* **1996.** 24, 2779-2780.

74. Tachibana, Y., Matsubara, N., Nakajima, F., Tsuda, T., Tsuda, S., Monde, K. and Nishimura, S. *Tetrahedron* **2002.** 58, 10213-10224.

75. Goff, H.D. and Regand, A. *Journal of Dairy Science.* **2006**. 89, 49-57.

76. Rulis, A.M. *Agency Response Letter.* U.S. Food and Drug Administration, Centre for Food Safety and Applied Nutritions, Office of Food Additive Safety. **2003**. available from; http://www.cfsan.fda.gov/~rdb/opa-g117.html, accessed November 7th 2008

77. Payne, S.R. and Young, O.A. *Meat Sci.* **1995.** 41, 147-155.

78. Kaufman, C.S. and Rewcastle, J.C., Technol. *Cancer Res. Treat.* **2004.** 3, 165-176.

79. Rees, J., Patel, B., MacDonagh, R. and Persad, R. *BJU Int.* **2004.** 93, 710-714.

80. Koushafar, H. and Rubinsky, B. *Urology.* **1997.** 49, 421.

81. Pham, L., Dahiya, R. and Rubinsky, B. *Cryosurgery.* **1999.** 38, 169.

82. Arav, A., Rubinsky, B., Fletcher, G. and Seren, E. *Mol. Reprod. Dev.* **1993**. 36, 488-493.

Chapter 2

Goals and Objectives

2.1 Synthesis of AFGPs and AFGP Analogues

Antifreeze glycoproteins are obtained primarily from the blood of teleost fish. Due to the low natural abundance of these "*O*-linked" compounds and the difficulty in purifying them, traditional methods of isolation have proven inadequate. In order to obtain large quantities of analytically pure glycoproteins for commercial applications and research, alternative strategies are required. Unlike AFPs which have been readily cloned with yeast expression vectors,[1, 2, 3] cloning of AFGPs has not been accomplished due to the incompatibility of the carbohydrate functionality with established cloning techniques. Laboratory synthesis of antifreeze glycoproteins is an attractive alternative. Synthetic approaches allow for the construction of AFGPs and AFGP analogues for structure-activity relationship (SAR) studies.

The most common antifreeze target for chemical synthesis is AFGP8. The relative simplicity of AFGP8 makes it amenable to synthetic approaches and as a result, analogues for SAR investigations are predicated upon this glycoprotein.

The first reported synthesis of an AFGP analogue was Anderson's tripeptide glycoprotein.[4] This synthesis employed a convergent approach consisting of separate construction of the disaccharide and peptide components (**Scheme 2.1.1**). In order to achieve this, benzoyl protected galactose bromide **1** was coupled with a benzyl protected galactose derivative **2,** via AgOTf to afford the core disaccharide **3**. This was followed by conversion of the anomeric substituent to the corresponding chloride **4,** and AgOTf mediated coupling with orthogonally protected tripeptide **5**. The coupling was achieved

in 60 % yield. Finally, removal of protecting groups with Pd/C and H_2 afforded *O*-linked AFGP analogue **6**.

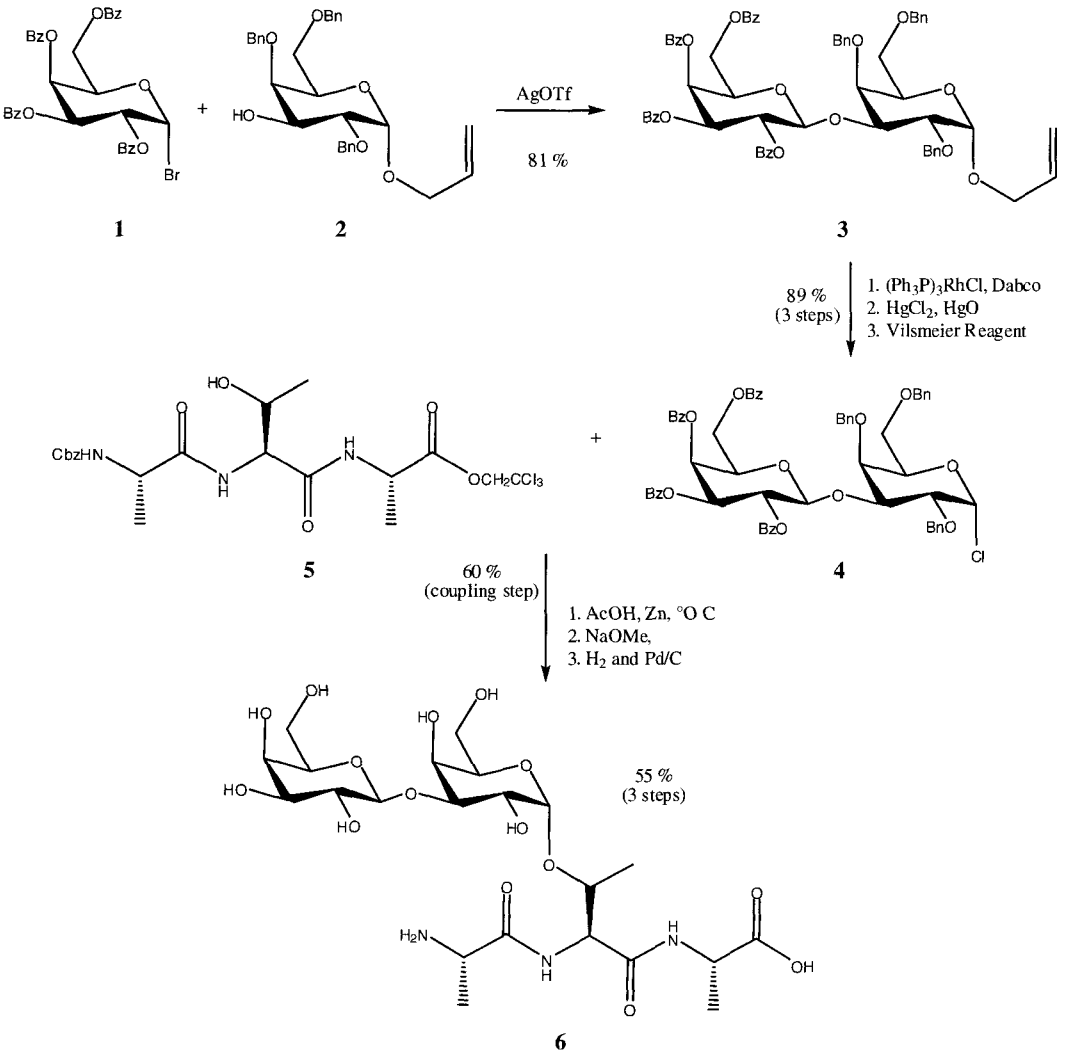

Scheme 2.1.1 Anderson's convergent synthesis of *O*-linked AFGP.

Drawbacks inherent to Anderson's convergent approach are poor diastereoselectivity during coupling (resulting in α/β mixtures), low reactivity of the threonine hydroxyl and poor solubility of the peptide chain under glycosylation conditions.[5, 6] The stepwise assembly of glycosylated amino acids in a linear fashion is an alternative strategy which can overcome these limitations. Linear approaches to

AFGP synthesis include Filira's continuous flow solid phase synthesis (SPS) of β-linked galactose.[7] In contrast to AFGP8 which possess an α-glycosidic linkage and a disaccharide, Filira's synthesis incorporates a β-glycosidic linkage and a galactose residue. This modification was performed in order to mimic the terminal galactose moiety of native AFGP8.

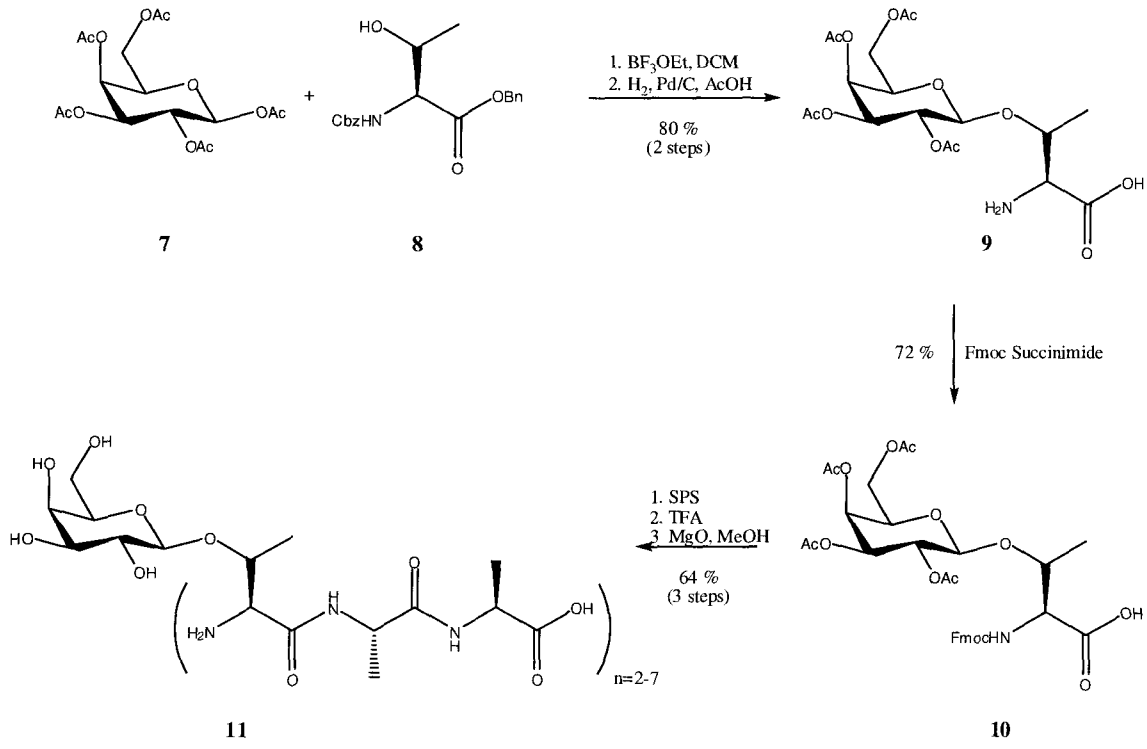

Scheme 2.1.2 Filira's linear solid phase synthesis strategy.

Filira's approach (**Scheme 2.1.2**) involved treatment of commercially available D-galactose pentaacetate **7** with selectively protected L-threonine **8** in the presence of $BF_3{\cdot}OEt_2$, followed by deprotection of the amino acid moiety to afford **9.** N-terminus reprotection with base labile Fmoc succinimide furnished the building block **10.** Stepwise addition of the amino acids was then accomplished on a Pepsyn KA solid-phase

resin using continuous flow solid-phase peptide synthesis, followed by TFA mediated cleavage from the resin and acetyl deprotection to afford the glycoprotein **11**.

The first synthesis of native *O*-linked AFGPs was accomplished by Nishimura and Tsuda[8] (**Scheme 2.1.3**). The disaccharide moiety was synthesized by coupling a galactosyl trichloroacetimidate donor **12** with a glycosyl fluoride acceptor **13** in the presence of TMSOTf. The product, **14**, was then coupled with orthogonally protected tripeptide **15** via cyclopentadienylzicronium dichloride and silver perchlorate to afford **16** in 64 % yield. Reduction of the azide with $NiCl_2$ and $NaBH_4$, followed by acetylation with Ac_2O furnished the protected disaccharide moiety. Deprotection of the carbohydrate and peptide functionalities afforded the AFGP monomer. Finally, diphenylphosphorylazide (DPPA) promoted polymerization of the unprotected monomer afforded a mixture of glycopeptides (**17**) in 69 % yield. The low yields of the coupling step and subsequent polymerization, in addition to the generation of a mixture of glycopeptides (with n= 10, 11 and 12) requiring laborious separation make this approach inexpedient.

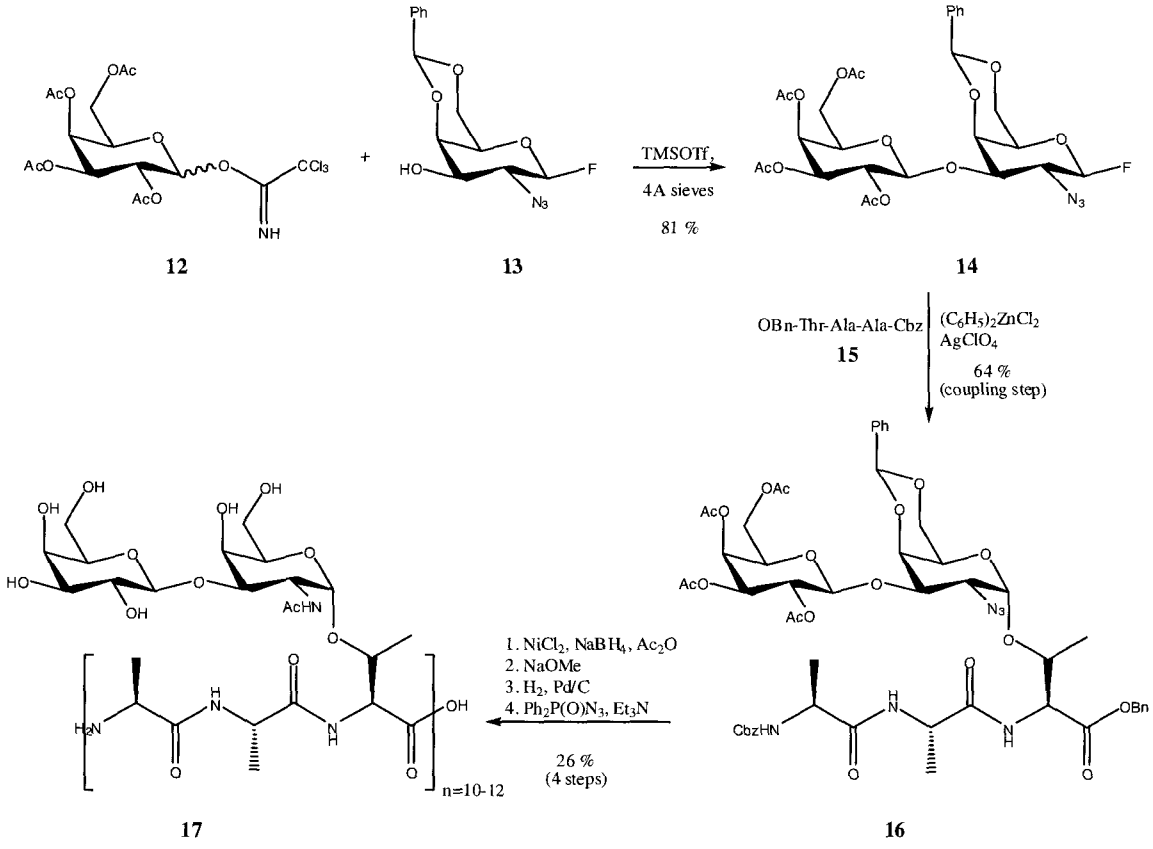

Scheme 2.1.3 Nishimura's first synthesis of native AFGP.

Chen and colleagues[9] reported the second synthesis of native *O*-linked AFGP via an Fmoc based solid phase peptide synthesis approach (**Scheme 2.1.4**). An important feature of this synthesis is the ability to control the length of the polymer chain using SPS. Reaction of selenyl glycoside **18** with selectively protected L-threonine afforded a monoglycoside. Treatment of the monoglycoside with thiourea to liberate the C3-hydroxyl for subsequent coupling afforded **19** in 83 % yield. Coupling of the glycoconjugate with thioglycoside **20** in the presence of an electrophilic iodine promoter (NIS) furnished the disaccharide **21** in 93 % yield. Deprotection of the C-terminus and concomitant reduction of the azide, followed by acetylation afforded Gal-NHAc

disaccharide building block **22**. SPPS followed by cleavage from the resin and NaOMe deprotection yielded **23** with 4 and 8 repeating units (**Scheme 2.1.4**.).

An advantage of Chen's solid-phase approach is direct control over the amino acid composition, allowing for the construction of a polypeptide with the desired amino acid sequence. As a consequence, the cumbersome separation of a complex mixture of glycoproteins required by Nishimura's approach is avoided.

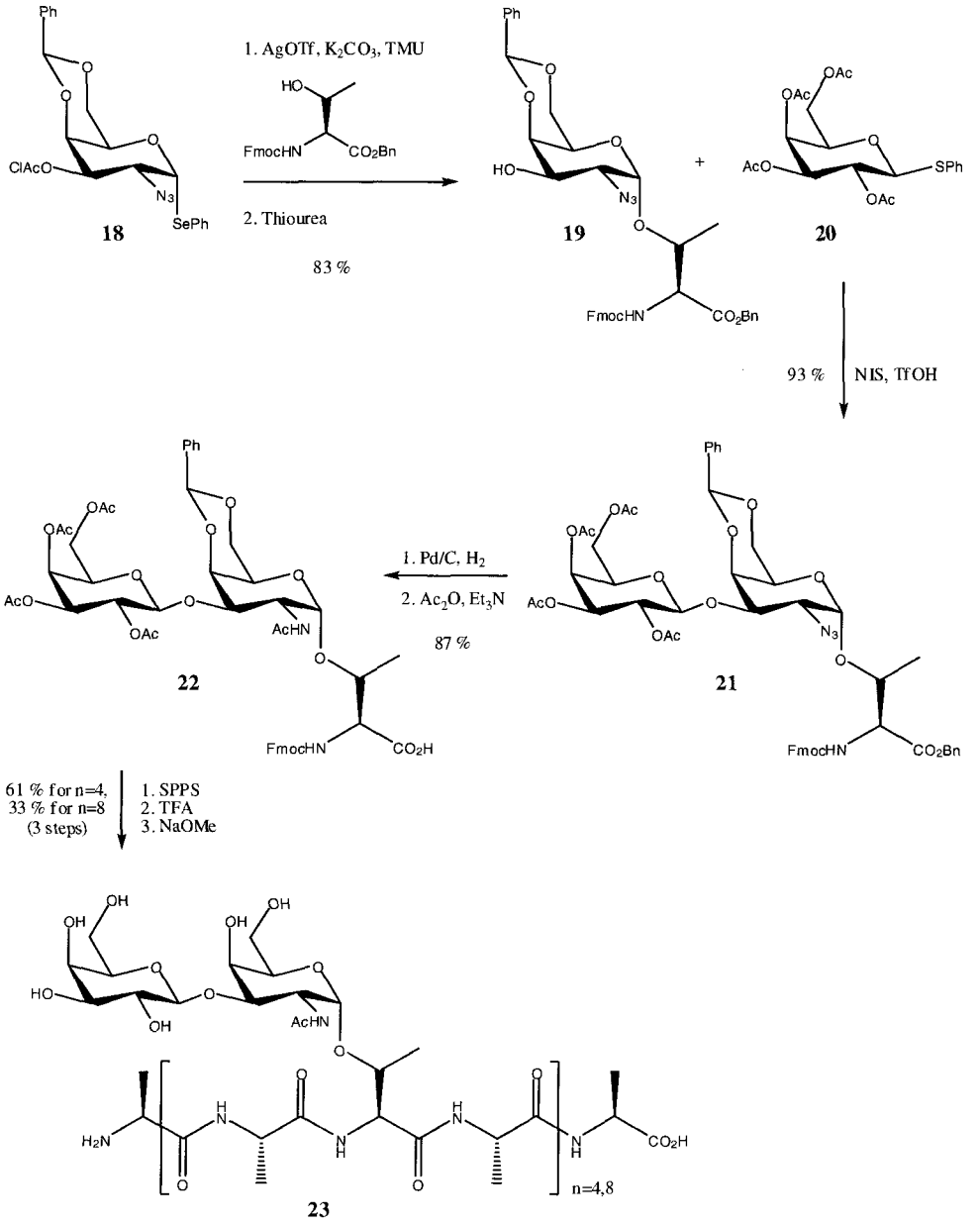

Scheme 2.1.4 Chen's SPPS approach to native AFGPs.

2.2 *C*-Linked AFGP Analogues

The L-threonine-disaccharide motif exhibited by native AFGPs is an example of an "*O*-linkage." Native *O*-linked glycoproteins are unstable due to the sensitivity of the glycosidic linkage to enzymes, acids and bases. Hydrolysis in acidic media results in the formation of an oxocarbenium cation, while cleavage of the glycosidic bond via β-elimination occurs in basic media (**Figure 2.2.1**).

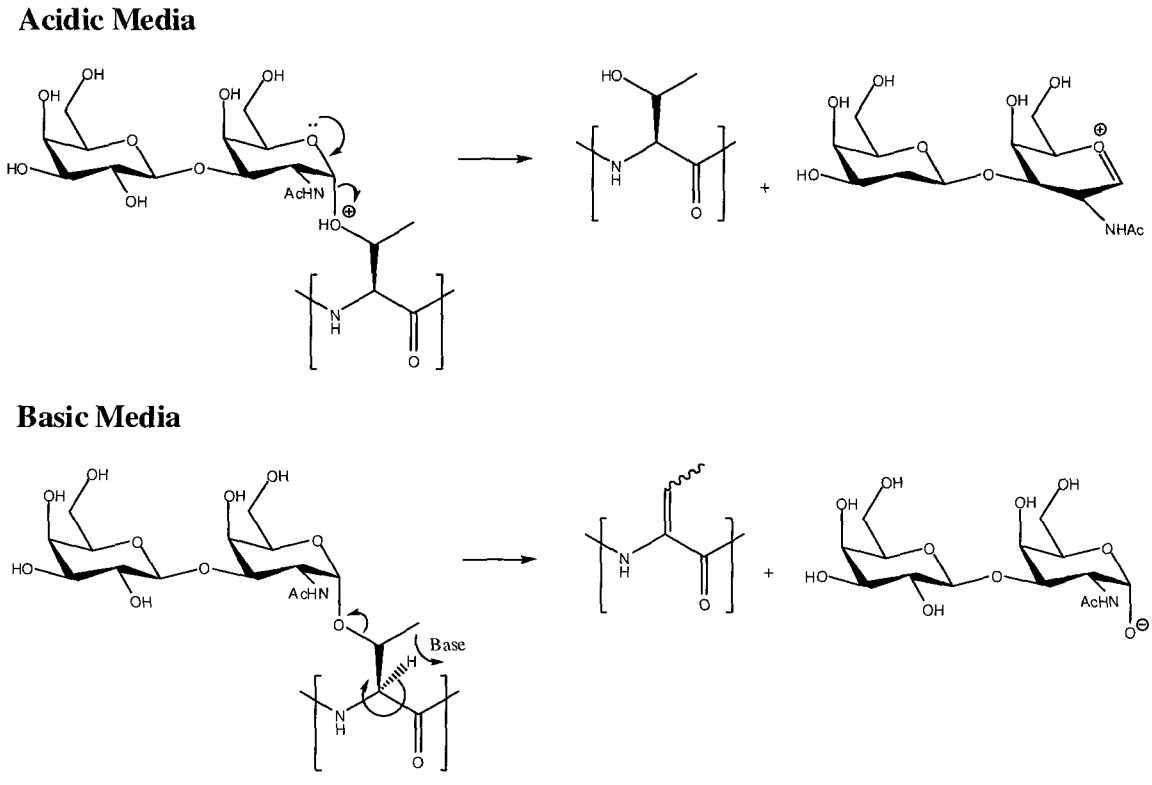

Figure 2.2.1 Hydrolysis of the labile glycosidic linkage in acidic media yielding the oxocarbenium cation, and cleavage in basic media via β-elimination.

The instability of *O*-linked glycopeptides and the challenges in synthesizing these compounds have led to the development of less labile *C*-linked analogues.[10, 11, 12] *C*-glycoproteins are less prone to enzymatic cleavage and are stable to acidic and basic

conditions. Furthermore, these variants are important for structure-function elucidation and drug discovery. Synthesis of these *C*-linked compounds is predicated upon common synthetic strategies and numerous syntheses have been reported.[10, 11, 12]

Despite the significant change in electronics upon replacement of an oxygen atom with a methylene group, *C*-linked glycopeptides exhibit similar conformation to their *O*-linked counterparts.[13, 14, 15] Kishi[16] has shown that *C*-glycoproteins adopt similar solution conformation as their *O*-linked counterparts. These results have been corroborated by receptor-ligand binding studies. X-Ray crystallographic analysis of *C*-lactose bound to peanut lectin reveals "an almost perfect exo-anomeric conformation" of the saccharide, and an overall conformation which is "virtually identical to its parent *O*-lactose."[17]

The conformational similarity of *C*-linked glycopeptides with their *O*-linked counterparts and the added stability of *C*-glycoproteins make them ideal synthetic targets for structure-function studies and drug discovery. Work in our laboratory is focused on the exploration of *C*-glycopeptides as biological antifreezes.

2.3 *C*-Linked AFGP Analogues in the Ben Laboratory

For the purpose of our analyses, antifreeze glycoproteins can be reduced to three variable regions, the carbohydrate moiety, the linker region and the amino acid side chain (**Figure 2.3.1**). Work in our laboratory involves manipulation of these three regions to produce analogous compounds with custom tailored RI activity and no TH activity.

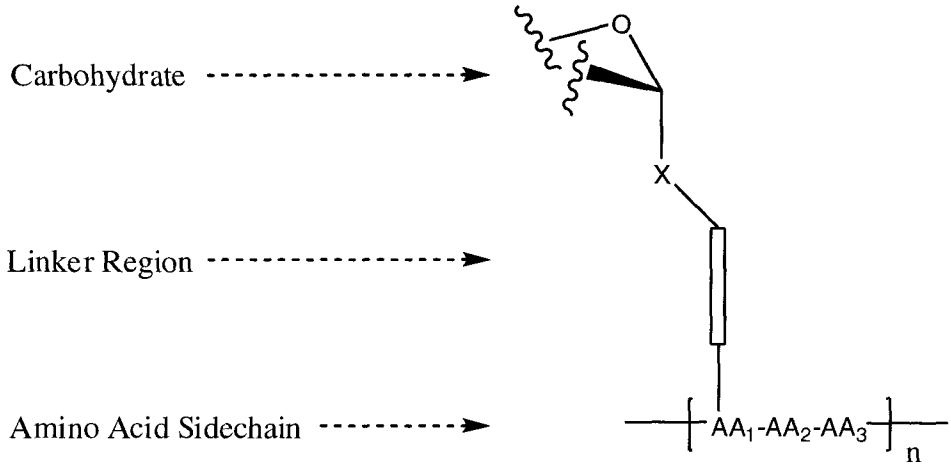

Figure 2.3.1 Core components of AFGPs. X= O in native systems, and X= CH_2 in *C*-linked analogues.

The main differences between native AFGPs and our first generation analogues are substitution of D-galactose for the disaccharide, L-lysine for L-threonine and the replacement of L-alanine in the peptide backbone with L-glycine (**Figure 2.3.2**).

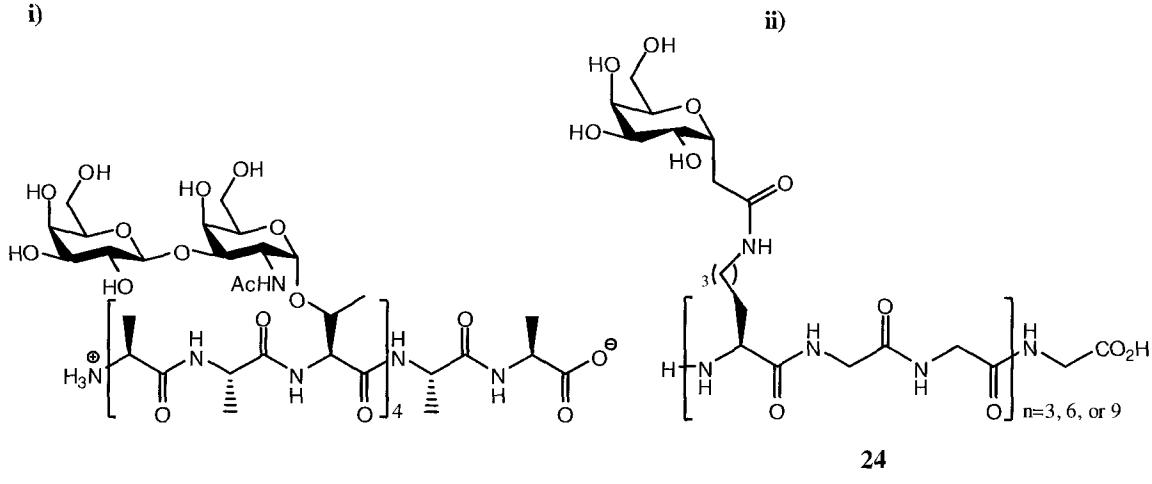

Figure 2.3.2 i) Native AFGP8 and **ii)** First Generation *C*-Linked AFGP Analogues.

Substitution of the disaccharide moiety with galactose was performed to simplify the synthesis. Early SAR work by Feeney[18] indicates that the terminal galactose residue is essential for antifreeze activity, and later studies by Nishimura[19] reveal that antifreeze activity is retained upon substitution of the β-D-galactosyl-(1→3)-α-*N*-acetyl-D-galactosamine disaccharide subunit with a monosaccharide. The replacement of L-lysine for L-threonine was predicated upon the fact that AFGPs from Arctic and North Atlantic cod possess L-arginine in place of L-threonine. The amide bond in our analogues mimic the guanidine functionality in L-arginine based AFGPs. Finally, the amino acid composition of the peptide backbone was altered from L-alanine to L-glycine to avoid possible racemization during amino acid coupling sequences. No racemization has been reported from the use of solid phase peptide synthesis in our lab.

Polypeptides possessing tripeptide repeats of 3, 6 and 9 amino acid units were among the first generation of *C*-glycopeptides synthesized.[20] 3-mer polymers (n=3) were found to be devoid of RI activity (**Graph 2.3**, pg. 46) In contrast, longer biopolymers, 6 and 9-mers were found to exhibit weak RI activity. The lack of activity observed in 3-mers, coupled with the fact that native AFGP8 possess 4 repeating units, led to the hypothesis that the minimum length for activity may be 4 repeating units.

The synthesis of AFGP analogue **24** was accomplished by Ben and Enaide[21] via a CDI mediated coupling of the carboxylic acid **25** with the protected tripeptide **26** to yield building block **27**. Deprotection with Pd/C and H_2 followed by SPPS furnished biopolymer **28**. TFA cleavage from the Wang resin followed by NaOMe deprotection afforded the 3-mer **24(a),** the 6-mer **24(b)** and the 9-mer **24(c)** (**Scheme 2.3.1**).

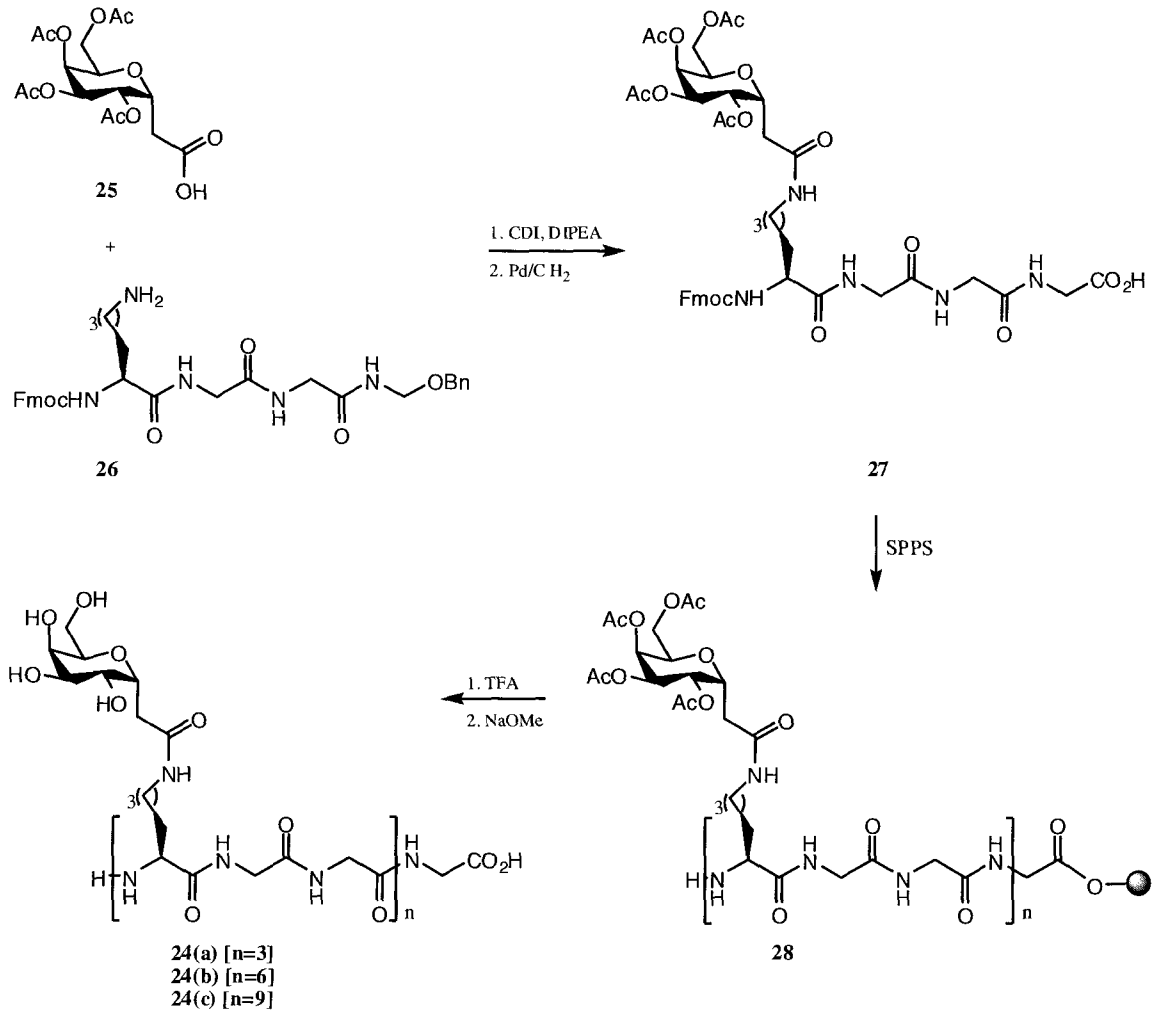

Scheme 2.3.1 Synthesis of our first generation *C*-linked AFGP analogues.

Second generation analogues were constructed with the same features of first generation AFGP analogues; however, the polypeptide core contained 4 repeating units (**Figure 2.3.3**). 4-mers, $[LGG]_4$[Gal] analogue **29,** and $[LAA]_4$[Gal] analogue **30** did not exhibit measurable antifreeze activity. In contrast, when a methylene unit was removed from the linker region, analogue **31** exhibited significant recrystallization inhibition activity (**Graph 2.3**, pg. 46). Replacement of L-lysine with L-ornithine in **31** indicates that there may be a correlation between the length of the linker and recrystallization inhibition activity.

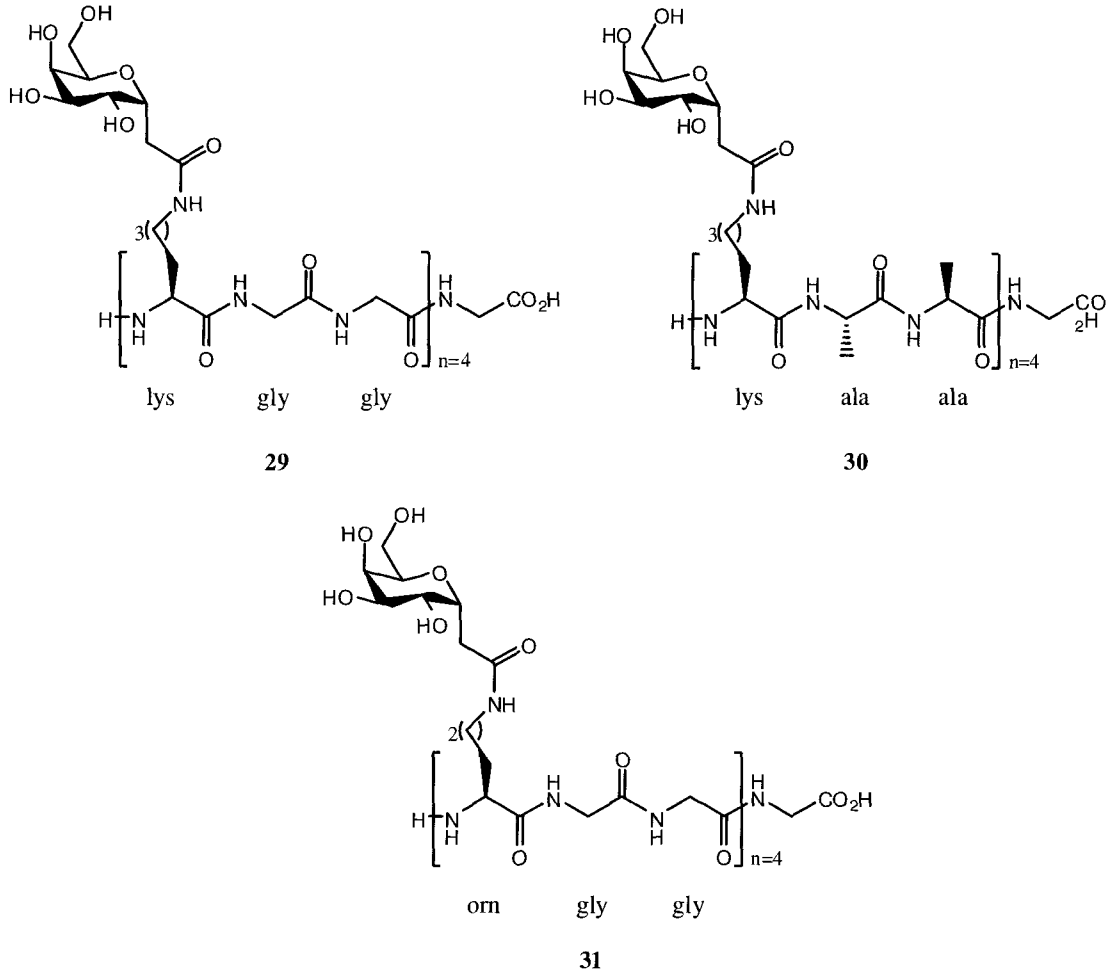

Figure 2.3.3 Second generation *C*-linked AFGP analogues.

Recently, third generation analogues have been synthesized in our lab with interesting results (**Figure 2.3.4**). These analogues possess an all carbon linker (no amide bond) between the sugar and the polypeptide backbone. *C*-serine analogue **34** exhibited greater recrystallization inhibition (RI) activity than our $[OGG]_4[Gal]$ benchmark **31** (**Graph 2.3**, pg. 46). Furthermore, **34** displays comparable RI activity to AFGP8. Curiously, analogues **32** and **33** exhibited no RI activity. The lack of recrystallization inhibition activity in **32** and **33** may be due solely to the length of the linker, or may be due to enhanced flexibility of the longer side chains in **32** and **33**. Further study on the linker is required to establish the importance of rigidity in this region.

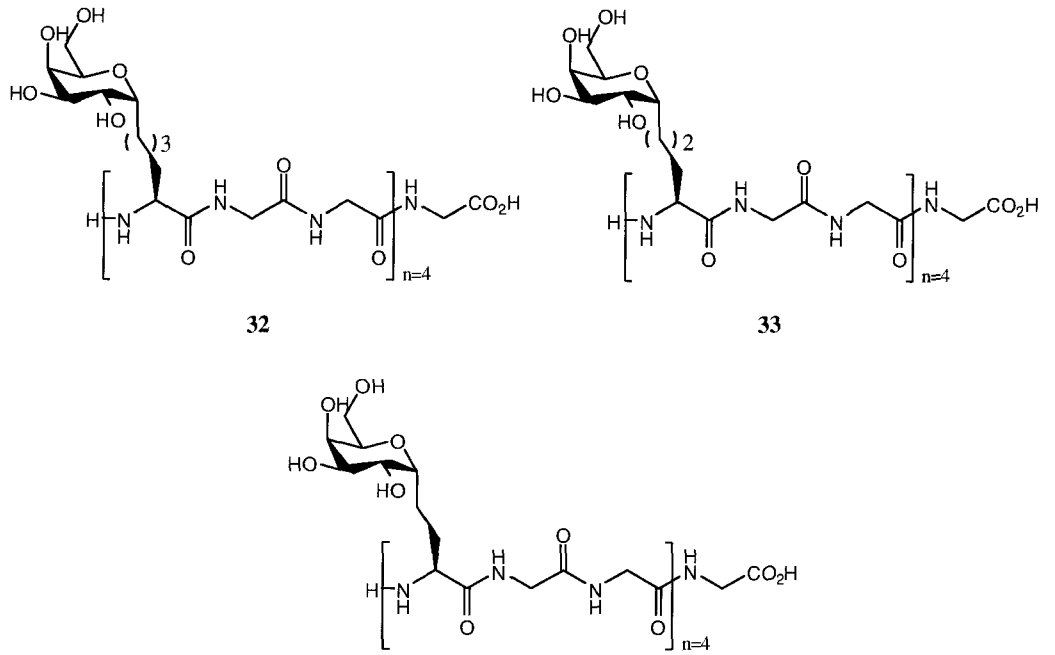

Figure 2.3.4 Third generation *C*-linked AFGP analogues.

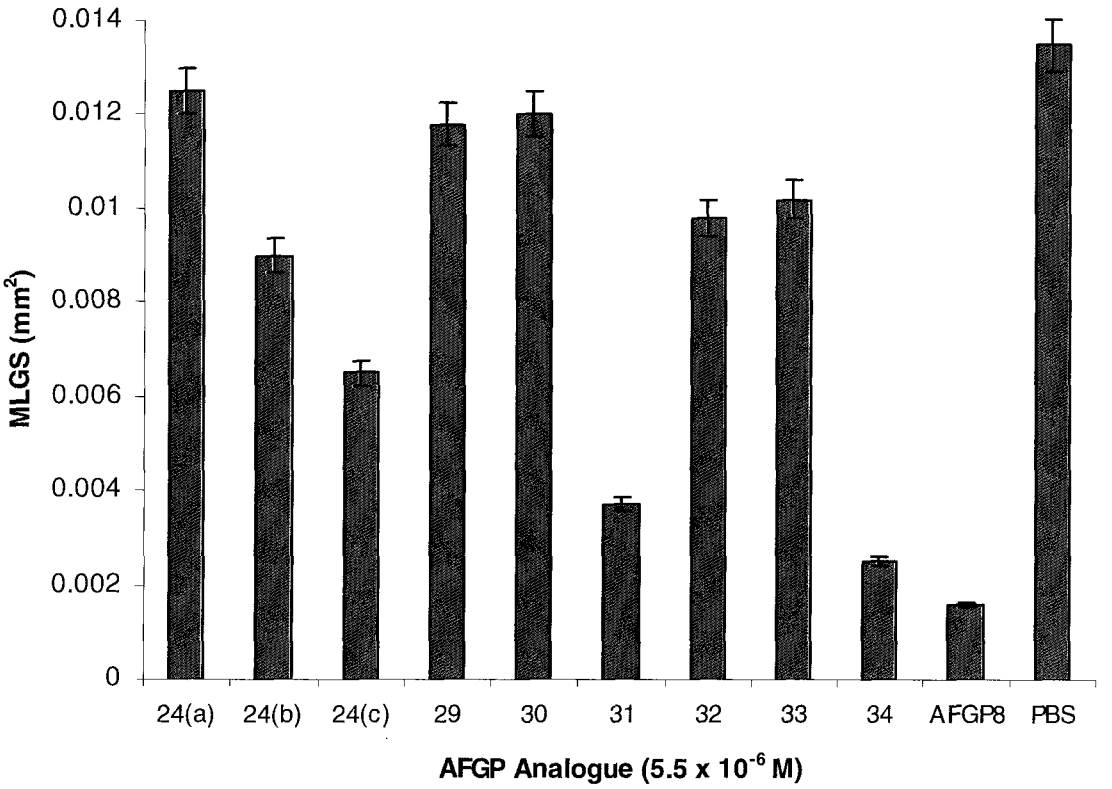

Graph 2.3 RI activity of AFGP analogues measured by mean largest grain size.

2.4 Goals and Objectives

Results from our second generation analogues suggest that there may be a specific linker configuration for optimal RI activity, while third generation analogues suggest that an all carbon linker is a suitable replacement for the *O*-linkage in native AFGP8.

An important question which has yet to be answered is the role of the amide bond in our $[OGG]_4$[Gal] analogue **31**. Since our third generation analogues indicate that activity can be retained with a linker consisting strictly of methylene units, the possibility of an all carbon ornithine analogue intrigued us.

In order to elucidate the function of the amide bond in **31**, we proposed the synthesis of **35,** an $[OGG]_4$[Gal] analogue possessing an internal olefin (**Figure 2.4.1**). This amide isostere would help to uncover the role of the amide moiety in the RI activity of $[OGG]_4$[Gal]. An isostere is a mimic of a parallel functional group/compound. The amide bond in **31** exhibits partial double bond character (*trans*) and thus, an analogue with an internal *trans*-double bond would serve as a mimic. Observation of RI activity in **35** would indicate whether the antifreeze activity expressed by **31** is due to the rigidity imparted by the amide bond, or perhaps due to some other phenomenon. The partial double bond character of the amide in **31** may limit the extent of free rotation of the carbohydrate moiety and consequently stabilize it in certain orientations, maximizing carbohydrate-ice interactions. Another possible explanation for the function of the amide bond in **31** is hydrogen bonding directly with the ice lattice itself, or perhaps with the sugar hydroxyls.

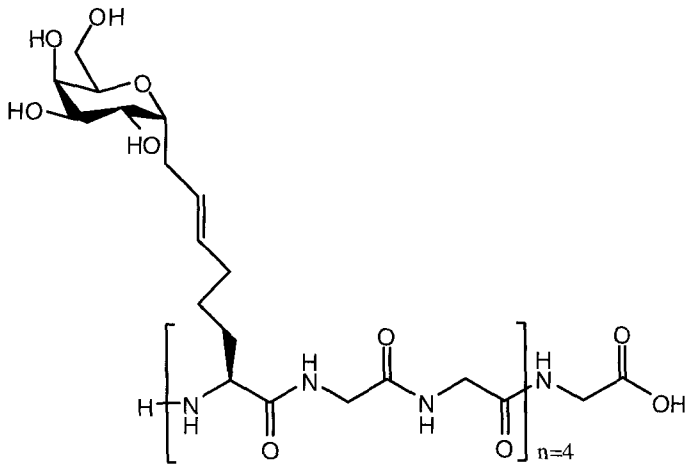

35

Figure 2.4.1 *C*-linked AFGP analogue containing an all carbon backbone and an internal olefin as an amide isostere.

In order to discern the role of the amide bond in the recrystallization inhibition activity of **31**, we decided to synthesize **35** according to **Scheme 2.4.1**. Our strategy consists of the solid phase peptide synthesis of the N-terminus protected building block **36**. We hypothesized that the building block could be obtained from the ring opening and subsequent Corey-Schmidt[22] oxidation of **37**. We envisioned synthesis of glycoconjugate **37** via a Wittig reaction[23] of the benzyl protected phosphonium salt of D-galactose **38** with chiral aldehyde **39**. The chiral aldehyde was envisaged via coupling of a 2 carbon linker **40** with chiral oxazolidin-2-one **41**. The chiral reagent can be obtained from L-serine via the approach described by Sibi and Renhowe.[24]

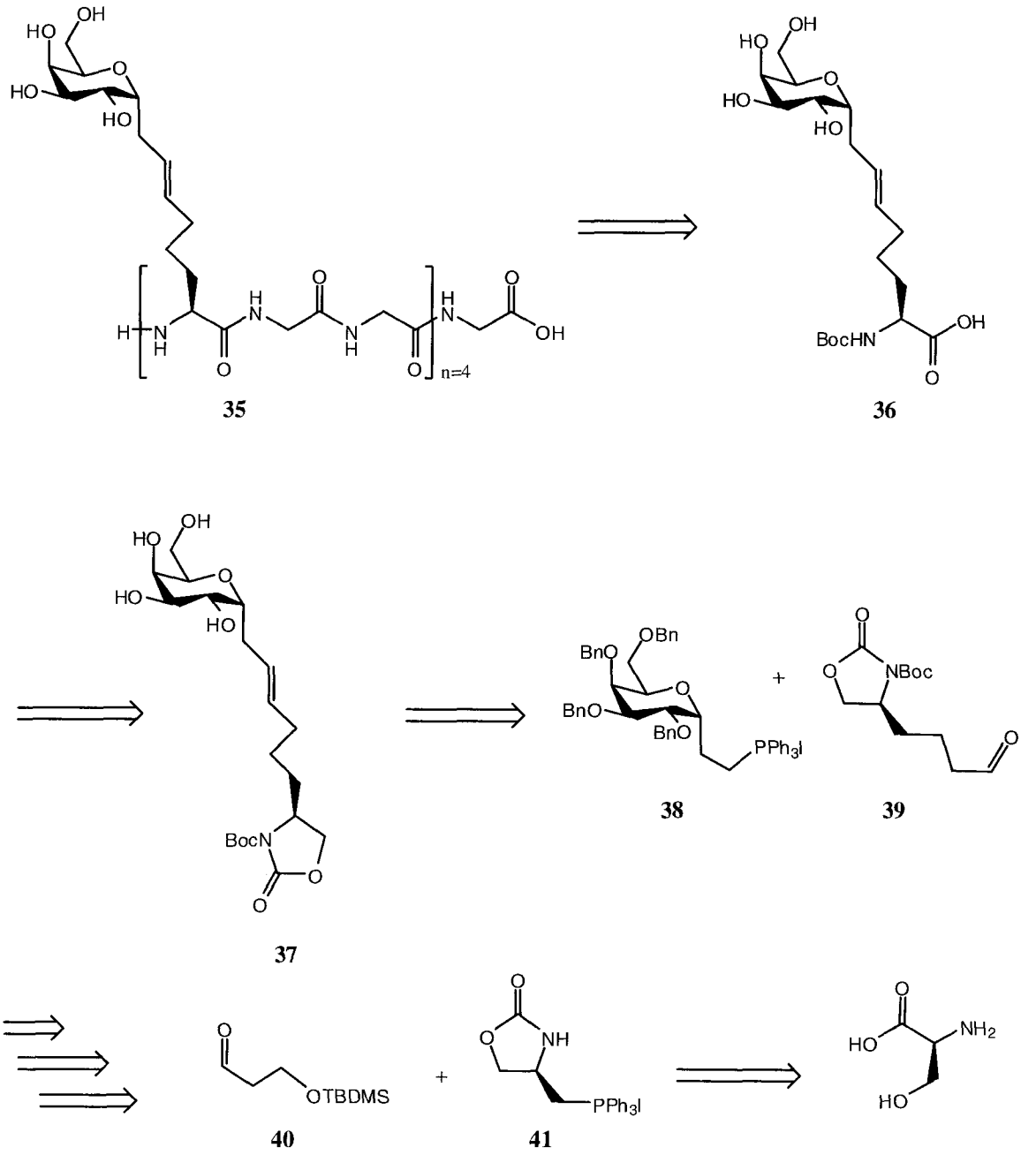

35 36 37 38 39 40 41

Scheme 2.4.1 Retrosynthetic analysis of AFGP analogue **35**.

References:

1. McKown, R.L. and Warren G. J. *Cryobiology.* **1991**. 28, 474-482.

2. Warren, G.J., Hague, C.M., Corroto, L.V. and Mueller, G. M. *FEBS Letters.* **1993.** 321, 116-120.

3. Driedonks, R.A., Toschka, H.Y. van Almkerk, J.W, Schäffers and Verbakel, J.M.A. *Yeast.* **1995.** 11(9), 849-864.

4. Anisuzzaman, A.K.M., Navia, J.L. and Anderson, L. *Carbohydr. Res.* **1988.** 174, 265-278.

5. Meldal, M. and Jensen, K.J. J. *Chem. Soc. Chem. Commun.* **1990.** 483-485.

6. Maeji, N.J., Inoue, Y. and Chujo, R. *Carbohydr. Res.* **1986.** 146, 174-176.

7. Rocchi, R., Peggion, E., Mammi, S., Foffani, M.T., Scolaro, B., Biondi, L. and Filira, F. *Int. J. Biol. Macromol.* **1990.** 12, 41-49.

8. Tsuda, T. and Nishimura, S.I. *Chem. Commun.* **1996**. 2779-2780.

9. Tseng, P.H., Jiaang, W.T., Chang, M.Y., and Chen, S.T. *Chem. Eur. J.* **2001.** 7, 585-590.

10. Marcaurelle, L.A. and Bertozzi, C.R., *Chem. Eur. J.* **1999.** 5, 1384-1390.

11. Eniade, A.A., Hauer, L. and Ben, R.N. *Org. Lett.* **1999.** 1, 1759-1762.

12. Ben, R.N. *Chem Biochem.* **2001.** 2, 161-166.

13. Marcaurelle, L.A., and Bertozzi, C.R. *Chem. Eur. J.* **1999.** 5, 1384-1390.

14. Kishi, Y. *Pure Appl. Chem.* **1993.** 65, 771-778.

15. Jimenez-Barbero, J., Espinosa, J.F., Asensio, J.L., Canada, F.J. and Poveda, A. *Adv. Carbohydr. Chem. Biochem.* **2001.** 56, 235.

16. Wei, A., Boy, K.M. and Kishi, Y. *J. Am. Chem. Soc.* **1995.** 117, 9432-9436.

17. Ravishankar, R., Surolia, A., Vijayan, M., Lim, S. and Kishi, Y. *J. Am. Chem. Soc.* **1998.** 120, 11297-11303.

18. Komatsu, S.K., DeVries, A.L., and Feeney, R.E. *J. Biol. Chem.* **1970.** 245, 2909-2913.

19. Tachibana, Y., Fletcher, G.L., Fujitani, N., Tsuda, S., Monde, K. and Nishimura, S. *Angew. Chem. Int. Ed.* **2004**. 43, 856-862.

20. Eniade, A., Puroshotham, M., Wang, J.B., Horwath, K. and Ben, R.N. *Cell Biochem. and Biophys.* **2003.** 38, 115.

21. Eniade, A.A., Hauer, L. and Ben, R.N. *Org. Lett.* **1999.** 1, 1759-1762.

22. Corey, E.J. and Schmidt, G. *Tetrahedron Lett.* **1979.** 20, 399.

23. Wittig, G. and Schöllkopf, U. *Chemische Berichte*. **1954.** 87, 1318.

24. Sibi, M.P. and Renhowe, P.A. *Tet. Lett.* **1990.** 31(51), 7407-7410.

Chapter 3

Preparation of *C*-Linked AFGPs

3.1 Original Approach to *C*-Linked [OGG]$_4$[Gal] Olefin Building Block

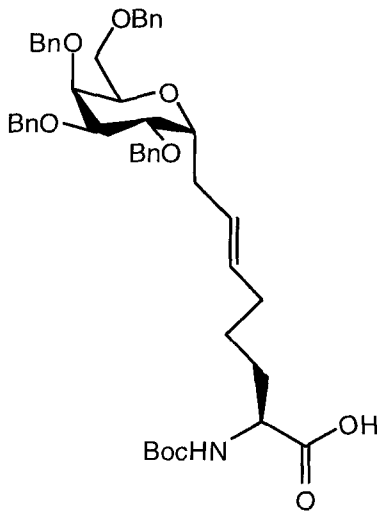

1

Figure 3.1 Structure of *C*-linked [OGG]$_4$[Gal] olefin monomer.

An important structural feature of our building block is the presence of an internal *trans*-double bond. The significance of the double bond has been highlighted in the previous section. This amide isostere can be incorporated using a number of synthetic strategies such as the Peterson Reaction,[1] the Julia Olefination,[2,3] Olefin Cross Metathesis[4,5,6] and the Wittig Reaction.[7,8,9] Synthesis of **1** via the Peterson Reaction would require a preassembled glycoconjugate tethered to a β-hydroxysilane. There is no readily accessible route to such a compound. Furthermore, removal of sugar protecting groups such as benzyl ethers by reducing metals employed in a typical Julia Olefination make this approach unfavourable.[10] Finally, problems associated with cross-product selectivity, including the presence of homo-coupled products make olefin cross metathesis a poor choice towards the synthesis of **1**.

Our original approach towards the synthesis of **1** was based upon Bertozzi and Bednarksi's synthesis of a *C*-glycosyl analog of β-Galactose-*O*-Serine **2**.[11] This strategy employed the Wittig reaction of benzyl protected D-galactose aldehyde **4** and a phosphonium salt derived from L-serine **5**. The β-stereochemistry at the anomeric center of **2** is due to the aldehyde,[11] while the L-stereochemistry of the α-amino acid component of **2** arises from the Wittig reagent.[12] The key step involved coupling of aldehyde **4** with the ylide generated from phosphonium salt **5** to afford **3** in 34 % yield, and a 15:1 *trans/cis* mixture of olefins. Reduction of the double bond, followed by ring opening, Fmoc protection and Jones oxidation furnished **2** (49 % from **3**). Considering the structural similarity of our target with glycoconjugate **2**, we decided to adopt this approach.

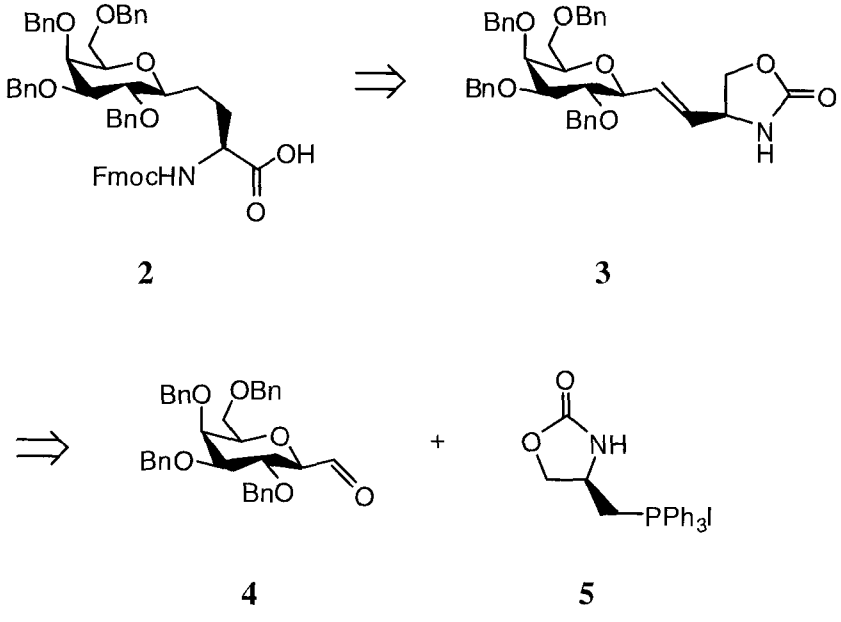

Scheme 3.1.1 Bertozzi and Bednarski's[11] approach to *C*-glycosyl analog of β-Gal-*O*-Ser **2**.

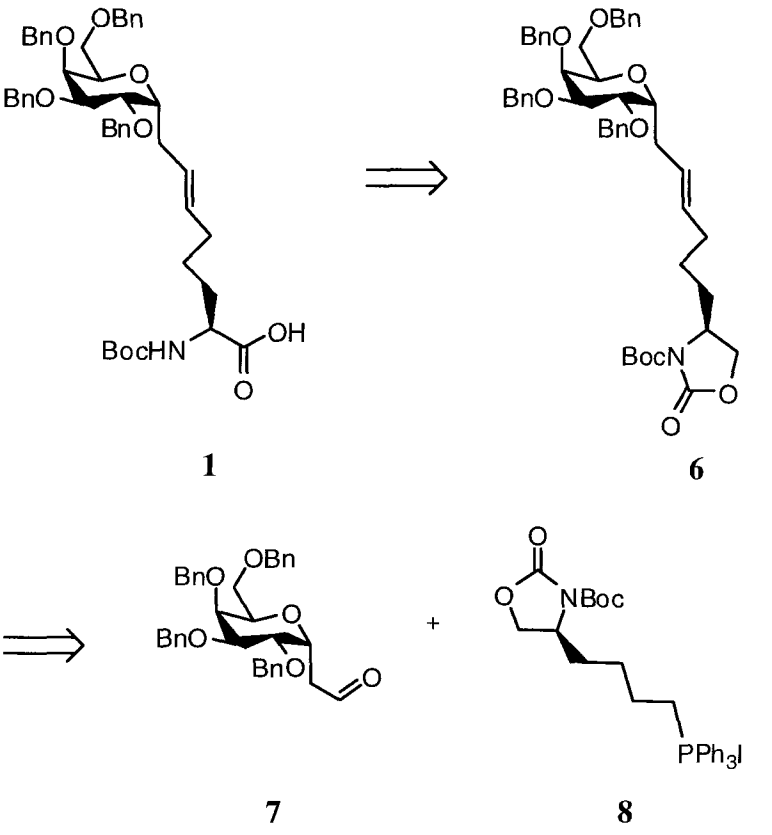

Scheme 3.1.2 Retrosynthetic analysis of our first approach to *C*-linked $[OGG]_4[Gal]$ building block with an internal double bond **1**.

The retrosynthesis of our approach to **1** is described in **Scheme 3.1.2** and is based upon a Wittig reaction of aldehyde **7** with the ylide generated from phosphonium salt **8**.

3.2 Preparation of Carbohydrate Coupling Partner 7

The requisite aldehyde was synthesized according to previously established protocols in our lab.[13] This involved bromination of commercially available β-D-galactose pentacetate **9** with HBr in acetic acid. The resulting α-bromo-pyranose **10** was obtained in 98 % yield (**Scheme 3.2.1 i**). The α-stereochemistry of the bromo sugar arises from nucleophilic attack of the bromide anion on the oxocarbenium intermediate. Although both epimers are possible, the α-product is preferred[14, 15] Overlap of the antiperiplanar oxygen lone pair with the σ*C-Br orbital stabilizes the α-anomer. (**Scheme 3.2.1 ii**).

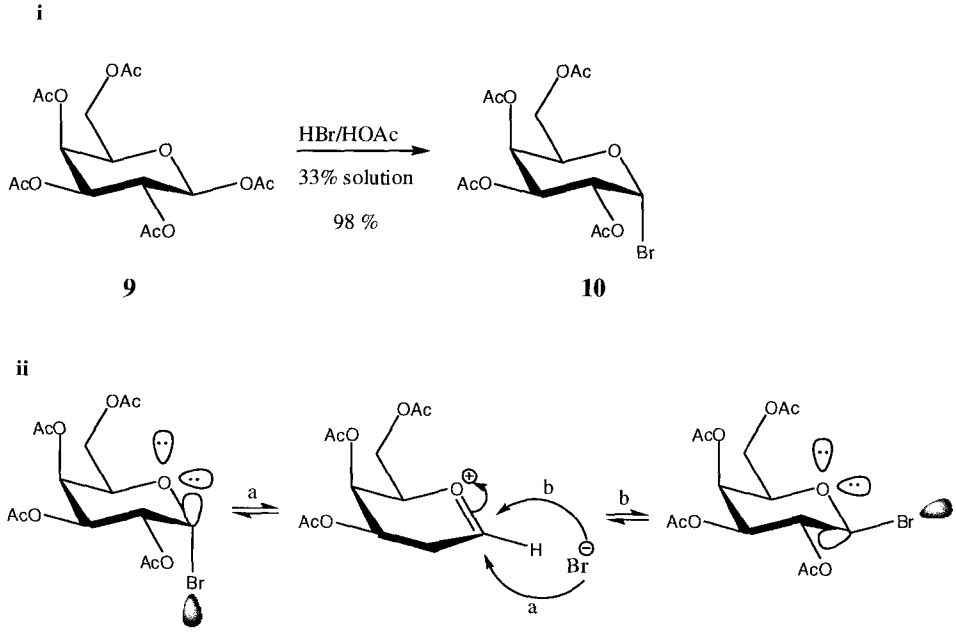

Scheme 3.2.1 i) Bromination of β-D-galactose pentacetate **9** to afford α-D-bromo galactose tetratacetate **10. ii)** Preference of the α-anomer due to the anomeric effect.[14, 15]

α-Allyl-D-galactose tetratacetate **11** was generated from the reaction of allyl reagents with anomeric glycosyl radical precursors. The labile C-Br bond is ideal for homolytic cleavage, resulting in the generation of stable anomeric radicals.[16] According to the protocol established by Magnusson,[17] photochemical mediated allylation of α-bromo- D-galactose tetracetate was achieved with stoichiometric quantites of bis-tributyl tin and phenyl allyl sulfone to afford exclusively α-allyl-D-galactose tetracetate in 88 % yield (**Scheme 3.2.2**).

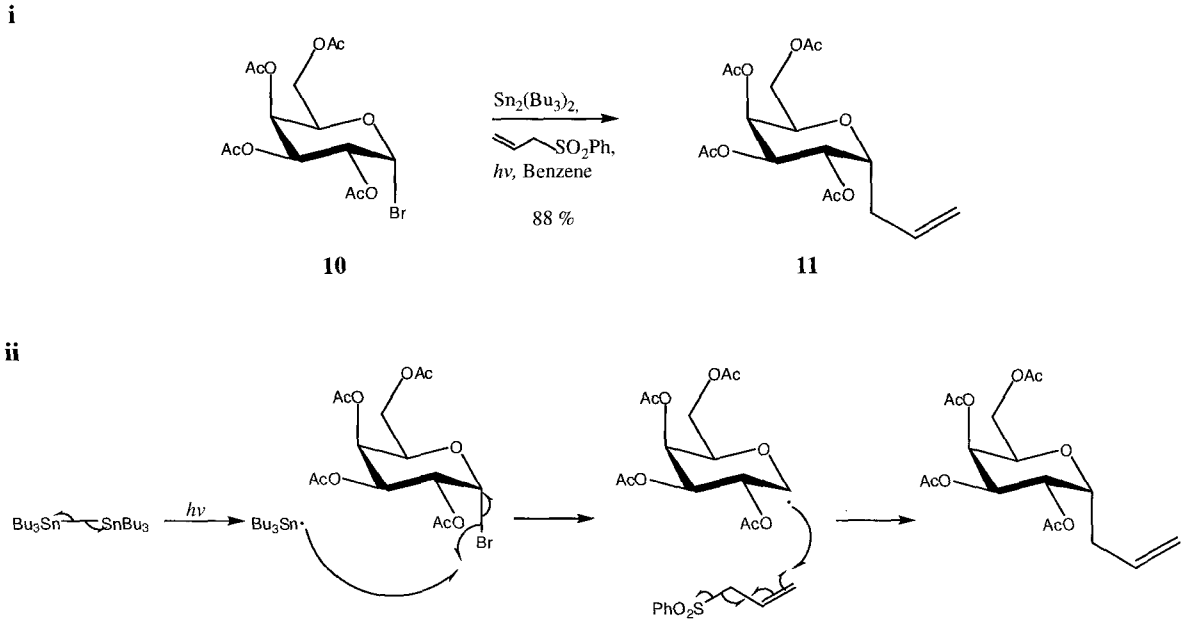

Scheme 3.2.2 Allylation of α-bromo-galactose tetracetate

Deprotection of the monosaccharide with NaOMe in methanol was achieved cleanly and quantitatively to afford **12**. Treatment of **12** with NaH, followed by addition of BnBr via cannula furnished benzyl protected allyl sugar **13** in 85 % yield. The choice of benzyl protecting groups for the carbohydrate component was predicated upon the incompatibility of acetate protecting groups with standard Wittig conditions.

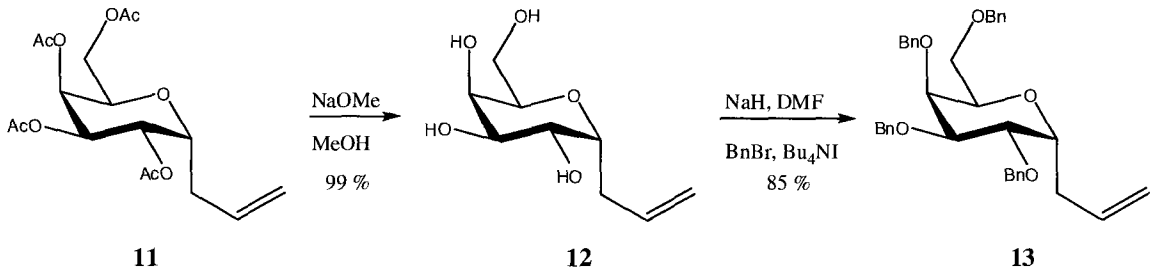

11 12 13

Scheme 3.2.3 Deprotection and reprotection to furnish **13**.

Benzyl protected α-*C*-allyl-D-galactose was subject to ozonolysis in dicholoromethane followed by reductive workup with triphenylphosphine. However, the reaction did not proceed cleanly (**Scheme 3.2.4**). In addition to the desired aldehyde, a mixture of unidentifiable aldehydes were also produced, ostensibly due to overoxidation. Integration of the ^{1}H NMR (9-10 ppm region) indicated the presence of numerous aldehydes. Attempts at separation and purification via flash chromatography and glass backed analytical TLC proved fruitless.

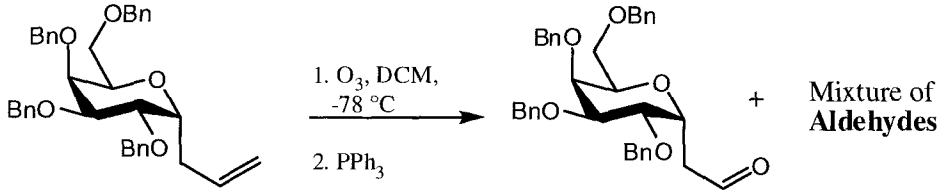

13 7

Scheme 3.2.4 Ozonolysis of olefin **13**

A possible explanation for the formation of byproducts in such reactions has been proposed by Defaye and Utille. They reported the mild deprotection of benzyl ethers in the presence of ozone. [18] Cleavage of benzyl ethers via ozonolysis was observed for benzyl protected methyl D-glucopyranosides, yielding the corresponding alcohols.

Defaye and Utille suggested that debenzylation involves insertion of ozone into the methylene bond of benzyl ethers, followed by decomposition and the formation of alcohol/polyol species (**Scheme 3.2.5 i**).

An alternate explanation may involve anomeric epimerization. Zou and coworkers reported the epimerization of 2'-carbonyl-α-*C*-glycopyranosides (including **7**) to their corresponding β-anomers[19] via treatment with 4 % NaOMe. Epimerization occurs via an acyclic α,β-unsaturated aldehyde formed from enolization of the sugar and subsequent β-elimination, followed by ring closure through an intramolecular 1,4-addition (**Scheme 3.2.5 ii**). Scala and Byram have reported similar results.[20, 21]

i

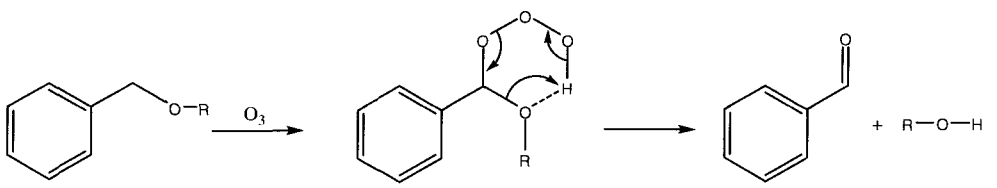

ii

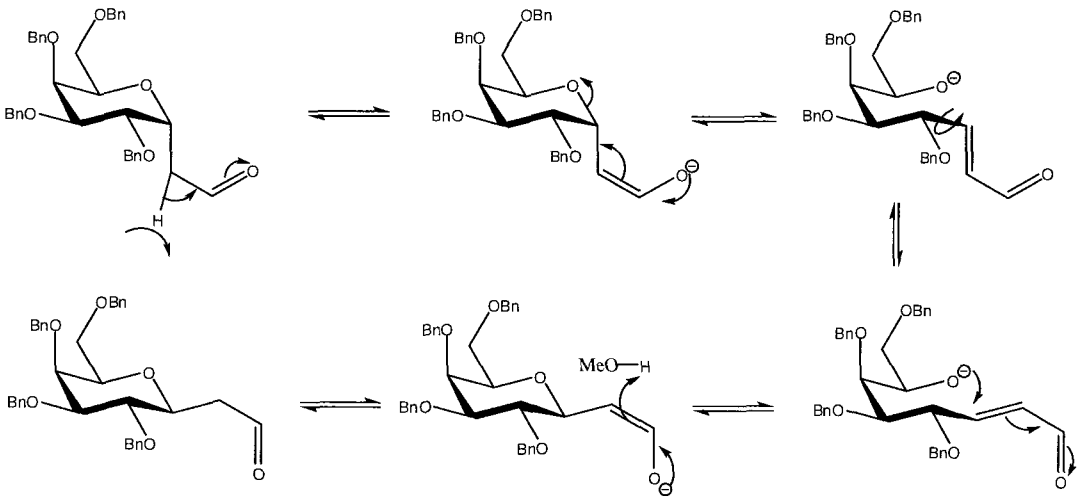

Scheme 3.2.5 i) Cleavage of benzyl ether protecting groups by ozone and **ii**) epimerization of 2-(2,3,4,6-Tetra-*O*-benzyl-α-D-galactopyranosyl)-ethyl aldehyde with 4 % NaOMe.

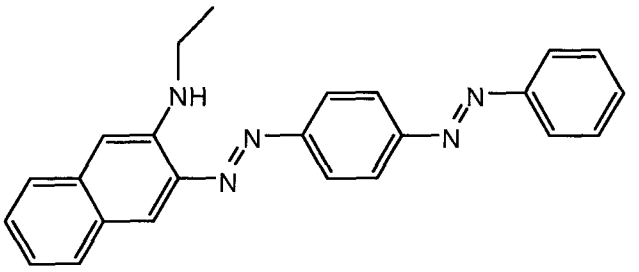

Figure 3.2 Structure of Sudan Red 7B

In order to overcome the problem of over oxidation during ozonolysis we decided to use the azo-dye Sudan Red 7B (**Figure 3.2**) as an indicator. The colourimetric change of a Sudan Red-aldehyde solution is indicative of excess ozone and therefore completion of ozonolysis. Using the indicator Sudan Red 7B, aldehyde **7** was obtained cleanly in near quantitative yield (**Scheme 3.2.6**).

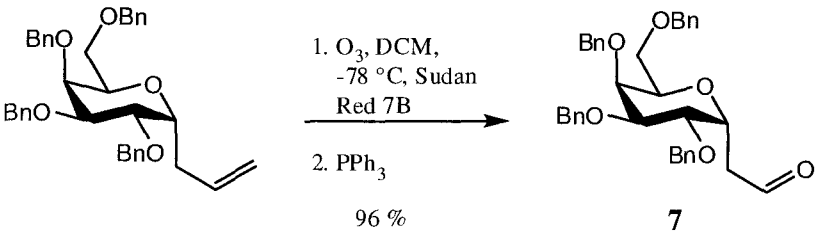

Scheme 3.2.6 Ozonolysis in the presence of Sudan Red 7B.

3.3 Preparation of Amino Acid Coupling Partner 8

The next step in our synthesis of building block **1** was construction of the amino acid moiety **8**. We envisioned **8** via Wittig reaction of silyl protected aldehyde **15** and the ylide generated from chiral phosphonium salt **16**. The chiral phosphonium salt is accessible from commercially available L-serine **17**.

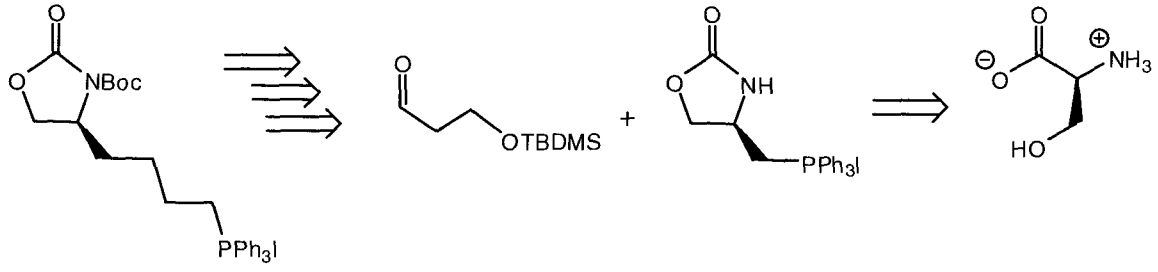

8 **15** **16** **17**

Scheme 3.3.1 Retrosynthesis of amino acid component.

The synthesis of **16** has been previously described by Sibi and Renhowe.[12] The key step in the synthesis of this Wittig reagent was oxazoldinone ring formation from **17**. In order to achieve this, Sibi and Renhowe combined L-serine methyl ester hydrochloride with phosgene (20% solution in toluene) in the presence of aqueous potassium carbonate. We attempted ring closure using alternatives to phosgene. The results are summarized in **Table 3.3**.

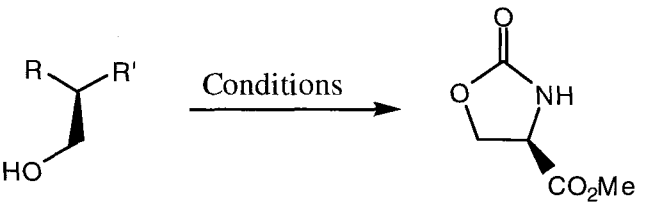

18

Entry	R	R'	Conditions	Yield (%)
1	CO_2Me	NH_2HCl	Et_2CO, aq K_2CO_3, 0°C, 3 hrs	0
2	CO_2Me	NH_2HCl	Et_2CO, aq K_2CO_3, 0°C/140 °C, 3 hrs	0
3	CO_2Me	NH_2HCl	$(CCl_3)_2CO$, aq K_2CO_3, 0°C, 3 hrs	0
4	CO_2Me	NH_2HCl	$(CCl_3)_2CO$, aq K_2CO_3, THF, 0°C, 3 hrs	0
5	CO_2Me	NH_2HCl	$(CCl_3)_2CO$, aq K_2CO_3, THF/Tol. 0°C, 3hrs	0
6	CO_2^-	NH_3^+	$(CCl_3)_2CO$ in dioxane, 1M NaOH, 0°C, 3 hrs/overnight stirring in MeOH[21]	83

Table 3.3 Conditions for oxazolidinone ring formation.

Our first attempts at ring closure with Et_2CO as a phosgene substitute proved fruitless (Entries **1** and **2**). Only L-serine methyl ester hydrochloride was recovered. This was followed by attempts with solid $(CCl_3)_2CO$ (triphosgene) (Entry **3**), but this also failed to produce acceptable results. Similarly, adjusting the solvent system to a biphasic aqueous/THF system, or an aqueous/THF/Toluene system was also unsuccessful (Entry **4** and **5**). We serendipitously discovered an alternate protocol involving the free amino acid published by Falb and Nudelman.[22] This procedure involved treatment of L-serine in NaOH with triphosgene dissolved in dioxane, followed by stirring overnight in methanol. This was successful, furnishing **18** as yellow oil in 83 % yield. The product was identical

(^{1}H NMR, ^{13}C NMR, mass spectrum, IR, and boiling point) to previous reports by Sibi and Renhowe.

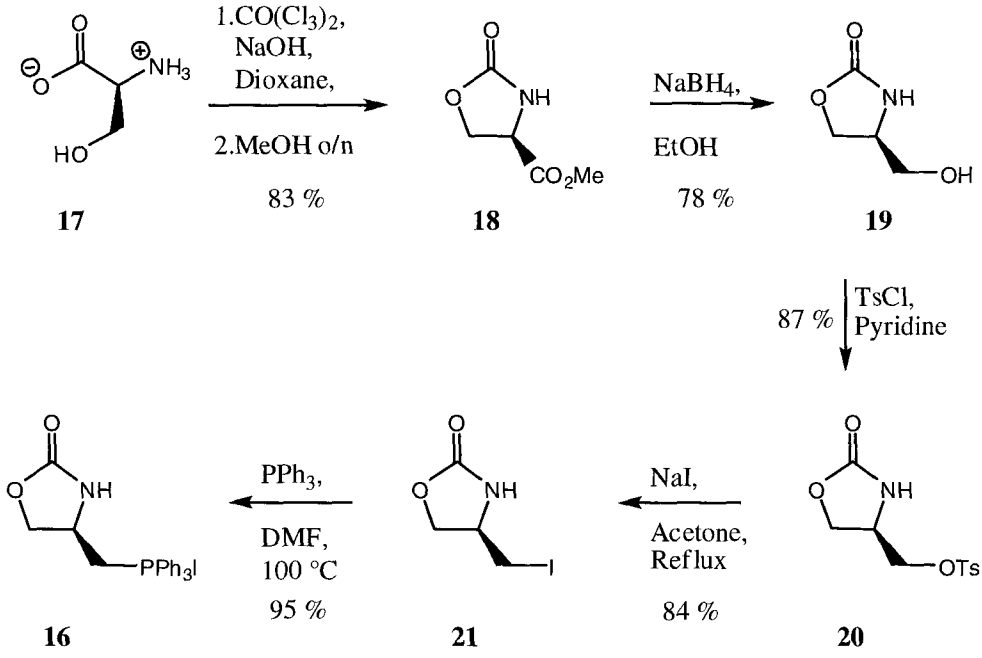

Scheme 3.3.2 Synthesis of chiral phosphonium salt **16**.

Reduction of the ester with $NaBH_4$ in ethanol followed by tosylation of the primary alcohol furnished **20**. Finklestein reaction of the tosylate with NaI in refluxing acetone yielded iodo auxillary **21**. Displacement of the iodine moiety in an S_N^2 fashion with excess triphenylphosphine afforded Wittig reagent **16**. The phosphonium salt was found to be hygroscopic and was consequently dried in a Kugelrohr and stored under Ar (g) in a dessicator.

Next, we attempted the synthesis of a 2-carbon unit as described by Pirrung and Webste[23] (**Scheme 3.3.3**). Coupling of **16** directly with the aldehyde **7** was not feasible since the product of such a coupling would lack two methylene units in the linker region and therefore would be structurally dissimilar to amide $[OGG]_4[Gal]$. In addition, there is no convenient route directly to **8** or to a synthetic equivalent of **8**. As a result, TBDMS protection of commercially available but-3-en-1-ol furnished the protected olefin **23** in 95 % yield. Ozonolysis of the olefin, followed by reductive workup with dimethyl sulfide afforded the protected aldehyde **24** as a colourless oil. The aldehyde was found to be unstable and was stored under an inert atmosphere at -20 °C.

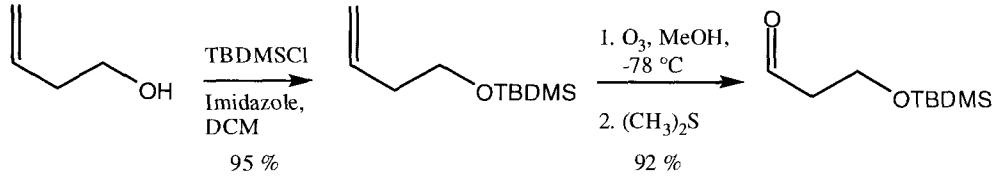

22 **23** **24**

Scheme 3.3.3 Synthetic scheme for the synthesis **24**.

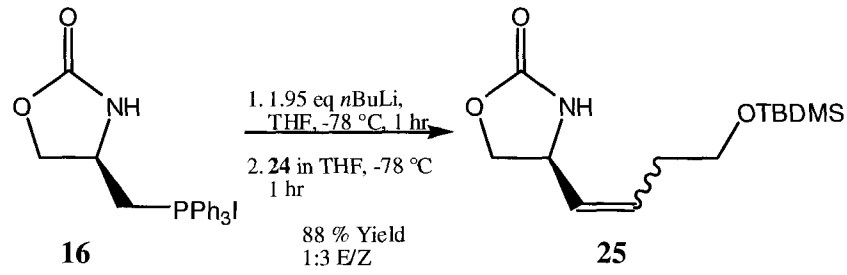

Scheme 3.3.4 Wittig reaction of **16** and **24** to furnish **25** as a mixture of *E/Z* olefins.

Wittig reaction of **16** and **24** proceeded smoothly to afford **25** as a 4:1 mixture of *E/Z* olefins in 88 % yield. Coupling required treatment of the salt with 1.95 equivalents of base. This was performed to ensure double deprotonation of **16**, since the pKa of the amide proton (N<u>H</u>) is approximately 20.6, while the pKa of the α-methylene protons (RC<u>H</u>$_2$PPh$_3$) are approximately 21. Addition of a single equivalent of base would result in competitive deprotonation of N<u>H</u> versus C<u>H</u>$_2$, resulting in a dramatic reduction in yield. In addition, Sibi and Renhowe have theorized that treatment of the salt with a single equivalent of base results in loss of chirality via β-elimination.[24] Bis-deprotonation with 2 equivalents of base precludes β-elimination and therefore prevents racemization (**Scheme 3.3.5**).

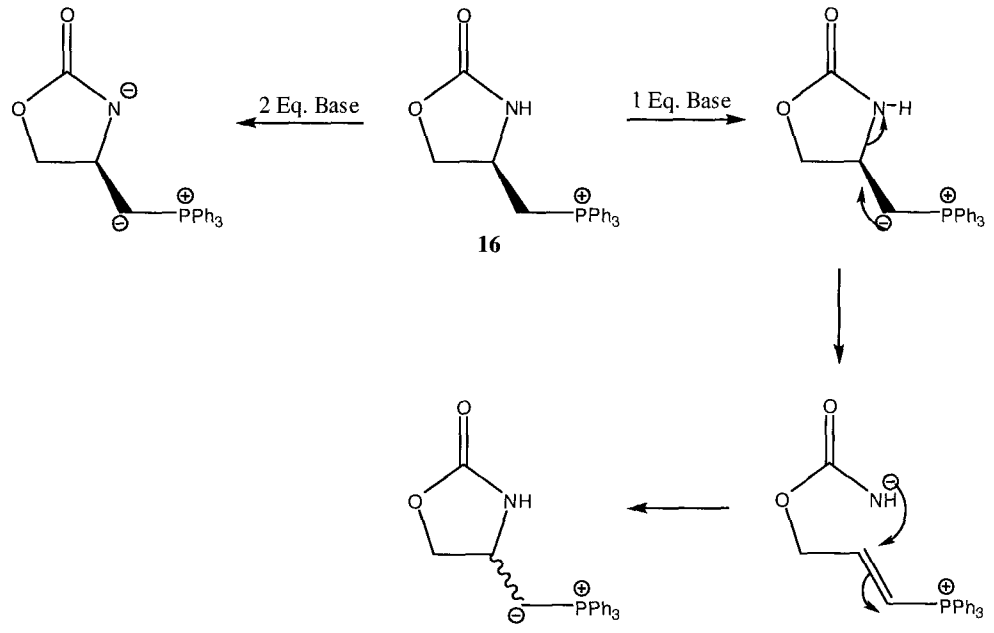

Scheme 3.3.5 Comparison between the use of one and two equivalents of base in the deprotonation of phosphonium salt **16**.

Removal of the silyl protecting group with TBAF furnished the free alcohol **26**. This was followed by catalytic reduction of the double bond with Pd/C and H_2 (g) to afford **27**. We hypothesized that Garreg reaction of **27** would yield iodo auxillary **28** and convenient access to phosphonium salt **29**. However, this was not the case. Instead, starting material (**27**) was recovered in addition to an unexpected polycyclic product. Attempts at tosylation and mesylation of the primary alcohol also proved unsuccessful (**Scheme 3.3.6**).

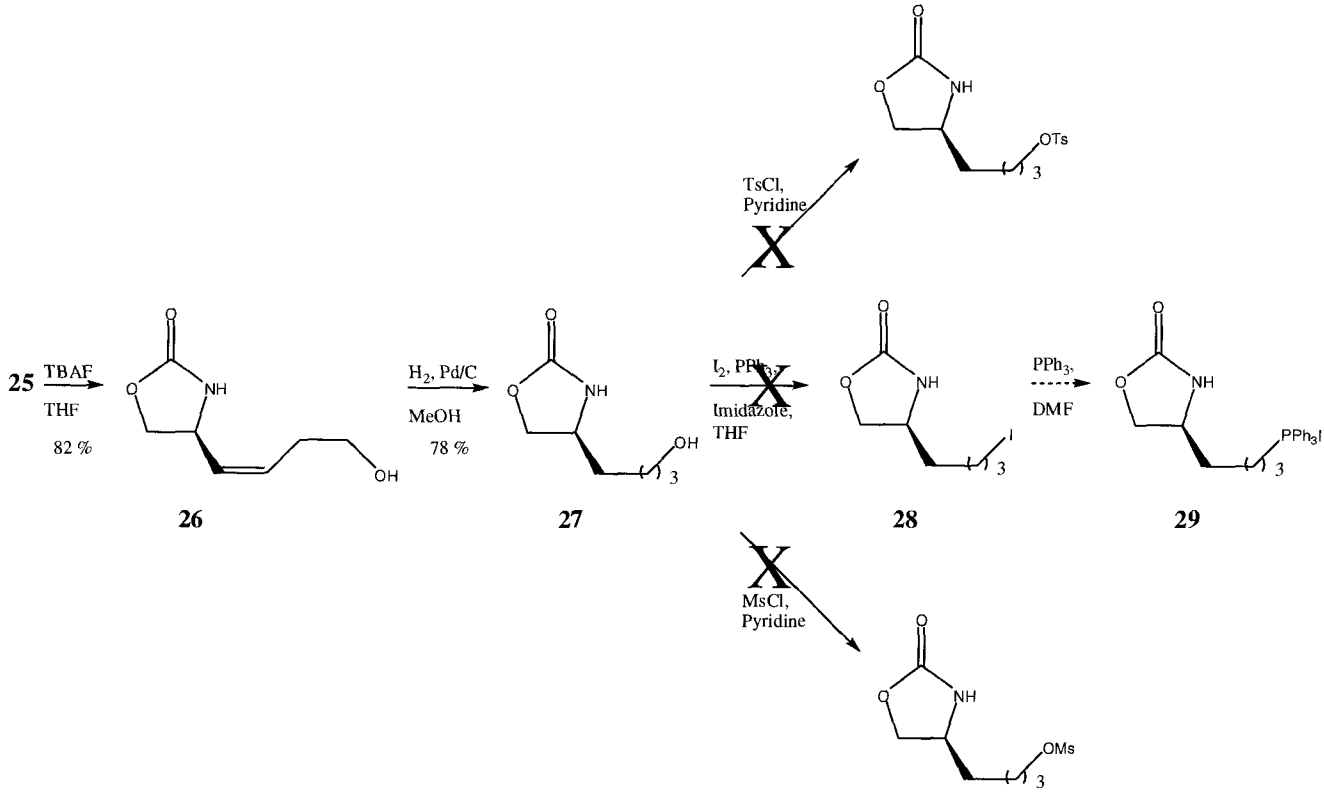

Scheme 3.3.6 Attempts at derivatization of **27** with TsCl, I_2 and MsCl.

We speculated that the unhindered and slightly nucleophilic amide nitrogen in **27** may be responsible for the absence of product. We hypothesized that formation of a 6-membered intramolecular ring, followed by ring opening upon aqueous workup was responsible for the regeneration of starting material and the polycyclic product (**Scheme 3.3.7**).

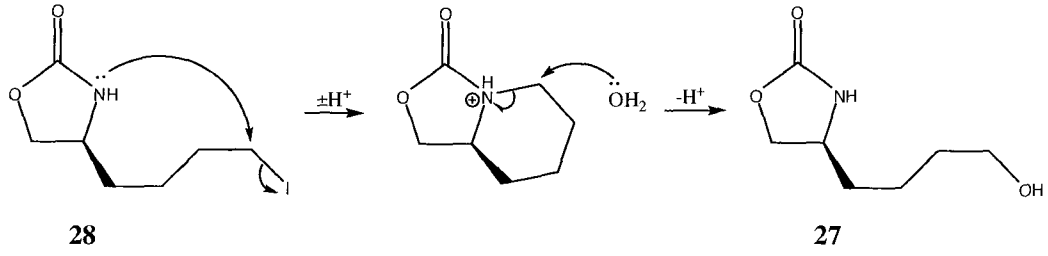

Scheme 3.3.7 Possible mechanism for the regeneration of **27**.

We tested this hypothesis by protecting the amide with di-*tert*-butyl dicarbonate to afford *t*-BOC derivative **30**. This was followed by TBAF mediated silyl deprotection to yield **31** and reduction with Pd/C and H_2 (g) to furnish alcohol **32**. We attempted the Garreg reaction again, but this time with the amide nitrogen protected as a *tert*-butoxy carbonyl functionality. The reaction proceeded smoothly, yielding **33** and supporting our assertion of amide nitrogen involvement. Stirring the primary iodide overnight with excess triphenylphosphine in DMF afforded the second coupling partner, phosphonium salt **8**.

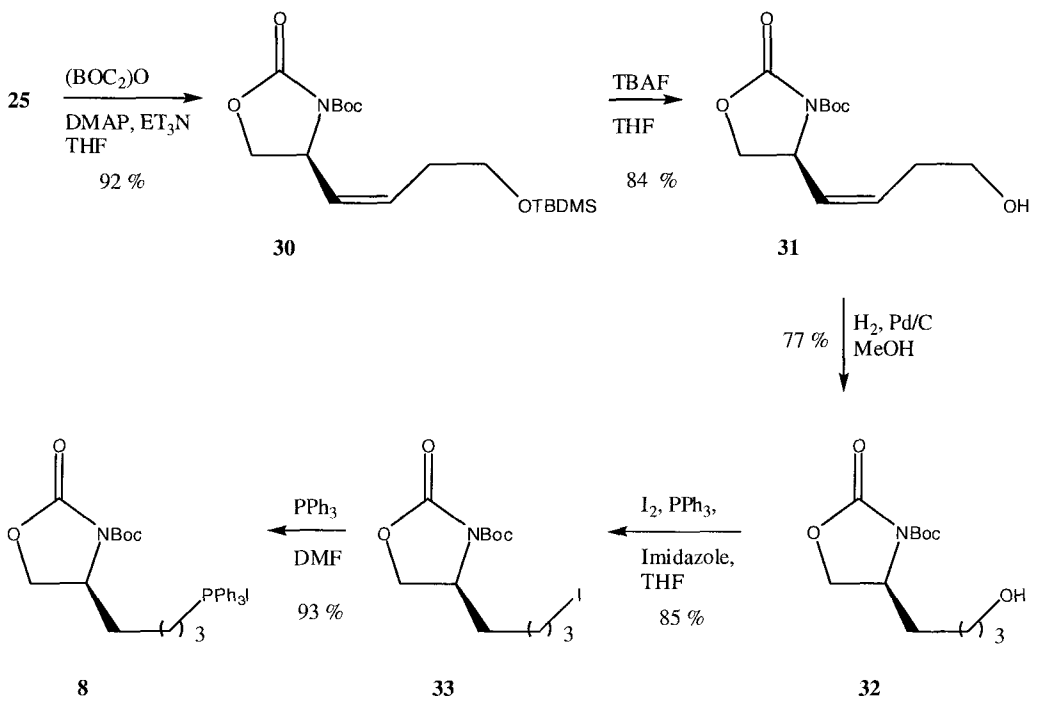

Scheme 3.3.8 Generation of the amino acid coupling partner **8**.

3.4 Coupling of Carbohydrate and Amino Acid Components

With coupling partners **7** and **8** available, we sought to couple the two components using a Wittig reaction (**Scheme 3.4**). Unfortunately, this proved unsuccessful. Initial attempts were made with *n*BuLi and the more hindered tertiary anion, *t*BuLi. In both instances phosphonium salt **8** and aldehyde **7** were recovered quantitatively. In addition, the absence of any triphenylphosphine oxide byproduct indicated that condensation failed to occur. It was unclear precisely why the coupling did not proceed. Possible explanations for the lack of product were speculated to be either; 1) failure to generate the ylide (although unlikely, especially in the presence of strong BuLi bases), or 2) failure to generate the betaine intermediate/oxaphosphetane ring, due to steric hindrance from the bulky benzyl protected aldehyde.

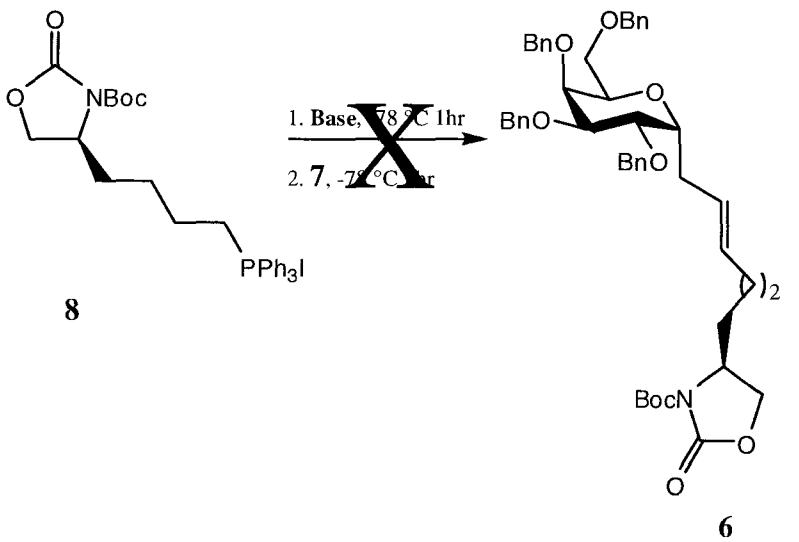

Scheme 3.4 Wittig reaction of aldehyde **7** and salt **8**.

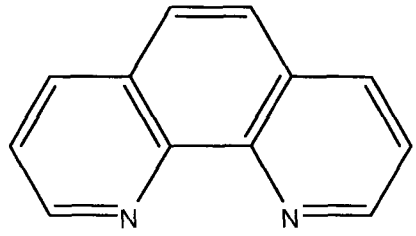

Figure 3.4 Structure of 1, 10-Phenanthroline

We performed a series of test reactions with a well known aldehyde to determine why the reaction failed. Phosphonium salt **8** was treated with a variety of bases and quenched with benzaldehyde. The results are summarized in **Table 3.4**. Attempts at ylide generation with *n*BuLi (**Entry 1**), followed by quench with benzaldehyde proved unsuccessful. The reaction was then performed under the same conditions, but with 1,10-phenanthroline (**Entry 2**). Phenanthroline is an indicator often used in the titration of alklyl lithiums (**Figure 3.4**). The presence of a deep red colour in solutions containing 1,10-phenanthroline is indicative of excess base. We added the indicator to a solution of **8** in THF and added sufficient quantities of *n*BuLi to impart a visible red hue. The solution was stirred for 1 hour at -78 °C and quenched again with benzaldehyde. No product was detected, and only starting materials were recovered. Attempts with *t*BuLi (**Entry 3**), NaH (**Entry 4**), LDA (**Entry 5**) and LiHMDS (**Entry 6**) also proved unsuccessful. In all cases, starting material **8** and benzaldehyde accounted for the mass balance. These results indicated that the problem lay with the phosphonium salt.

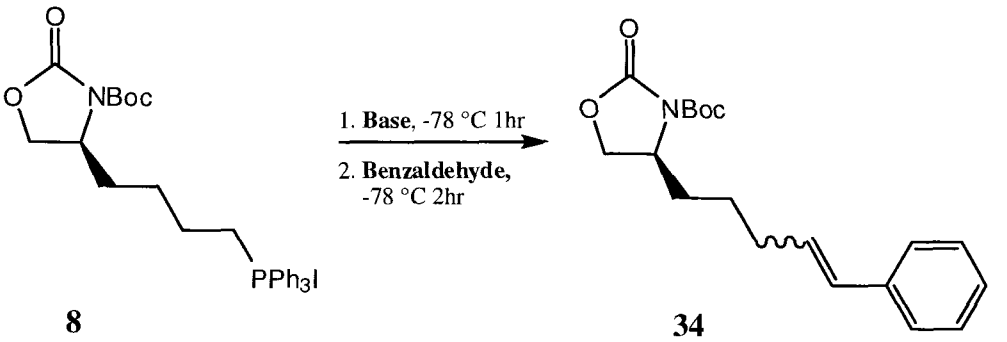

8 **34**

Entry	Base	Yield of 34 (%)
1	*n*BuLi	0*
2	*n*BuLi with 1, 10-Phenanthroline	0*
3	*t*BuLi	0*
4	NaH	0*
5	LDA	0*
6	LiHMDS	0*

*Starting material recovered.

Table 3.4 Test reactions of **8** with Benzaldehyde.

3.5 Revised Approach

Our failure to generate **6**, and our inability to couple **8** with benzaldehyde prompted a change in strategy. It was evident that the difficulty in coupling the two components was due to the amino acid coupling partner. Consequently, we decided to 'switch' coupling partners by converting **8** into its corresponding aldehyde **35,** and **7** into its corresponding phosphonium salt **36** (**Scheme 3.5.1**). This approach was based on the strategy elucidated by Kihlberg and colleagues.[25]

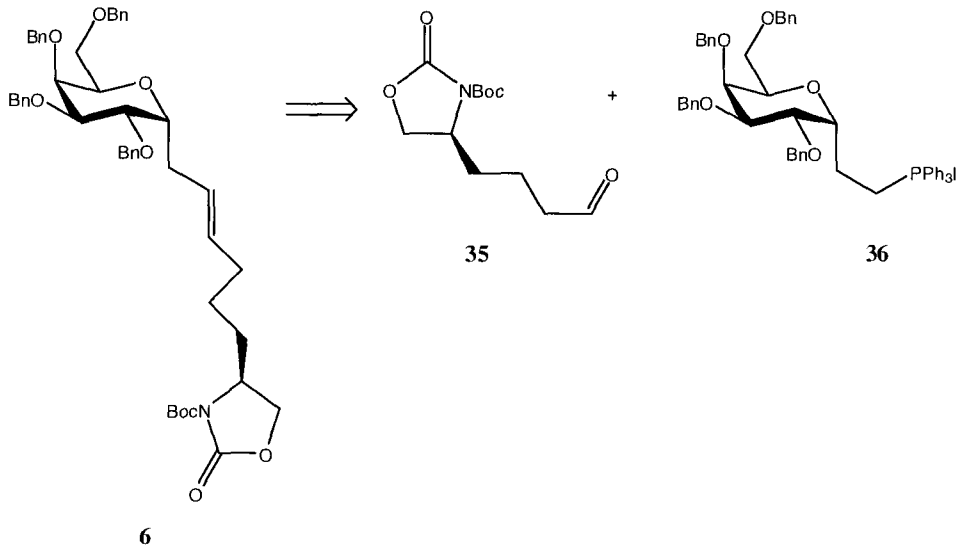

Scheme 3.5.1 Revised approach to olefin **6** involving the 'swap' of coupling partners.

Before implementing the revised approach, we decided to explore the reactivity of **35** to Wittig olefination. Therefore, we attempted oxidation of **31** to its corresponding aldehyde. Swern oxidation cleanly furnished coupling partner **35** in over 90 % yield (**Scheme 3.5.2**).

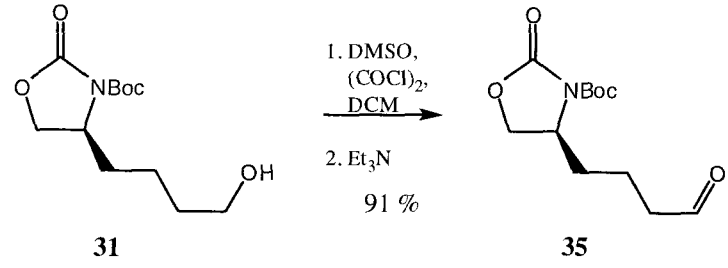

Scheme 3.5.2 Swern oxidation of **31**.

Next, we tried coupling **35** with methyltriphenylphosphonium iodide, **37**. Methyltriphenylphosphonium iodide was readily precipitated from a stirred solution of CH_3I and PPh_3, dried in Kugelrohr and stored under argon in a dessicator until ready for

use. Coupling of **37** and the aldehyde with *n*BuLi was successful, furnishing the monosubstituted olefin **38** in 61 % yield.

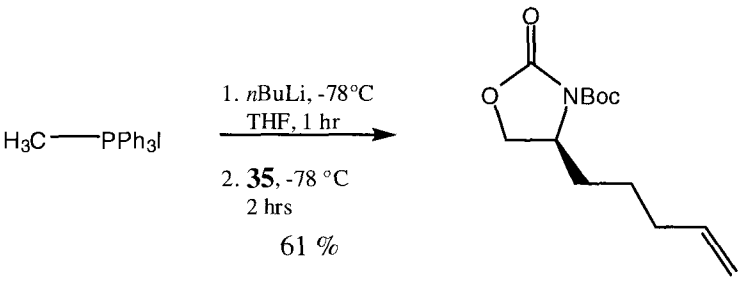

37 **38**

Scheme 3.5.3 Test coupling of aldehyde **35** with methyltriphenylphosphonium iodide.

Encouraged by these results, we sought convenient access to phosphonium salt **36**. With **13** already available, we surmised that the synthetic handle on **13** could be exploited for easy access to the salt. In fact, the precursor to **36**, benzyl protected α-iodoethyl *C*-galactose (**40**), has already been reported from **13** by Nolen and coworkers.[26] Ozonolysis of **13** was performed again, but this time followed by reductive workup with $NaBH_4$ to furnish **39** cleanly and in excellent yield. This was followed by Garreg reaction with PPh_3, I_2 and imidazole according to the procedure described by Nolen to afford iodo sugar **40** in 86 % yield. However, α-iodoethyl *C*-glycosides are prone to forming bicyclic structures with concomitant loss of the *C*2 *O*-benzyl group upon storage for extended periods of time.[26] Therefore, we moved quickly, stirring the iodide in excess PPh_3 overnight to furnish phosphonium salt **36** in quantitative yield.

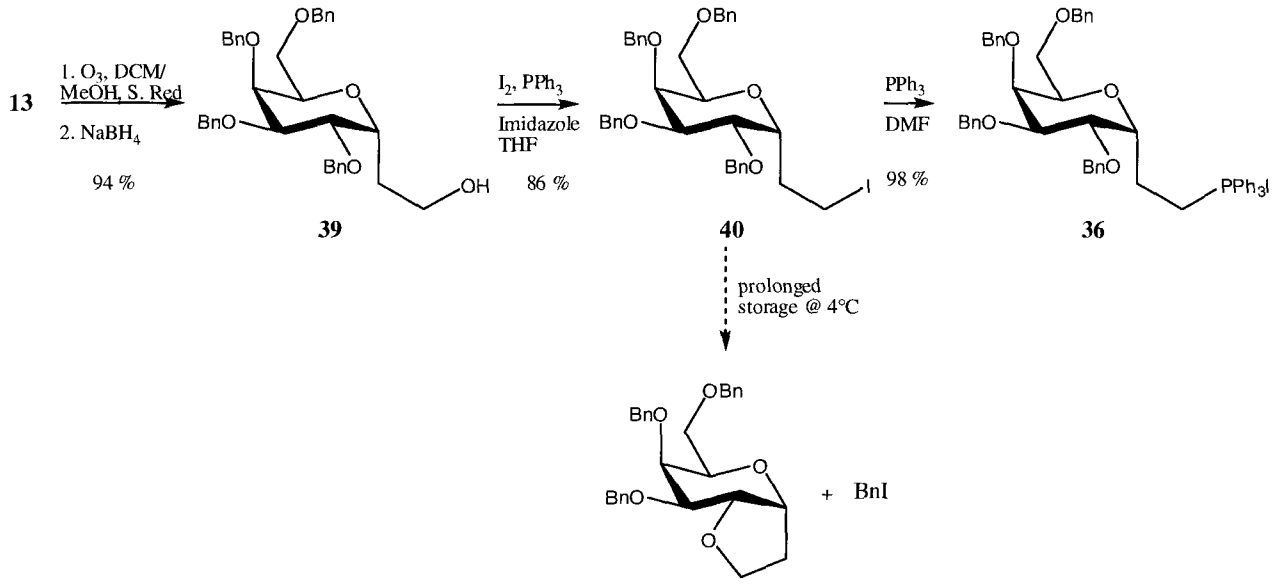

Scheme 3.5.4 Generation of Wittig reagent **36**.

Next, we attempted coupling monosaccharide **36** with amino acid **35** under the same conditions as our previous attempts. This time coupling was successful, yielding **41** as a 1:4 mixture of *E:Z* isomers in 38 % yield. In addition, we obtained the ring opened product **42** in 15 % yield. The *in situ* ring opening of **41** was unexpected.

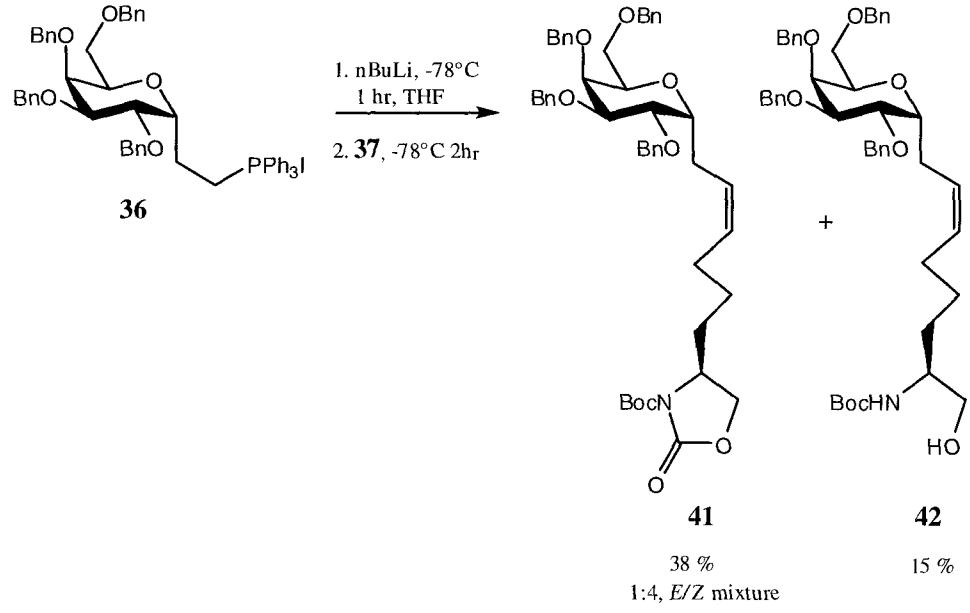

Scheme 3.5.5 Coupling of phosphonium salt **36** with aldehyde **37**.

Although the coupling was successful, our initial target was the *trans* diastereomer. Attempts to photochemically isomerize the olefin with I_2 in chloroform failed. Photochemical isomerization with Ph_2S_2 based upon established protocols was also attempted and proved unsuccessful.[27] In both cases, decomposition of the starting material was observed upon exposure to a 450 W Hg lamp.

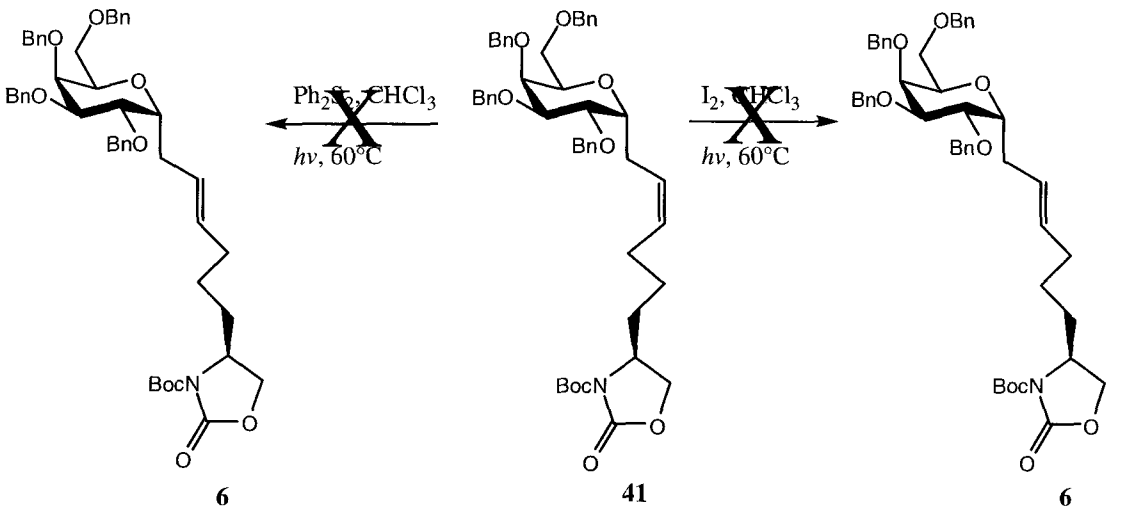

Scheme 3.5.6 Attempts at photochemical isomerization of **41**.

Although the *cis* diastereomer was not what we originally set out to produce, we hypothesized that a *cis* double bond in the linker region would still allow for assessment of the amide functionality on AFGP activity.

Oxazolidinone ring opening with $CsCO_3$ in MeOH afforded **42** in 87 % yield. Numerous approaches were considered for the oxidation of **42** to its corresponding carboxylic acid. Popular single step techniques include chromium based strategies such

as the Jones Oxidation[28] and Corey Schmidt Oxidation.[29] Corey-Schmidt Oxidation with PDC in DMF furnished building block **43** in 78 % yield.

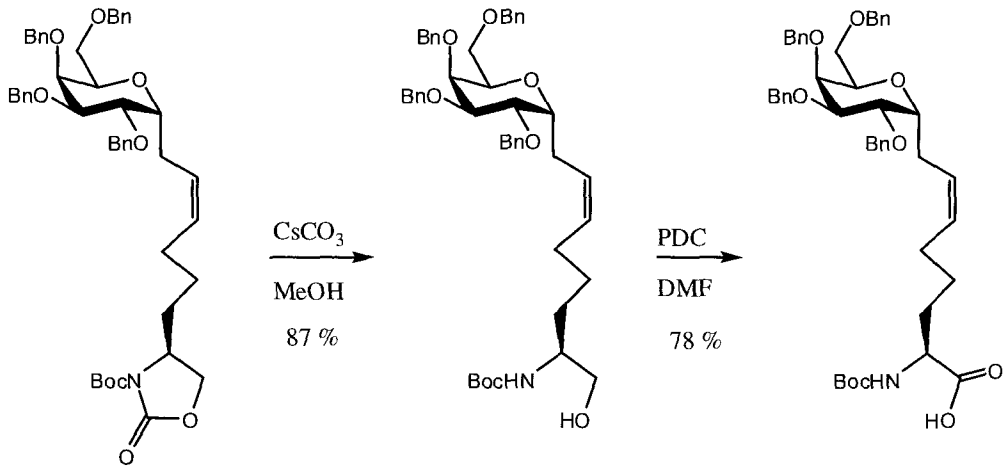

Scheme 3.5.7 Deprotection and oxidation of glyconjugate **41** to afford building block **43**.

3.6 Conclusion

Although we were unable to synthesize exclusively the trans $[OGG]_4[Gal]$ building block we originally planned, we were able to obtain the *Z*-diastereomer by modifying the coupling partners. A *cis*-double bond in the linker region still allows for assessment of amide rigidity on AFGP activity.

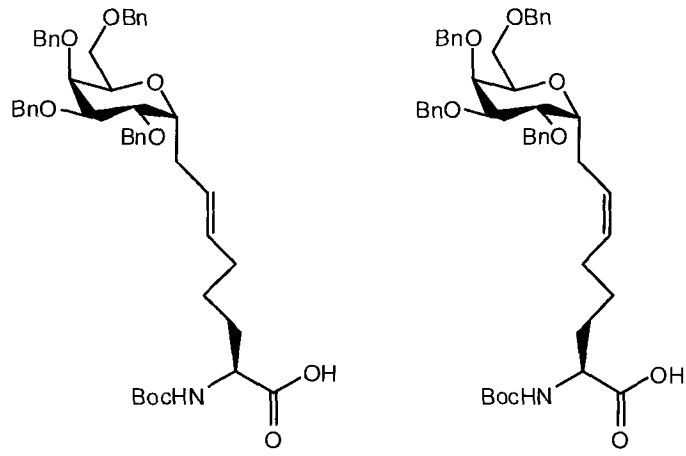

Figure 3.6 Original *trans* target (left), and *cis* isomer actually obtained (right).

3.7 Future work

Solid Phase Peptide Synthesis (SPPS) of the building block according to the approach elucidated by Merrifield[30] is the next step (**Scheme 3.7.1**). SPPS involves immobilization of the substrate on an insoluble, yet porous support, and stepwise assembly of the peptide. Classical techniques for peptide synthesis (i.e. solution phase) are often labour, time and skill intensive. Furthermore, solution phase techniques suffer from low yields due to the difficulties involved in separating and purifying often poorly

soluble intermediates. In contrast, SPPS is high yielding (individual coupling and deprotection steps are virtually quantitative), allows for easy purification (requires simply washing off excess reagents, since the peptide is immobilized) and is amenable to automation.

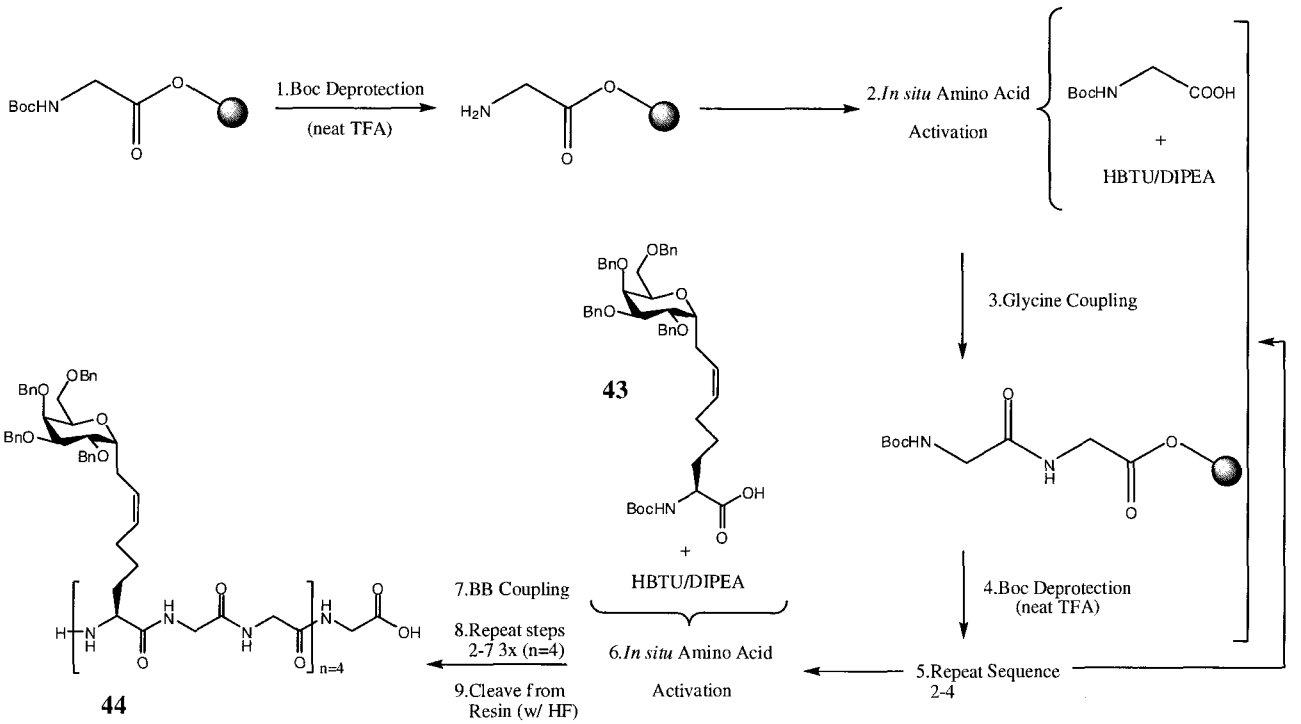

Scheme 3.7.1 SPPS of building block **43.**

Debenzylation of polymer **44** can be accomplished with BCl_3,[31, 32, 33] followed by reverse phase HPLC purification to furnish **45**, $[OGG]_4[Gal]$ analogue with an internal double bond (**Scheme 3.7.2**).

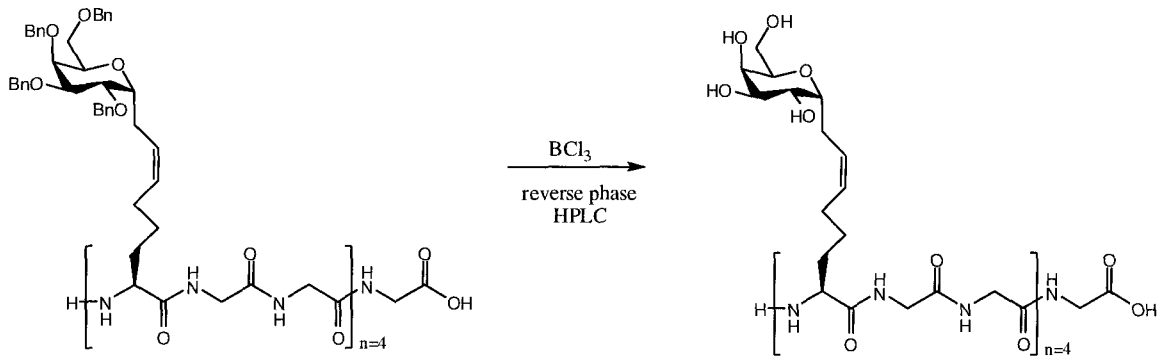

44 **45**

([OGG]$_4$[Gal] analogue w/ an internal olefin)

Scheme 3.7.2 Debenzylation of benzyl protected AFGP analogue with an internal double bond **44**.

Assessment of the analogue for thermal hysteresis (TH) activity and dynamic ice shaping (DIS) can be conducted with nanolitre osmometry.[34] Recrystallization inhibition (RI) activity can be assessed via the "splat assay" described by Knight *et al.*[35] and the secondary structure can be determined by circular dichroism (CD) spectroscopy.[36]

Finally, the analogue can be evaluated for cytotoxicity and cryotoxicity by *in vitro* testing in a human embryonic cell line using the MTT assay.[37]

References:

1. Peterson, D. J. *J. Org. Chem.* **1968.** 33(2), 780–784.

2. Julia, M. and Paris, J.-M. *Tet. Lett.* **1973.** 14, 4833-4836.

3. Kocienski, P. J., Lythgoe, B. and Ruston, S. *J. Chem. Soc., Perkin Trans. 1* **1978.** 829.

4. Grubbs, R. H. and Chang, S. *Tetrahedron* **1998**. 54, 4413-4450.

5. Grubbs, R.H. *Tetrahedron* **2004.** 60(34), 7117–7140.

6. Hérisson, J.-L. and Chauvin, Y. *Macromol. Chem.* **1970.** 141, 161.

7. Wittig, G. and Schöllkopf, U. *Chemische Berichte* **1954.** 87, 1318.

8. Wittig, G. and Haag, W. *Chemische Berichte* **1955.** 88, 1654–1666.

9. Maryanoff, B.E. and Reitz, A.B. *Chem. Rev.* **1989.** 89(4), 863–927.

10. Greene, T.W. and Wuts, P.G.M. *Greene's Protective Groups in Organic Synthesis, 4th Edition* Wiley-Interscience, **2007.**

11. Bertozzi, C.R., Hoeprich, P.D. and Bednarski, M.D. *J. Org. Chem.* **1992.** 57, 6092-6094.

12. Sibi, M.P. and Renhowe, P.A. *Tet. Lett.* **1990.** 31(1), 7407-7410.

13. Thapa, I. M.Sc. Thesis. **2006.** University of Ottawa.

14. Lemieux, R.U. *Can. J. Chem.* **1969.** 47, 4427.

15. Juaristi, E. and Cuevas, G. *Tetrahedron* **1992.** 48, 5019–5087.

16. Keck, G.E. and Enholm, E.J. *Tetrahedron.* **1985.** 41, 4079-4094.

17. Ponten, F. and Magnusson, G. *J. Org. Chem.* **1996.** 61, 7463-7466.

18. Angibeaud, P., Gadelle, A., Defaye, J. and Utille, J-P. *Syn. Commun.* **1985.** 1123-1125.

19. Wang, Z., Shao, H., Lacroix, E., Wu, S-H., Jennings, H.J. and Zou, W. *J. Org. Chem.* **2003.** 68, 8097-8105.

20. Allevi, P., Anastasia, M., Ciuffreda, P., Fiecchi, A. and Scala, A. *J. Chem. Soc., Perkin Trans. 1* **1989.** 1275.

21. Ohrui, H., Jones, G.H., Moffatt, J.G., Maddox, M.L., Christensen, A.T. and Byram, S.K. *J. Am. Chem. Soc.* **1975**. 97, 4602.

22. Hassner, A., Falb, E. and Nudelman, A. *Syn. Comm.* **1993.** 23(20), 2839-2844.

23. Pirrung, M.C. and Webste, N.J.G. *J. Org. Chem.* **1987.** 52, 3603-3613.

24. Rutherford, D., Li, B., Renhowe, P.A. and Sibi, M.P. *J. Am. Chem. Soc.* **1999.** 121, 7509-7516.

25. Wellner, E., Gustafsson, T., Backlund, J., Holmdahl, R. and Kihlberg, J. *Chembiochem* **2000.** 1, 272-280.

26. Watts, M.M., Fowler D.J. and Nolen, E.G. *Org. Lett.* **2002.** 4(22), 3963-3965.

27. Thalmann, A., Oertle, K., and Gerlach, H. *Org. Syn. Coll.* **1990.** 7, 470; **1985.** 63, 192.

28. Bowden, K., Heilbron, I.M. and Jones, E.R.H. *J. Chem. Soc.* **1946**. 39.

29. Corey, E.J. and Schmidt, G. *Tetrahedron Lett.* **1979.** 20, 399.

30. Merrifield, R.B. *J. Am. Chem. Soc.* **1963.** 85(14), 2149–2154.

31. Williams, D.R., Brown, D.L. and Benbow, J.W. *J. Am. Chem. Soc.* **1989**. 111, 1923–1925;

32. Tamura, S., Abe, H., Matsuda, A. and Shuto, S. *Angew. Chem., Int. Ed.* **2003.** 42, 1021–1023;

33. Stolz, F., Reiner, M., Blume, A., Reutter, W. and Schmidt, R.R. *J.Org. Chem.* **2004.** 69, 665–679.

34. Kao, M., Fletcher, G.L., Wang, N.C. and Hew C.L. *Can. J. Zool.* **1986**. 64, 578-582.

35. Knight, C.A., Hallett, J. and DeVries, A.L. *Cryobiology* **1988.** 25, 55–60.

36. Greenfield, N.J. *Nature protocols* **2006.** 1(6), 2876–90.

37. Mosmann, T. *J. Immunol. Methods* **1983.** 65, 55-63.

Chapter 4

Experimental: Materials and Methods

4.1 General

Dichloromethane, acetonitrile and triethylamine were distilled over calcium hydride prior to use. Benzene, ether and tetrahydrofuran (THF) were distilled over sodium-benzophenone before use. *N,N*-dimethylformamide (DMF), methanol and acetone were dried with activated molecular sieves (4 Å) overnight prior to use. Solution phase reactions were conducted under an inert atmosphere (N_2 (g) or Ar (g)), unless specified otherwise. Reactions were monitored by thin layer chromatography; visualized with U.V. light (254 nm), and/or i) aqueous ceric ammonium molybdate (CAM), or ii) aqueous potassium permanganate ($KMnO_4$) stains. Purification via flash chromatography was conducted with silica gel (Merck) of 240-400 mesh and columns fixed with fritted glass filters. Titration of organolithium reagents was conducted with commercially available *N*-benzylbenzamide in THF according to established protocols.[1] Ozonolysis was performed with a Yanco Industries ozonolysis apparatus.

^{1}H and ^{13}C NMR analyses were performed with an INOVA 500 MHz spectrometer and Bruker Avance 400 and 500 MHz spectrometers. NMR experiments were performed mainly with deuterated chloroform. Deuterated methanol, water and benzene were also employed. Chemical shifts are reported in parts per million (ppm) and are referenced to the appropriate deuterated solvent. ^{1}H integration is denoted in parentheses and coupling constants are reported in Hz. ^{1}H signal splitting patterns are indicated by s-singlet, br-broad singlet, d-doublet, t-triplet, m-multiplet and dd-doublet of doublets. Infrared (IR) spectra were obtained from an FTIR-8400 Fourier Transform

[1] Burchat, A.F., Chong, M.J. and Nielsen, N. *J. Organometallic Chem.* **1997.** 542, 281-283.

Infra Red Spectrophotometer (Simadzu). Mass spectral analyses were conducted with an Electrospray mass spectrometer. All spectral analyses were performed at facilities located at the University of Ottawa.

4.2 Protocol for the Preparation of Carbohydrate Components

Preparation of 2,3,4,6-tetra-*O*-acetyl-α-D-galactopyranosyl bromide (10)

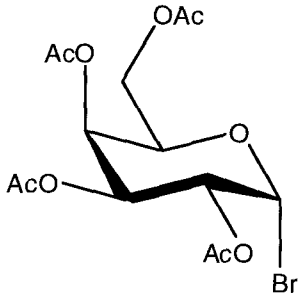

10

According to established protocols,[2,3] a flame dried 250 ml round bottom flask with a N_2 (g) feed was charged with a stir bar and commercially available β-D-galactose pentacetate (10 g, 25.12 mmmol). The flask was cooled in an ice bath and a solution of 33 % HBr in acetic acid (50 ml) was added. The ice bath was removed and the solution stirred for 2hrs. The solution was diluted with 150 ml of DCM and added to a separatory funnel. The organic layer was washed repeatedly with water until the pH of the aqueous layer was ≈ 7. The organic layer was dried over $MgSO_4$, filtered through Whatman paper and concentrated *in vacuo* to yield a white paste. Coevaporation with toluene furnished a white solid. The solid was recrystallized from Et_2O to afford the title compound (10.29 g, 98 %).

^{1}H NMR (400 MHz, $CDCl_3$), δ: 6.69 (1H, d, J=4.0 Hz), 5.51 (1H, dd, J=1.2, 3.3 Hz), 5.40 (1H, dd, J=3.3, 10.6 Hz), 5.04 (1H, dd, J=4.0, 10.6 Hz), 4.48 (1H, t, J= 6.7 Hz), 4.18 (1H, dd, J= 6.3, 11.4 Hz), 4.10 (1H, dd, J=6.8, 11.4), 2.15 (3H, s), 2.11 (3H,s), 2.06 (3H, s), 2.01 (3H, s);

---

[2] Conchie, J. and Levvy, G.A. Meth. *J. Carbohydr. Chem.* **1963** 2. 335.

[3] Paulson, H. *Angew. Chem.* **1982.** 94, 184.

^{13}C NMR (400 MHz, $CDCl_3$), δ: 170.1, 169.8, 169.6, 169.5, 87.9, 70.8, 67.7, 67.5, 66.7, 60.6, 20.5, 20.4, 20.4, 20.3:

MS (ESI, MeCN) calcd. For $C_{14}H_{19}BrO_9$, m/z: (M^+) 410.02, found 433.0 [($M+Na^+$)].

Preparation of 2,3,4,6-tetra-*O*-acetyl-α-1-allyl-D-galactopyranoside (11)

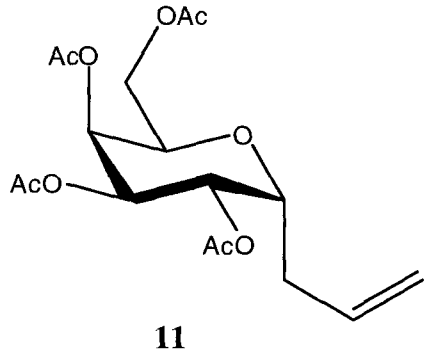

11

Compound **10** (1.50 g, 3.41 mmol) was added to a flame dried flask equipped with an Ar (g) inlet and a stir bar according to established protocols[4]. The flask was charged with benzene and flushed for 30 minutes, followed by addition of allyl phenyl sulfone (1.5 mL, 8.0 mmol) and *bis*-tributyl tin (2.2 ml 4.4 mmol). The resulting solution was sonicated under Ar (g) for an additional 40 min. The Ar (g) feed and sonicator were removed and the flask sealed with parafilm. The flask was irradiated with a 450 W mercury lamp for ≈ 18 hours and monitored by TLC. Upon completion, the reaction mixture was loaded directly onto a silica gel column and flushed with hexanes to remove excess *bis*-tributyl tin. The column was then eluted with 10:1, 8:1 and 6:1 hexanes: ethyl acetate until phenyl allyl sulfone started to elute. Upon elution of phenyl allyl sulfone, the column was subject to 3:1 hexanes: ethyl acetate until the title compound was

[4] Ponten, F. and Magnusson, G. *J. Org. Chem. Soc.* **1996.** 61, 7463-7466.

recovered. Removal of the solvent *in vacuo* afforded **11** as a crystalline solid (1.20 g, 88 %).

^{1}H NMR (400 MHz, $CDCl_3$), δ: 5.70- 5.81 (1H, m), 5.42 (1H, dd, J=2.4, 0.7 Hz), 5.27 (1H, dd, J=5.0, 9.3 Hz), 5.21 (1H, dd, J=3.2, 9.3 Hz), 5.09- 5.16 (2H, m), 4.26-4.33 (1H, m), 4.20 (1H, dd, J= 8.9, 12.8 Hz), 4.06-4.11 (2H, m), 2.41- 2.55 (1H, m), 2.21- 2.39 (1H, m), 2.12 (3H, s), 2.07 (3H,s), 2.04 (3H, s), 2.00 (3H, s);

^{13}C NMR (400 MHz, $CDCl_3$), δ: 170.6, 170.1, 169.9, 169.8, 133.3, 117.6, 71.4, 68.3, 67.9, 67.6, 61.4, 30.9, 20.8, 20.7, 20.7, 20.6:

MS (ESI, MeCN) calcd. For $C_{17}H_{24}O_9$, m/z: (M^+) 374.12, found 411.1 [($M+K^+$)].

Preparation of α-1-allyl-D-galactose (12)

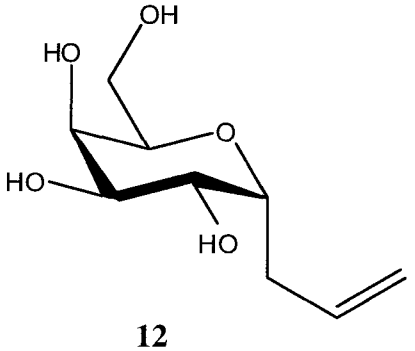

12

2.0 g, 5.31 mmol of **11** was added to a solution of freshly prepared NaOMe (pH ≈ 10) and stirred overnight. The reaction was monitored by TLC, and upon completion treated with Amberlite IR 120(H) ion-exchange resin. Sufficient resin was added to ensure a pH of 7. The beads were filtered off with Whatman paper and the solution concentrated to yield α-1-allyl-D-galactose as a white solid in 99 % yield (1.10 g).

^{1}H NMR (500 MHz, MeOD), δ: 5.83- 5.94 (1H, m), 5.09- 5.15 (1H, m), 5.02- 5.06 (1H, m), 3.87- 4.03 (3H, m), 3.66- 3.89 (4H, m), 2.34- 2.50 (2H, m);

^{13}C NMR (500 MHz, MeOD), δ: 136.8, 116.9, 75.7, 74.2, 72.0, 70.2, 70.0, 63.0, 31.1;

MS (ESI, MeOH) calcd. For $C_9H_{16}O_5$, m/z: (M^+) 204.10, found 205.1 [($M + H^+$)];

IR (MeOH) cm^{-1}: 3323, 1074 and 1024.

Preparation of 2,3,4,6-tetra-*O*-benzyl-α-1-allyl-D-galactopyranoside (13)

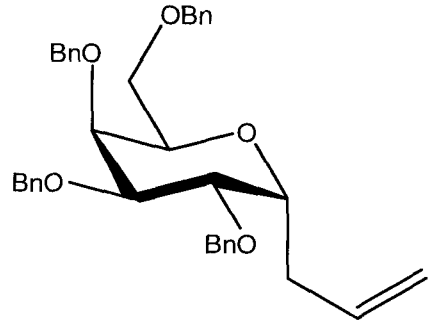

13

A flame dried flask equipped with a N_2 (g) feed and stir bar was charged with 400 mg, 2.0 mmol, of α-1-allyl-D-galactose and 5 ml of dry DMF. 500 mg (5.0 mmol) of NaH and catalytic $^tBuNH_4^+I^-$ were quickly transferred to a second round bottom flask containing 5 mL of dry DMF and a stir bar. The α-1-allyl-D-galactose solution (first flask) was transferred to the second flask via cannula. The flask was then submerged in an ice bath and BnBr (2.5g, 13.0 mmol) was added dropwise via syringe. Additional DMF was added to the flask to maintain a stirable slurry. The ice bath was removed and the slurry stirred overnight. The solution was diluted with water and extracted repeatedly with ethyl acetate (8x). The combined organic extracts were dried over $MgSO_4$ and concentrated under vacuum. Flash chromatography (8:1, hexanes:ethyl acetate) yielded the title compound as a colourless oil (0.95g, 85 %).

^{1}H NMR (400 MHz, $CDCl_3$), δ: 7.25-7.34 (20H, m), 5.70- 5.81 (1H, m), 5.01- 5.09 (2H, m), 4.47- 4.72 (8H, m), 4.04- 4.09 (1H, m), 3.98- 4.02 (2H, m), 3.81- 3.87 (2H, m), 3.69- 3.73 (2H, m), 3.66 (1H, dd, J= 4.7, 10.6), 2.29-2.42 (2H, m);

^{13}C NMR (400 MHz, $CDCl_3$), δ: δ: 138.5, 138.4, 138.4, 138.2, 137.7, 135.1, 133.7, 128.3, 128.3, 128.2, 127.9, 127.8, 127.7, 127.5, 127.5, 127.4, 116.7, 76.4, 74.2, 73.1, 73.3, 73.0, 72.9, 72.5, 70.8, 70.7, 67.2, 32.2;

MS (ESI, MeCN) calcd. For $C_{37}H_{40}O_5$, m/z: (M^+) 564.29, found 587.3 [($M+Na^+$)];

IR (CH_2Cl_2) cm^{-1}: 3050, 1501 and 1454.

Preparation of 2,3,4,6-tetra-*O*-benzyl-α-D-galactopyranosyl-ethyl aldehyde (7)

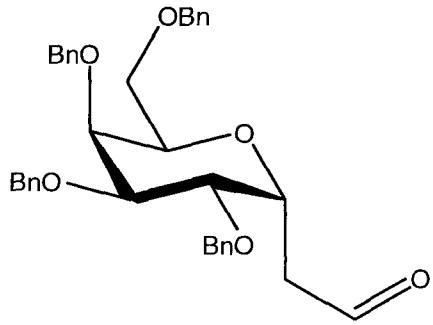

7

1.0 g, 1.95 mmol, of **13** was added to a 25 mL round bottom flask containing freshly distilled DCM, ≈ 1 mg of Sudan Red 7B and a stir bar. The solution was cooled to -78 °C in an acetone/dry ice bath and treated with ozone while stirring until the reddish colour disappeared (≈ 20 min). The solution was then flushed with nitrogen for 20 min and quenched with triphenylphosphine. The bath was removed and the solution was stirred overnight. Column chromatography (6:1 hexanes: ethyl acetate) furnished the aldehyde **7** as a colourless oil (0.96 g, 96 %).

^{1}H NMR (400 MHz, $CDCl_3$), δ: 9.68 (1H, t, J=2.2 Hz), 7.27- 7.37 (18H, m), 7.20-7.24 (2H, m), 4.44- 4.72 (9H, m), 3.98- 4.07 (2H, m), 3.76- 3.87 (2H, m), 3.62- 3.72 (2H, m), 2.63 (2H, dd, J= 2.2, 6.6 Hz), 2.14 (3H, s), 2.11 (3H,s), 2.05 (3H, s), 2.00 (3H, s);

^{13}C NMR (400 MHz, $CDCl_3$), δ: 200.6, 138.3, 138.3, 138.2, 137.7, 128.4, 128.4, 128.4, 128.3, 128.1, 127.9, 127.8, 127.7, 127.7, 127.6, 127.5, 76.1, 73.8, 73.3, 73.3, 73.1, 73.0, 67.0, 42.9;

MS (ESI, MeCN) calcd. For $C_{36}H_{38}O_6$, m/z: (M^+) 566.27, found: 567.3 [($M+H^+$)];

IR (CH_2Cl_2) cm^{-1}: 2671, 1741, 1503, and 1451.

Preparation of 2,3,4,6-tetra-*O*-benzyl-α-D-galactopyranosyl-ethanol (39)

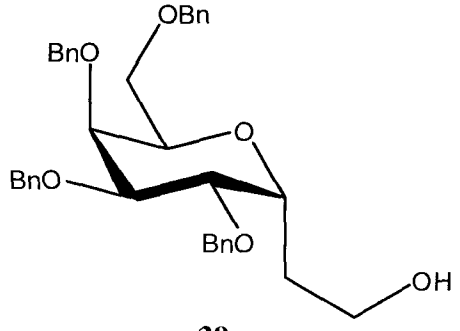

39

50 mg, 0.117 mmol, of **13** was added to a 5 mL round bottom flask containing 1.0 ml of freshly distilled DCM, Sudan Red 7B (≈ 2 mg) and a stir bar. The solution was cooled to -78 °C in an acetone/dry ice bath and treated with ozone while stirring until the reddish hue disappeared (≈ 5 min). The solution was then flushed with nitrogen for 20 min and treated with 15 mg, 0.340 mmol, of $NaBH_4$. The bath was removed and the solution was stirred for 2 hours. Column chromatography (3:1 hexanes: ethyl acetate) furnished the alcohol **39** as a colourless oil (0.47 g, 94 %).

^{1}H NMR (400 MHz, $CDCl_3$), δ: 7.24-7.36 (20H, m), 4.70 (1H, dd, J= 5.08, 11.8 Hz), 4.63 (1H, dd, J=4.2, 11.8 Hz), 4.49-4.56 (4H, m), 4.16-4.22 (1H, m), 4.08-4.13 (1H, m), 3.95.(2H, m), 3.74 (4H, m), 3.50 (1H, dd, J= 3.7, 10.6 Hz), 2.78 (1H, br), 1.93-2.03 (1H, m) 1.63-1.70 (1H, m);

^{13}C NMR (400 MHz, $CDCl_3$), δ: 138.4, 138.2, 138.0, 137.9, 128.4, 128.3, 128.0, 127.9, 127.8, 127.7, 127.6, 127.6, 127.5, 77.0, 76.7, 74.2, 73.3, 73.2, 73.1, 73.0, 72.1, 67.7, 61.2, 29.8;

MS (ESI, MeCN) calcd. For $C_{36}H_{40}O_6$, m/z: (M^+) 568.28, found 569.3 [($M+H^+$)].

Preparation of 2,3,4,6-tetra-*O*-benzyl-α-D-galactopyranosyl-ethyl iodide (40)

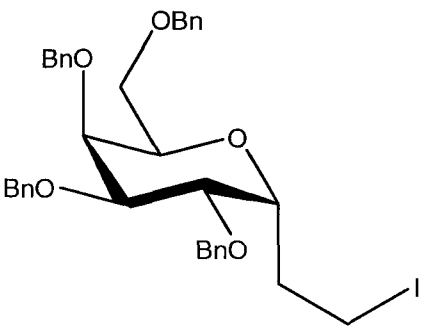

40

350 mg (0.62 mmol) of 2,3,4,6-tetra-*O*-benzyl-α-1-allyl-D-galactopyranosyl-ethanol was added to a 10 mL round bottom flask containing 3.0 ml of freshly distilled THF and a stir bar as described by Nolen.[5] 240 mg (0.90 mmol) of triphenylphosphine, 170 mg (2.5 mmol) of imidazole and 170 mg (0.70 mmol) of I_2 were sequentially added to the solution. The solution was stirred for 30 minutes, concentrated under reduced pressure and dissolved in 5 ml of EtOAc. The organic layer was washed successively

[5] Watts, M.M., Fowler D.J. and Nolen, E.G. *Org. Lett.* **2002.** 4, 22, 3963-3965.

with sodium sulfite (until the yellow colour dissipated), distilled water (2x) and brine (1x). The organic phase was dried over $MgSO_4$, filtered and concentrated *in vacuo.* Column chromatography (10:1 hexanes: ethyl acetate) furnished **40** as a colourless oil (360 mg, 86 %).

^{1}H NMR (400 MHz, $CDCl_3$), δ: 7.26-7.36 (18H, m), 7.15- 7.25 (2H, m), 4.45-4.75 (8H, m), 4.09 (1H, m), 3.97 (1H, m), 3.83 (1H, m), 3.76.(1H, m), 3.64- 3.70 (2H, m), 3.12-3.28 (2H, m), 2.12- 2.22 (1H, m), 1.90- 2.00 (1H, m);

^{13}CN MR (400 MHz, $CDCl_3$), δ: 138.5, 138.4, 138.3, 138.0, 128.5, 128.4, 128.4, 128.3, 128.0, 127.9, 127.9, 127.7, 127.7 127.6, 127.5, 77.2, 76.8, 76.4, 74.1, 73.4, 73.2, 73.0, 72.6, 67.7, 61.2, 31.6, 3.1;

MS (ESI, MeCN) calcd. For $C_{36}H_{39}O_5$, m/z: (M^+) 678.18, found 701.2 [($M+Na^+$)].

Preparation of 2,3,4,6-tetra-*O*-benzyl-α-D-galactopyranosyl-ethyl triphenylphosphonium iodide (36)

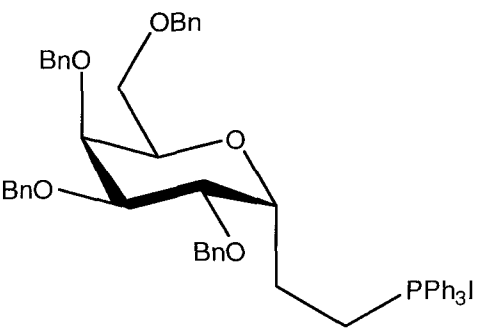

36

To a flame dried round bottom flask equipped with a stir bar, 262 mg, 1.00 mmol, of triphenylphosphine was added to a solution of **40** (100 mg, 0.143 mmol) in 2 ml of dry

DMF. The solution was stirred at 40 °C overnight under a nitrogen atmosphere. Upon completion of the reaction (as judged by TLC), DMF was removed under vacuum to yield a thick oil. Excess triphenylphosphine was removed by repeated ether and THF washes to furnish a white paste. Recrystallization from toluene furnished **36** as a white amorphous solid (133 mg, 98 %). The solid was dried in a Kugelrohr and stored in a dessicator under argon.

^{1}H NMR (400 MHz, $CDCl_3$), δ: 7.58-7.77 (15H, m), 7.10-7.35 (20H, m), 4.43-4.73 (8H, m), 4.18 (1H, m), 3.87-4.05 (4H, m), 3.73.(1H, dd. J= 2.7, 6.1 Hz), 3.56-3.68 (1H, m), 3.33 (1H, m), 1.93 (2H, m);

^{13}C NMR (400 MHz, $CDCl_3$), δ: 138.4, 138.3, 138.1, 138.0, 135.0, 134.9, 133.5, 133.4, 130.5, 130.3, 128.9, 128.2, 128.2, 127.7, 127.6, 127.6, 127.5, 127.4, 127.4, 125.2, 118.2, 117.4, 76.3, 73.6, 73.2, 73.1, 72.8, 72.7, 72.4, 67.7, 21.9, 21.3, 19.7, 19.1;

MS (ESI, H_2O) calcd. For $C_{54}H_{54}IO_5P$, m/z: (M^+) 940.28, found 940.3 [M^+];

IR (CH_2Cl_2) cm^{-1}: 3048, 1581 and 1279.

4.3 Protocol for the Preparation of Amino Acid Components

Preparation of (S)-4-methoxycarbonyloxazolidin-2-one (18)

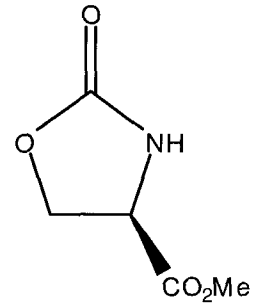

18

Commercially available L-serine (0.525 g, 5 mmol) was dissolved in 1M NaOH (15 ml, 15 mmol) and added to triphosgene (1.5 g, 5 mmol) in *p*-dioxane (10 ml) as described by Falb.[6] The mixture was stirred at room temperature for 2 hrs. The solvent was evaporated, and the crude solids were dissolved in methanol (30 ml) and the mixture stirred overnight. The solvent was decanted and evaporated to yield a viscous oil which was washed with acetonitrile (15 ml) and filtered. The filtrate was subject to roto-evaporation to afford **18** as a yellow oil (0.61 g, 83 %).

^{1}H NMR (400 MHz, $CDCl_3$), δ: 6.45 (1H, br), 4.61 (1H, dd, J=9.55, 8.95 Hz), 4.52 (1H, dd, J=8.95, 4.50), 4.43 (1H, dd, J=9.55, 4.50), 3.81 (3H, s);

^{13}C NMR (400 MHz, $CDCl_3$), δ: 170.6, 159.2, 66.8, 53.8, 53.1;

MS (ESI, MeCN) calcd. For $C_5H_7NO_4$, m/z: (M^+) 145.04, found: 146.0 [($M+H^+$)], 86.0 [($M+H^+$)- CO_2Me];

IR (CH_2Cl_2) cm^{-1}: 3327 and 1765.

---

[6] Hassner, A., Falb, E. and Nudelman, A. *Syn. Comm.* **1993.** 23, 20, 2839-2844.

Preparation of (R)-4-hydroxymethyloxazolidin-2-one (19)

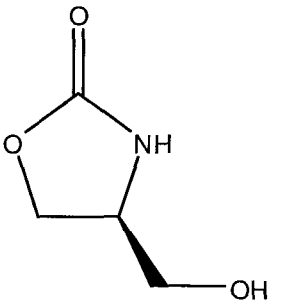

19

According to the procedure described by Sibi,[7] a dry 100 ml round-bottom flask equipped with a stirbar, 1.0 g (50 mmol) of $NaBH_4$ was added in portions to a solution of **18** (3.5 g, 0.025 mmol) in ethanol (50 ml). The solution was stirred for 2 hours, after which it was treated with saturated ammonium chloride, and stirred for an additional 10 minutes. The solids (mostly salt) were filtered off and the filtrate was concentrated to yield a crude white paste (2.80 g, 98 %). Flash chromatography with 9:1 ethyl acetate:methanol afforded the title compound as white crystals (2.2 g, 78 %).

^{1}H NMR (400 MHz, D_2O), δ: 4.57 (1H, t, J=9.01 Hz), 4.30 (1H, dd, J=8.93, 5.15 Hz), 4.11-4.04 (1H, m), 3.68 (1H, J=12.01, 3.76 Hz), 3.60 (1H, dd J=12.01, 4.40 Hz);

^{13}C NMR (400 MHz, D_2O), δ: 164.9, 70.5, 65.0, 56.3;

MS (ESI, MeOH) calcd. For $C_4H_7NO_3$, m/z: (M^+) 117.04, found:118.1 [(M+ H^+)], 117.0 [M^+];

IR (MeOH) cm^{-1}: 3372 and 1741.

---

[7] Sibi, P.M., Rutherford, D. and Sharma, R.. *J Chem. Soc., Perkin Trans.* 1, **1994**, 1675 – 1678.

Preparation of (S)-4-(4'-tolylsulfonyl)oxymethyloxazolidin-2-one (20)

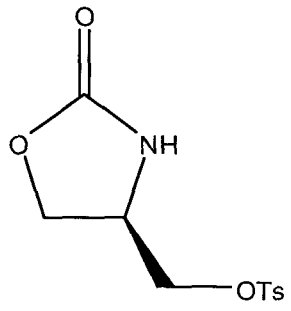

20

According to the procedure described by Sibi,[8] TsCl (8.6g, 45.1 mmol) was added to a round bottom flask containing **19** (3.4 g 29.3 mmol) dissolved in dry pyridine (15 ml). The solution was stirred for 4 hours and monitored periodically by TLC. Upon completion of the reaction, excess pyridine was removed via rotoevaporation to yield a dark red gel. The gel was dissolved in dichloromethane (50 ml) and rinsed with 1.5 M HCl (6 x 33 ml). The combined organic extracts were dried over $MgSO_4$, filtered and concentrated *in vacuo*. The resulting white solid was rinsed repeatedly with boiling hexanes to remove residual TsCl and afford **20** (87 %, 7.04 g) as a fluffy white solid.

^{1}H NMR (400 MHz, $CDCl_3$), δ: 7.79 (1H, d, J=8.31 Hz), 7.38 (1H, d, J=8.36 Hz), 5.8 (1H, br), 4.47 (1H, t, J=8.01Hz), 4.07 (4H, m), 2.46 (3H, s);

^{13}C NMR (400 MHz, $CDCl_3$), δ: 158.8, 145.6, 132.2, 130.2, 127.9, 69.7, 66.3, 50.9, 21.7;

MS (ESI, MeCN) calcd. For $C_{11}H_{13}NO_5S$, m/z: (M^+) 271.05, found: 294.0 [(M+ Na^+)], 271.1 [M^+];

IR ($CHCl_3$) cm^{-1}: 3437, 3181 and 1756.

---

[8] Sibi, P.M., Rutherford, D. and Sharma, R. *J Chem. Soc., Perkin Trans.* 1 **1994**, 1675 – 1678.

Preparation of (S)-4-iodomethyloxazolidin-2-one (21)

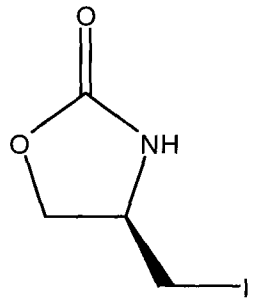

21

A mixture of 3.75 g (12.0 mmol) of tosylate **20**, and 9.0 g (56 mmol) of NaI were refluxed in 50 ml dry acetone under a N_2 (g) atmosphere as described by Sibi and Renhowe.[9] The reaction was stirred overnight under reflux, cooled to room temperature and excess NaI removed by filtration. The solids were rinsed with ethyl acetate and concentrated on a rotary evaporator to yield a crude red solid. The solid was dissolved in ethyl acetate and washed with a saturated Na_2SO_3 (50 ml) solution until the organic layer became colourless. The aqueous sodium sulfite layer was back-extracted repeatedly with ethyl acetate (10x 25 ml). The organic extracts were combined and dried over $MgSO_4$, filtered and the solvent removed by rotovaporation to furnish a crude orange solid. Column chromatography (3:1 ethyl acetate:hexanes) afforded the product, **21**, as a pale white solid (2.62 g, 87 %).

^{1}H NMR (500 MHz, $CDCl_3$), δ: 6.79 (1H, br), 4.50 (1H, dd, J=8.729, 8.41 Hz), 4.13 (1H, dd, J=4.87, 8.99), 4.07 (1H, m), 3.22 (2H, m);

^{13}C NMR (500 MHz, $CDCl_3$), δ: 159.4, 70.4, 53.2, 8.1;

[9] Sibi, M.P. Rutherford, D., Renhowe, P.A. and Li, B. *J. Am. Chem. Soc.* **1999.** 121, 7509-7516.

MS (ESI, MeCN) calcd. For $C_4H_6INO_2$, m/z: (M^+) 226.94, found 250.0, [(M+ Na^+)], 227.0 [M^+];

IR (CH_2Cl_2) cm^{-1}: 3472 and 1764.

Preparation of (S)-4-(2-oxazolidonyl)-methyltriphenylphosphonyl Iodide (22)

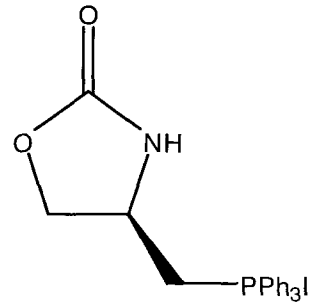

22

According to the protocol established by Sibi and Renhowe,[10] a flame dried round bottom flask equipped with a stir bar and N_2 (g) feed, 15.0 g (57.25 mmol) of triphenylphosphine was added to a solution of **21** (1.5 g, 6.6 mmol) in 8 ml of dry DMF. The solution was stirred at 100 °C overnight under a nitrogen atmosphere. Upon completion of the reaction (as judged by TLC), DMF was removed under vacuum to yield a viscous translucent yellow oil. The oil was triturated repeatedly with ether and THF to furnish a white solid. Mixed solvent recystallization with ethyl acetate and methanol afforded **22** (3.07 g, 95 %), as a white solid which was subsequently dried in a Kugelrohr and stored in a dessicator under argon.

^{1}H NMR (400 MHz, D_2O), δ: 7.80 (15H, m), 4.50 (1H, m), 4.35 (1H, dd J=9.22, 0.92 Hz), 4.01 (1H, dd, J= 5.01, 9.12 Hz), 3.94 (1H, m) 3.79 (1H, m);

[10] Sibi, M.P. Rutherford, D., Renhowe, P.A. and Li, B. *J. Am. Chem. Soc.* **1999.** 121, 7509-7516.

^{13}C NMR (400 MHz, D_2O), δ: 157.8, 132.4, 130.6, 127.3, 114.4, 67.8, 67.7, 44.3;

MS (ESI, H_2O) calcd. For $C_{22}H_{21}INO_4P$, m/z: (M^+) 489.04, found: 489.0 (M^+);

IR (CH_2Cl_2) cm^{-1}: 3324 and 1776.

Preparation of 1(-*tert*-butyldimethylsiloxy)-3-butene (23)

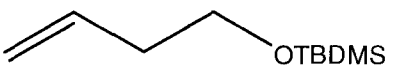

23

Commercially available 3-buten-1-ol (5.00g, 69.4 mmol) was added to a solution of tert-butyldimethylsilylchloride (TBDMSCl) (11.0 g, 72.0 mmol) and imidazole (5.0 g, 73.5 mmol) in 100 ml of dichloromethane as described by Webste and Pirrung.[11] The solution was stirred for 2 hours at room temperature, followed by repeated washes with 10 % HCl, water and brine. The organic phase was dried over $MgSO_4$ and concentrated on a rotary evaporator to yield the product as a clear oil (12.32 g, 95 %).

^{1}H NMR (400 MHz, $CDCl_3$), δ: 5.78- 5.86 (1H, m), 4.99- 5.09 (1H, m), 3.65 (1H, t J= 6.78 Hz), 2.24- 2.30 (1H, m), 0.90 (9H, s) 0.05 (6H, s);

^{13}C NMR (400 MHz, $CDCl_3$), δ: 135.3, 116.2, 62.8, 37.5, 25.9, 18.3,-5.3;

MS (ESI, MeCN) calcd. For $C_{10}H_{22}OSi$, m/z: (M^+) 186.14, found: 209.1 [(M+ Na^+)].

[11] Pirrung, M.C. and Webste, N.J.G. *J. Org. Chem.* **1987.** 52, 3603-3613.

Preparation of (3-*tert*-butyldimethylsiloxy)propanal (24)

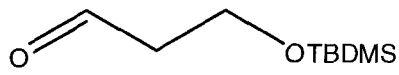

24

1.00 g (5.4 mmol) of **23** was added to a round bottom flask containing 15 ml of MeOH and a stir bar. The solution was cooled to -78 °C in a dry ice/acetone bath and a stream of ozone was bubbled through the solution. Bubbling was stopped once a pale blue colour developed (≈ 15 minutes), and the solution was flushed with dry nitrogen. Dimethyl sulfide (5 ml) was added and the solution was allowed to warm to room temperature (overnight). The solvent was removed under reduced pressure, and the crude oil was purified via flash chromatography (2:1, dichloromethane: hexanes) to afford the title compound as a colourless oil. The oil was stored under an inert atmosphere in the freezer.

^{1}H NMR (400 MHz, $CDCl_3$), δ: 9.80 (1H, t, J=2.0 Hz), 3.98 (2H, t, J=6.03), 2.60 (1H, td, J=2.0, 6.03 Hz), 0.88 (9H, s), 0.06 (6H, s);

^{13}C NMR (400 MHz, $CDCl_3$), δ: 201.8, 57.1, 46.3, 25.6, 18.0,-5.7;

MS (ESI, MeCN) calcd. For $C_9H_{20}O_2Si$, m/z: (M^+) 188.12, found: 211.1 [(M+ Na^+)], 189.1 [(M + H^+)];

IR (CH_2Cl_2) cm^{-1}: 2627, 1757, and 963.

Preparation of (*S*)-4-(4-(*tert*-butyldimethylsiloxy)but-1-enyl)oxazolidin-2-one (25)

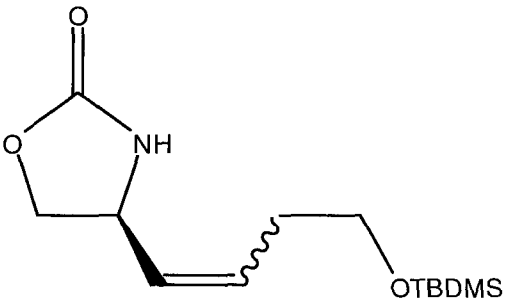

25

In a flame dried flask equipped with an Ar (g) inlet and a stir bar, a suspension of **22** (490 mg, 1 mmol) in 15 ml of freshly distilled THF was cooled to -78 °C. The suspension was treated with 1.95 mmol (0.80 ml) of *n*BuLi over a period of 10 minutes. The resulting orange-red suspension was stirred for 1 hour, followed by quench with **24** (179 mg, 0.95 mmol) in THF (2 ml). The solution was stirred for an additional 2 hours, followed by quench with saturated aqueous NH_4Cl (10 ml). THF was removed by rotovaporation and the aqueous layer extracted with ethyl acetate (5 x 15 ml). The combined organic extracts were dried over $MgSO_4$, filtered, and concentrated to afford a viscous dark yellow oil. Column chromatography with 1:1 ethyl acetate: hexanes furnished **25** as a viscous pale yellow oil (239 mg, 88 %).

^{1}H NMR (400 MHz, $CDCl_3$), δ: 5.64- 5.79 (1H, m), 5.45- 5.56 (1H, m), 5.38 (1H, br), 4.72 (1H, dd, J=15.88, 8.32 Hz), 4.51 (1H, t, J= 8.46) 4.02 (1H, t, J=8.48), 3.64 (2H, t, J=6.14 Hz), 2.20- 2.35 (2H, m), 0.89 (9H, m), 0.06 (6H, m);

^{13}C NMR (400 MHz, $CDCl_3$), δ: 159.4, 132.3, 129.4, 70.3, 62.1, 49.5, 31.2, 26.0, 18.5, -5.3;

MS (ESI, MeCN) calcd. For $C_{13}H_{25}NO_3Si$, m/z: (M^+) 271.16, found: 310.1 [($M+K^+$)];
IR (CH_2Cl_2) cm^{-1}: 3321, 1743, and 935.

Preparation of (S)-tert-butyl 4-(4-(tert-butyldimethylsilyloxy)but-1-enyl)-2-oxooxazolidine-3-carboxylate (30)

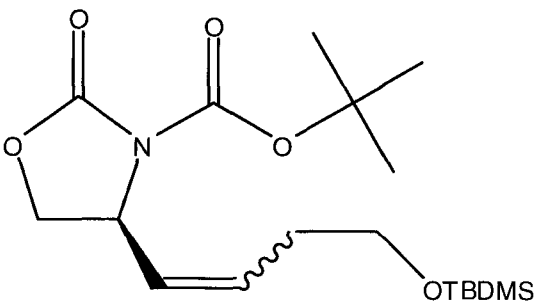

30

In a dry round bottom flask equipped with a stir bar, di-*tert*-butyldicarbonate (100 mg, 0.46 mmol) was added to a solution of **25** (100 mg, 0.36 mmol), triethylamine (250 µl, 2.0 mmol) and catalytic dimethylaminopyridine (DMAP) in THF (2.0 ml). The resulting yellow solution was stirred for 2 hours at room temperature, followed by concentration *in vacuo*. The yellow residue obtained after rotovaporation was dissolved in 5 ml of ethyl acetate, and extracted repeatedly with 10 % HCl (3x), water (2x) and brine (1x). The organic layer was dried over $MgSO_4$, filtered and concentrated to yield a dark yellow oil. Flash column chromatography (1:5 ethyl acetate: hexanes) furnished the title compound as white needles (122 mg, 92 %).

^{1}H NMR (400 MHz, $CDCl_3$), δ: 5.64- 5.73 (1H, m), 5.50- 5.57 (1H, m), 4.98- 5.06 (1H, m), 4.41 (1H, t, J= 8.6 Hz), 3.93 (1H, dd, J= 4.9, 8.7 Hz), 3.66- 3.74 (1H, m), 3.55- 3.64 (1H, m), 2.26- 2.44 (1H, m), 1.50 (9H, s), 0.88 (9H, s), 0.43 (6H, s);

^{13}C NMR (400 MHz, $CDCl_3$), δ: 152.2, 149.1, 131.0, 128.5, 83.8, 67.3, 62.1, 52.4, 31,3, 28.0, 25.9, 18.4, -5.3;

MS (ESI, MeCN) calcd. For $C_{18}H_{33}NO_5Si$, m/z: (M^+) 371.21, found: 371.2 [M^+], 271.2 [(M^+) -Boc];

IR (CH_2Cl_2) cm^{-1}: 1795 and 1728.

Preparation of (S)-*tert*-butyl 4-(4-hydroxybut-1-enyl)-2-oxooxazolidine-3-carboxylate (31)

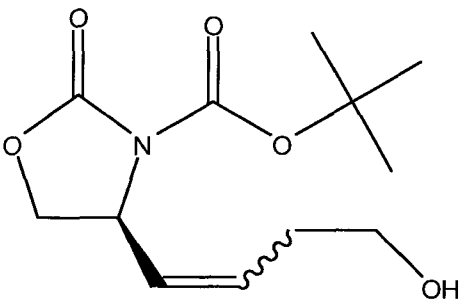

31

In a dry round bottom flask, TBAF$\circ H_2O$ (310 mg, 1.42 mmol) was added to a stirred solution of **30** (371 mg, 1.0 mmol) in 4 ml of tetrahydrofuran. The solution was stirred at room temperature for 1 hour. THF was promptly removed by rotovaporation to yield a thick yellow oil which was dissolved in ethyl acetate (5 ml) and extracted successively with water (3 x 5 ml) and brine (2 x 5 ml). The organic layer was dried over $MgSO_4$, filtered and concentrated to yield a translucent yellow oil. Column chromatography (1:1 ethylacetate: hexanes) afforded **31** as a colourless oil (215 mg, 84 %).

^{1}H NMR (400 MHz, $CDCl_3$), δ: 5.69- 5.82 (1H, m), 5.52- 5.62 (1H, m), 5.05- 5.13 and 4.65- 4.73 (total 1H, m) 4.43 (1H, m), 3.90- 4.04 (1H, m), 3.69 (2H, m), 2.30- 2.54 (2H, m), 2.22 and 1.66 (total 1H, br), 1.51 (9H, s);

^{13}C NMR (400 MHz, $CDCl_3$), δ: 152.0, 149.7, 132.3, 129.3, 84.3, 67.1, 61.4, 57.0, 35,3, 27.9;

MS (ESI, MeOH) calcd. For $C_{12}H_{19}NO_5$, m/z: (M^+) 257.13, found: 257.1 [M^+], 157.1 [(M^+) - Boc].

Preparation of (S)-*tert*-butyl 4-(4-hydroxybutyl)-2-oxooxazolidine-3-carboxylate (32)

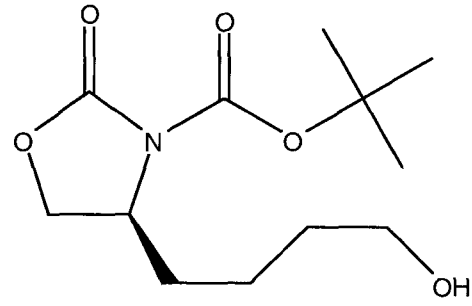

32

To a round bottom flask equipped with an inlet, 100 mg (0.386 mmol) of **31** was added to a stirred suspension of Pd/C (10 mg, 10 % w/w) in methanol (2.0 ml). The mixture was degassed with dry N_2 (g) for 20 minutes with stirring. H_2 (g) was bubbled through the suspension for 25 minutes, the inlet removed and solid Pd/C filtered off with Whatman paper. The filtrate was concentrated on a rotary evaporator to furnish a crude colourless oil. Flash chromatography (1:1 ethyl acetate: hexanes) furnished the product as a white crystalline solid (78 mg, 77 %).

^{1}H NMR (400 MHz, $CDCl_3$), δ: 4.34 (1H, t, J= 8.14 Hz), 4.20- 4.28 (1H, m), 4.05 (1H, dd, J= 8.39 , 2.74 Hz), 3.65 (2H, t, J= 6.26 Hz), 1.80- 1.92 (1H, m), 1.69- 1.78 (1H, m), 1.60 (2H, m), 1.53 (9H, s), 1.42 (2H, m);

^{13}C NMR (400 MHz, $CDCl_3$), δ: 152.2, 149.5, 83.9, 66.4, 62.3, 54.9, 32.7, 32.2, 28.0, 20.6;

MS (ESI, MeOH) calcd. For $C_{12}H_{21}NO_5$, m/z: (M^+) 259.14, found**:** 282.1 [(M+ Na^+)];

IR (CH_2Cl_2) cm^{-1}: 3423, 1797 and 1720.

Preparation of (S)-*tert*-butyl 4-(4-hydroxybutyl)-2-oxooxazolidine-3-carboxylate (37)

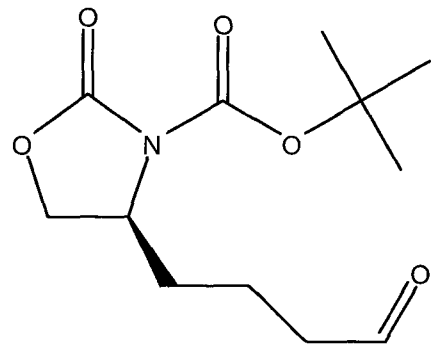

37

To a dry round bottom flask equipped with a stir bar and dicholoromethane (1.0 ml), DMSO (45 mg, 0.58 mmol) was added and the solution cooled to -78 °C in an acetone/dry ice bath. Oxalyl chloride (38 mg, 0.290 mmol) was added dropwise over 5 minutes and the solution stirred for 15 minutes. **32** (50 mg, 0.19 mmol) was diluted in dichloromethane and added via syringe over 5 minutes. The solution was stirred for an additional 30 minutes. Triethylamine (78 mg, 107 mmol) was diluted in dichloromethane and added to the solution over 5 minutes by syringe, and the solution stirred for an additional 30 minutes. The solution was allowed to warm to room temperature, extracted with 10 % HCl (2 ml x 3), water (2ml x 3) and brine (2ml x 1). The organic phase was dried over $MgSO_4$, filtered and concentrated. Column chromatography (2:1 hexanes: ethyl acetate) afforded **37** as a colourless oil (45 mg, 91 %).

^{1}H NMR (400 MHz, $CDCl_3$), δ: 9.88 (1H, t, J= 1.04 Hz), 4.35 (1H, t, J= 8.15 Hz), 4.25 (1H, m), 4.08 (1H, m), 2.55 (1H, t, J= 6.82 Hz), 2.45 (1H, t, J= 6.98 Hz), 1.73 (4H, m), 1.54 (9H, s);

^{13}C NMR (400 MHz, $CDCl_3$), δ: 201.1, 152.0, 149.2, 83.9, 66.2, 54.6, 43.0, 32.2, 27.9, 16.5; **MS** (ESI, MeCN) calcd. For $C_{12}H_{21}NO_5$, m/z: (M^+) 257.13, found: 280.1 [(M+ Na^+)], 257.1 [M^+] and 157.1 [(M^+)- Boc];

IR (CH_2Cl_2) cm^{-1}: 2761, 1802, 1761 and 1713.

4.4 Coupling of Carbohydrate and Amino Acid Components

Preparation of (4S)-tert-butyl 2-oxo-4-((Z)-6-((2R,3R,4R,5R)-3,4,5-tris(benzyloxy)-6-(benzyloxymethyl)tetrahydro-2H-pyran-2-yl)hex-4-enyl)oxazolidine-3-carboxylate (41)

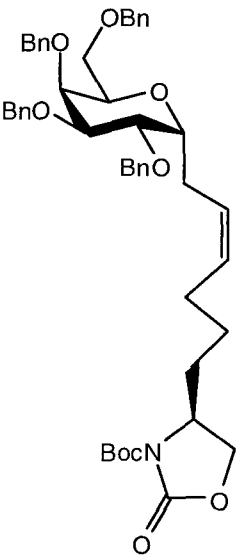

41

To a flame dried flask equipped with an Ar (g) inlet and a stir bar, a suspension of **36** (202 mg, 0.215 mmol) in 2 ml of freshly distilled THF was cooled to -78 °C. The suspension was treated with 0.215 mmol (127 µl) of *n*BuLi over a period of 5 minutes.

The resulting orange suspension was stirred for 20 minutes, followed by quench with **37** (60 mg, 0.230 mmol) in THF (1 ml). The solution was stirred for an additional 30 minutes at -78 °C, followed by quench with saturated aqueous NH_4Cl (1 ml). THF was removed on a rotary evaporator and the aqueous layer extracted with ethyl acetate (5 x 2 ml). The combined organic extracts were dried over $MgSO_4$, filtered, and concentrated to afford a viscous yellow oil. Column chromatography with 4:1 hexanes: ethyl acetate furnished **41** as a viscous yellow oil (65 mg, 38 %).

^{1}H NMR (500 MHz, $CDCl_3$), δ: 7.25-7.35 (20H, m), 5.40 (2H, m), 4.48- 4.75 (8H, m) 4.25 (1H, t, J=8.2), 4.15 (1H, m), 3.98- 4.05 (2H, m), 3.92- 3.96 (2H, m), 3.81- 3.87 (2H, m), 3.66 (1H, dd, J= 4.2, 10.4 Hz), 2.28- 2.37 (2H, m), 2.08- 2.02 (2H, m), 1.58-1.82 (4H, m), 1.53 (9H, s);

^{13}C NMR (500 MHz, $CDCl_3$), δ 152.3, 149.4, 138.6, 138.5, 138.4, 138.3, 130.3, 128.4, 128.3, 128.3, 127.9, 127.8, 127.7, 127.6, 127.6, 127.5, 126.9, 83.8, 76.7, 74.3, 73.2, 73.2, 73.1, 72.8, 67.4, 66.4, 54.9, 32.5, 28.0, 27.0, 24.2;

MS (ESI, MeCN) calcd. For $C_{48}H_{57}NO_9$, m/z: (M^+) 791.40, found**:** 814.4 [(M+ Na^+)];

IR (CH_2Cl_2) cm^{-1}: 1791, 1720 and 696.

Preparation of tert-butyl (2S,Z)-1-hydroxy-8-((2R,3R,4R,5R)-3,4,5-tris(benzyloxy)-6-(benzyloxymethyl)tetrahydro-2H-pyran-2-yl)oct-6-en-2-ylcarbamate (42)

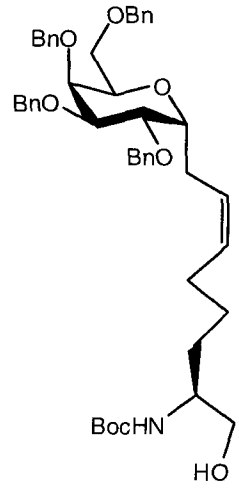

42

25 mg (0.032 mmol) of **42** was dissolved in 1ml of MeOH and stirred at room temperature. Catalytic $CsCO_3$ (3 mg) was added and the solution stirred until the reaction was judged complete (TLC, 1 hr). MeOH was removed *in vacuo* and the residue was dissolved in 1 ml of DCM. The solution was washed with 2 ml of 10 % citric acid (2x) and dried over $MgSO_4$, filtered and concentrated. Flash chromatography with 2:1 hexanes: ethyl acetate furnished the alcohol as a clear oil (21 mg, 87 %).

^{1}H NMR (500 MHz, $CDCl_3$), δ: 7.16-7.26 (20H, m), 5.31 (2H, m), 4.42- 4.66 (8H, m) 3.86- 4.00 (3H, m), 3.78 (1H, m), 3.64- 3.70 (2H, m), 3.60 (1H, m), 3.44- 3.58 (2H, m), 3.32- 3.38 (1H, m), 2.18-2.36 (2H, m), 1.88-2.04 (2H, m), 1.54 (1H, br), 1.37 (9H, s), 1.18- 1.36 (4H, m);

^{13}C NMR (500 MHz, $CDCl_3$), δ 156.5, 138.5, 138.4, 138.3, 138.2, 131.0, 128.3, 128.3, 128.3, 128.2 127.9, 127.8, 127.8, 127.7, 127.5, 127.5, 127.4, 126.3, 79.5, 76.6, 74.2, 73.2, 73.1, 73.0, 66.0, 52.8, 31.0, 28.4, 27.2, 26.0;

MS (ESI, MeOH) calcd. For $C_{47}H_{59}NO_8$, m/z: (M^+) 765.42, found**:** 788.4 [(M+ Na^+)].

Preparation of (2S,Z)-2-(tert-butoxycarbonylamino)-8-((2R,3R,4R,5R)-3,4,5-tris(benzyloxy)-6-(benzyloxymethyl)tetrahydro-2H-pyran-2-yl)oct-6-enoic acid (43)

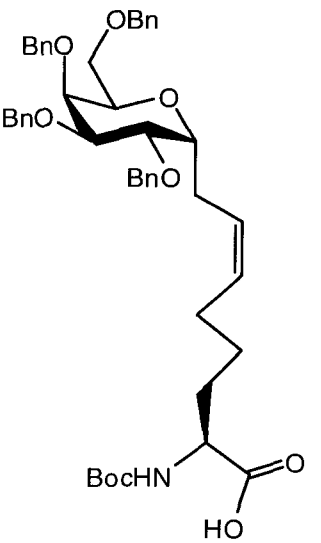

43

50 mg (0.0654 mmol) of **42** was added to a 5 ml round bottom flask containing a stir bar and 0.5 ml of dry DMF. 200 mg (0.65 mmol) of PDC was added and the solution stirred overnight. The solution was diluted with 3 ml of water and extracted with EtOAc (5 x 3 ml). The organic extracts were washed successively with 10 % HCl, distilled water and brine. The organic phase was dried over $MgSO_4$, filtered and concentrated to yield a crude yellow oil. Column chromatography with 13:1 DCM: MeOH furnished the product as a colourless oil (40 mg, 78 %).

^{1}H NMR (500 MHz, $CDCl_3$), δ: 7.22-7.33 (20H, m), 5.31-5.42 (2H, m), 5.08 (1H, br), 4.46- 4.70 (8H, m), 4.20- 4.28 (1H, m), 4.02- 4.08 (1H, m), 3.98 (1H, m), 3.89- 3.94 (1H, m), 3.71 (2H, m), 3.64 (1H, dd, J= 3.2, 8.1 Hz), 2.38 (1H, m), 2.25 (1H, m), 1.92-2.11 (2H, m), 1.50-1.88 (4H, m), 1.42 (9H, s);

^{13}C NMR (500 MHz, $CDCl_3$), δ 176.0,155.6, 138.4, 138.4, 138.3, 138.2, 131.0, 128.3, 128.3, 128.3, 128.2 127.9, 127.8, 127.8, 127.7, 127.5, 127.5, 127.4, 126.3, 79.5, 76.6, 74.2, 73.2, 73.1, 73.0, 66.0, 52.8, 31.0, 28.4, 27.2, 26.0;

MS (ESI, MeCN) calcd. For $C_{47}H_{57}NO_9$, m/z: (M^+) 779.40, found**:** 818.4 [(M+ K^+)], 802.4 [(M+ Na^+)];

IR (CH_2Cl_2) cm^{-1}: 3342, 1721 and 1703.

Appendix

^{1}H and ^{13}C NMR Spectra

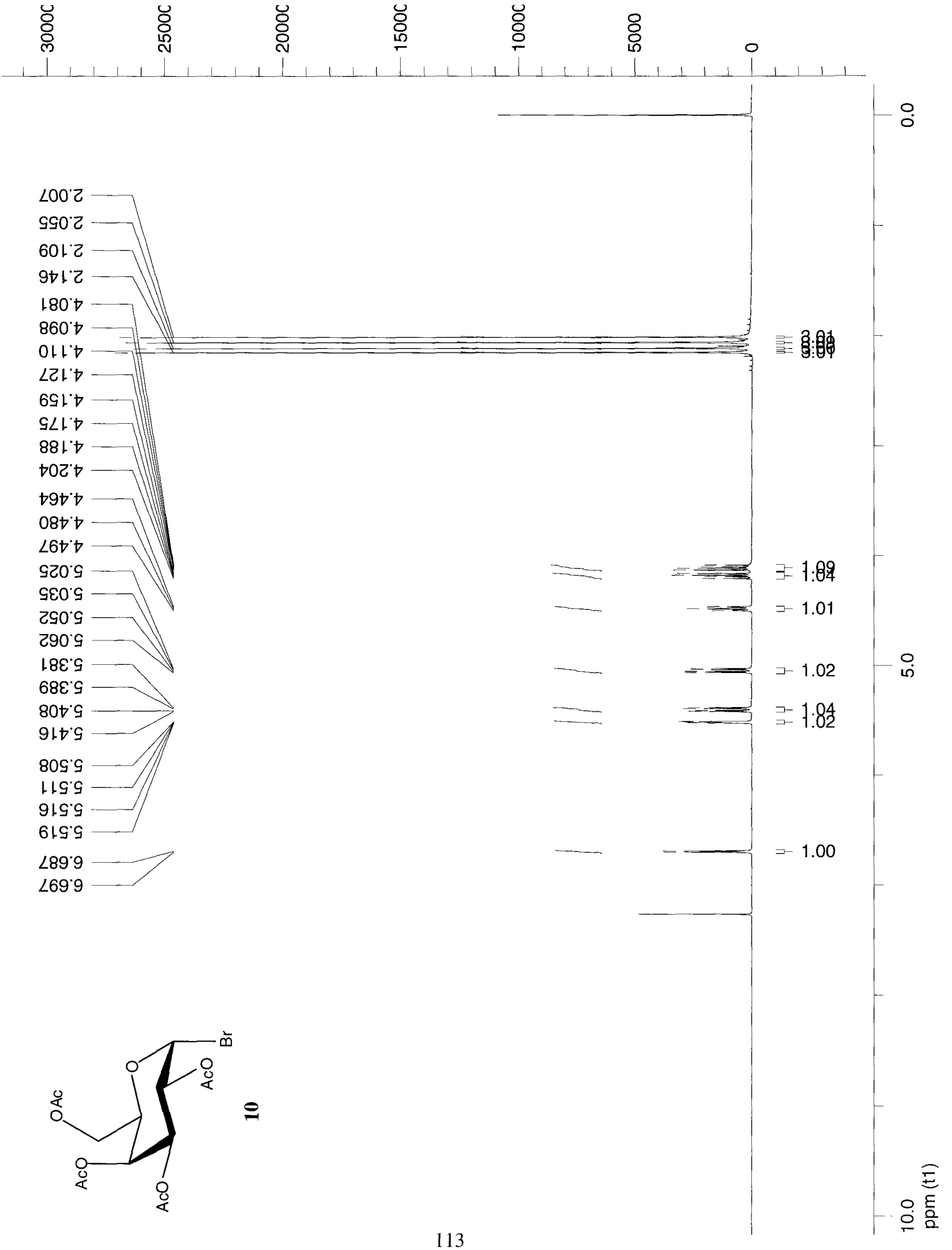
3000
2500
2000
1500
1000
500
0
2.007
2.055
2.109
2.146
4.081
4.098
4.110
4.127
4.159
4.175
4.188
4.204
4.464
4.480
4.497
5.025
5.035
5.052
5.062
5.381
5.389
5.408
5.416
5.508
5.511
5.516
5.519
6.687
6.697
3.01
1.09
1.04
1.01
1.02
1.04
1.02
1.00
0.0
5.0
10.0
ppm (t1)

OAc
AcO
AcO
O
AcO
Br

10

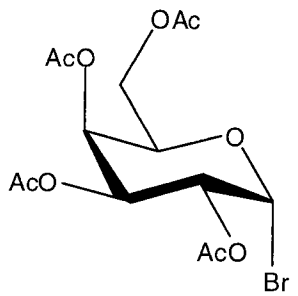

10

170,328
170,075
169,903
169,766

88,135

71,075
68,005
67,784
66,990
60,845

20,772
20,663
20,609
20,581

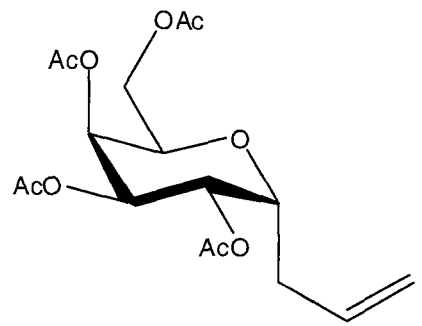
OAc
AcO
AcO
O
AcO

11

5.763
5.746
5.721
5.424
5.416
5.410
5.296
5.288
5.275
5.264
5.252
5.228
5.220
5.204
5.196
5.120
4.323
4.311
4.299
4.286
4.274
4.230
4.207
4.198
4.176
4.096
4.077
2.298
2.294
2.119
2.067
2.039
2.027
7000
6000
5000
4000
3000
2000
1000
0
-1000
1.04
1.05
1.07
1.11
1.19
10.0
5.0
0.0
ppm (t1)

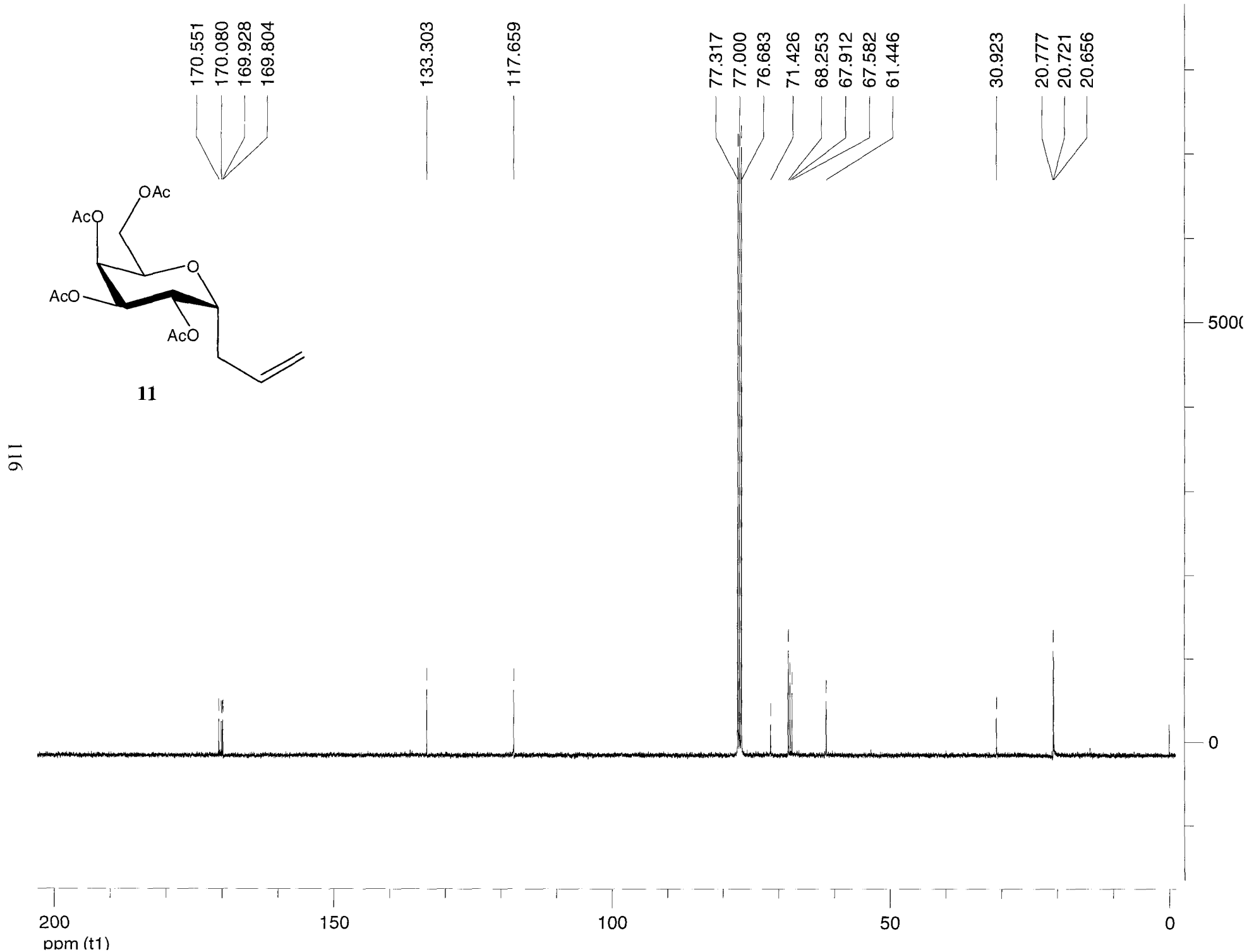
170.551
170.080
169.928
169.804
133.303
117.659
77.317
77.000
76.683
71.426
68.253
67.912
67.582
61.446
30.923
20.777
20.721
20.656
OAc
AcO
AcO
AcO
O
11
116
5000
0
200
150
100
50
0
ppm (t1)

7000
6000
5000
4000
3000
2000
1000
0
-1000
0.0
5.0
ppm (f1)
2,433
2,437
2,441
3,713
3,719
3,943
3,948
5,019
5,022
5,025
5,045
5,048
5,050
5,100
5,138
5,869
5,887
2.06
4.15
3.11
1.03
1.03
1.00

HO
OH
OH
O
OH

12

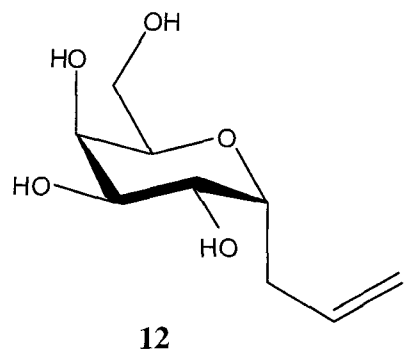
OH
HO
O
HO
HO

12

136.792
116.911
75.665
74.155
71.970
70.180
70.038
61.986
31.145
118
5000
0
200
150
100
50
0
ppm (t1)

60000
50000
40000
30000
20000
10000
0
0.0
5.0
10.0
ppm (t1)
2,387
3,645
3,656
3,671
3,683
3,721
3,727
3,839
3,846
4,001
4,004
4,060
4,069
4,582
4,606
5,031
5,034
5,036
5,047
5,051
5,746
5,763
7,295
7,308
2.14
1.02
1.93
0.98
1.97
0.89
8.00
2.00
1.00
20.37
OBn
BnO
BnO
BnO
O

13

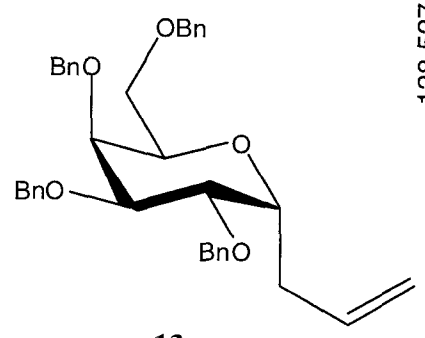
OBn
BnO
O
BnO
BnO

13

138,527
138,419
138,383
138,209
135,067
128,286
128,262
128,229
127,859
127,800
127,691
127,531
127,466
127,392
116,719
76,357
74,177
73,112
72,999
72,931
72,491
70,778
70,749
67,158
32,173
120
30000
25000
20000
15000
10000
5000
0
200
150
100
50
0
ppm (t1)

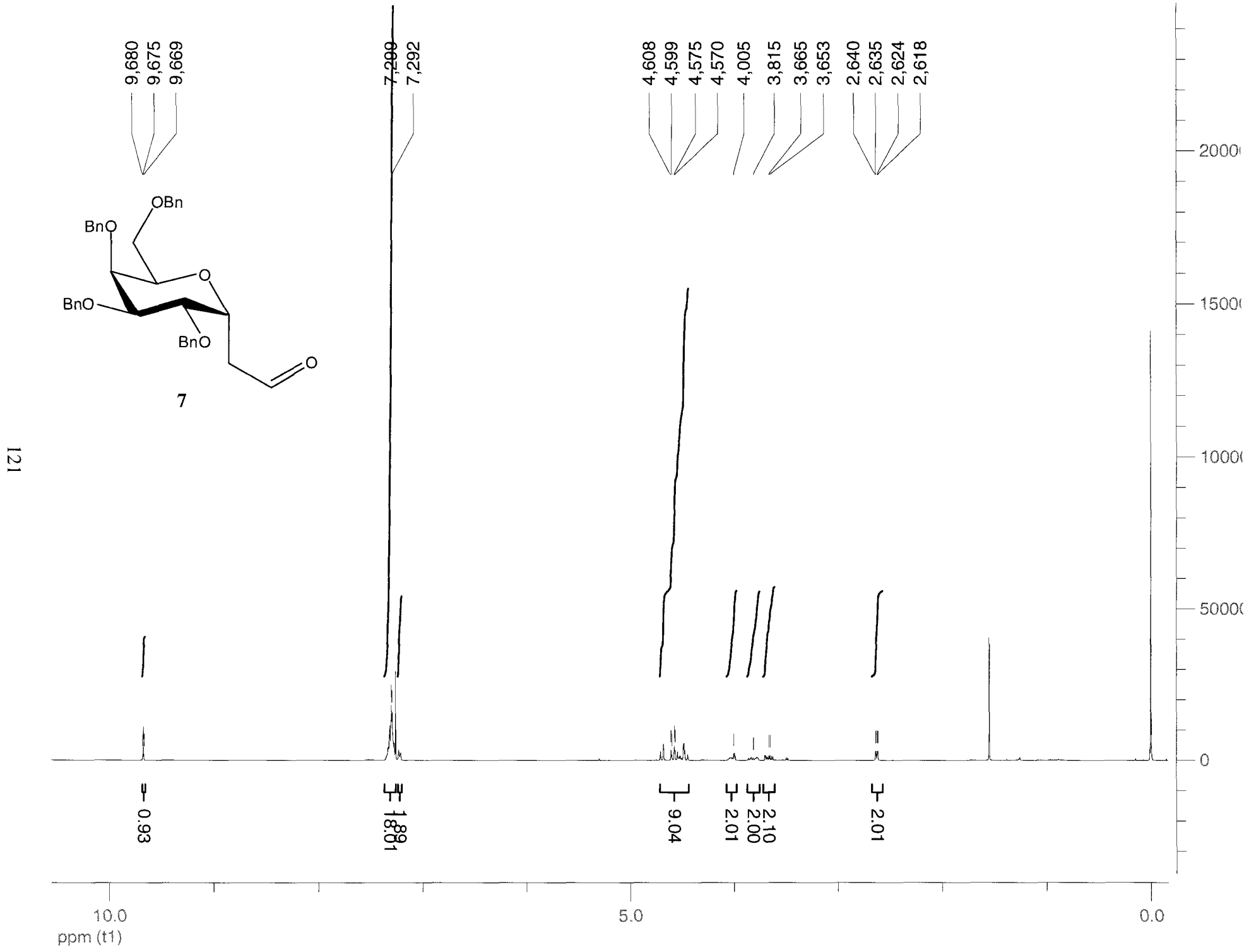
9,680
9,675
9,669
7,299
7,292
4,608
4,599
4,575
4,570
4,005
3,815
3,665
3,653
2,640
2,635
2,624
2,618
OBn
BnO
BnO
BnO
O
O
7
2000
1500
1000
500
0
0.93
1.89
1.81
9.04
2.01
2.10
2.00
2.01
10.0
5.0
0.0
ppm (t1)

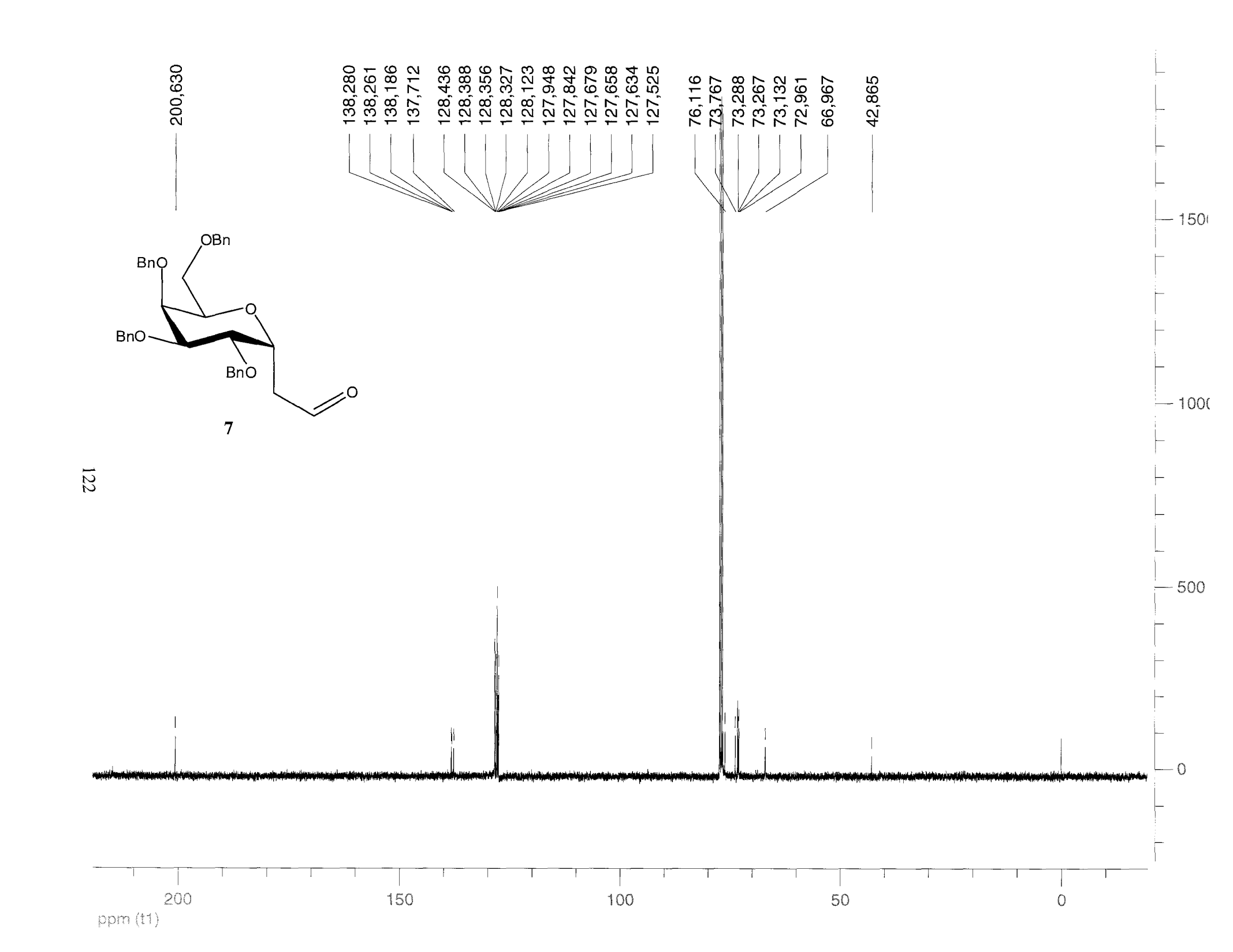
200,630
138,280
138,261
138,186
137,712
128,436
128,388
128,356
128,327
128,123
127,948
127,842
127,679
127,658
127,634
127,525
76,116
73,767
73,288
73,267
73,132
72,961
66,967
42,865
OBn
BnO
O
BnO
BnO
O
7
122
150
100
500
0
200
150
100
50
0
ppm (t1)

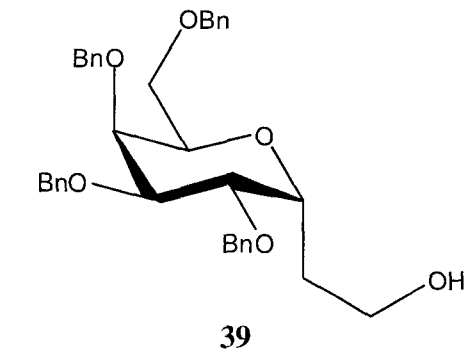
OBn
BnO
O
BnO
BnO
OH

39

7.303
4.725
4.712
4.695
4.682
4.647
4.636
4.617
4.606
4.562
4.534
4.504
4.493
4.198
4.171
4.117
3.944
3.737
3.512
3.503
3.486
3.477
1.986
1.651
123
19.55
2.08
3.88
1.00
0.87
1.05
1.08
10.0
5.0
0.0
ppm (t1)

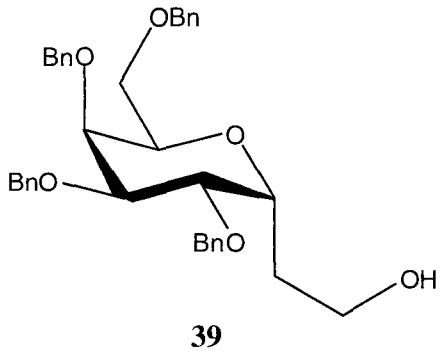
OBn
BnO
O
BnO
BnO
OH

39

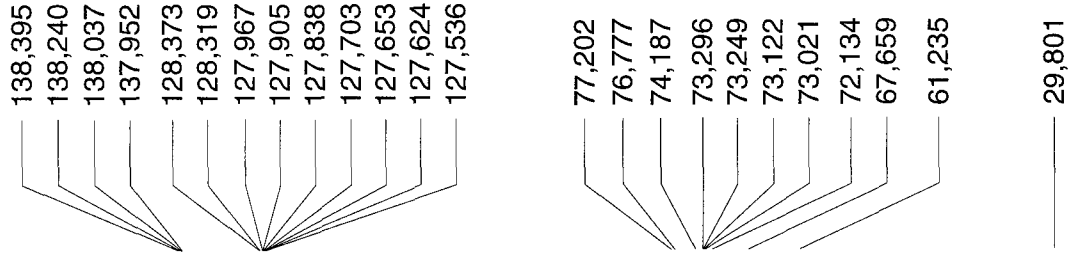
138,395
138,240
138,037
137,952
128,373
128,319
127,967
127,905
127,838
127,703
127,653
127,624
127,536
77,202
76,777
74,187
73,296
73,249
73,122
73,021
72,134
67,659
61,235
29,801

6000
5000
4000
3000
2000
1000
0
200
150
100
50
0
ppm (t1)

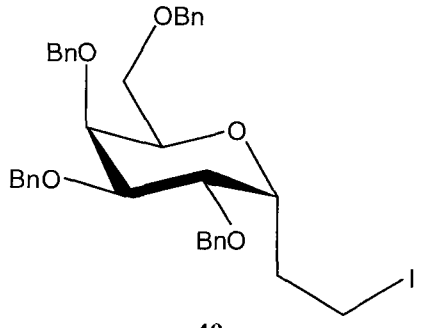
OBn
BnO
O
BnO
BnO
I

40

7.278
4.696
4.649
4.588
4.533
4.489
4.089
3.967
3.825
3.753
3.750
3.678
3.186
2.157
1.955
30000
25000
20000
15000
10000
5000
0
1.71
18.00
2.00
2.01
2.03
0.92
1.89
2.04
0.37
1.02
10.0
9.0
8.0
7.0
6.0
5.0
4.0
3.0
2.0
ppm (t1)

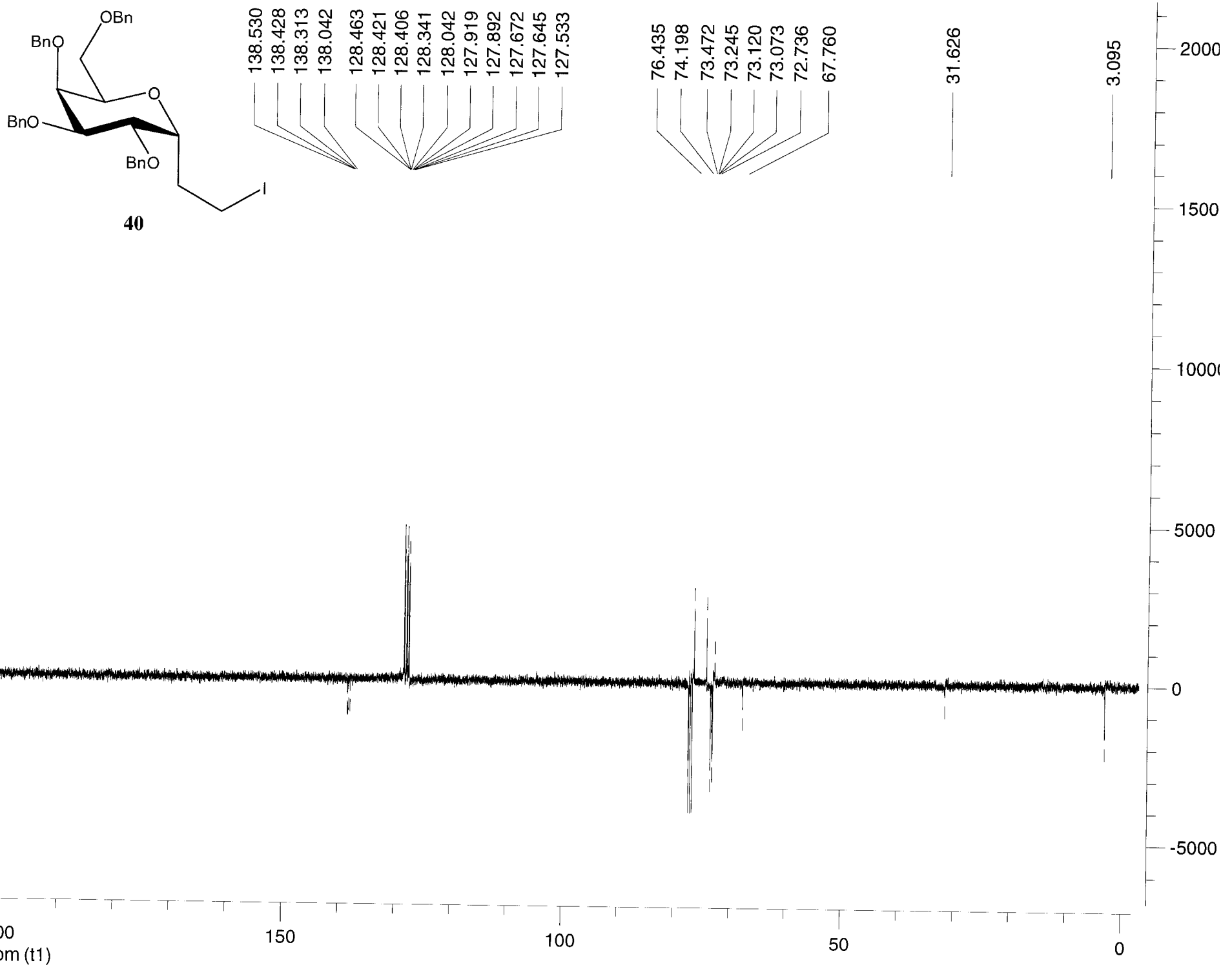
OBn
BnO
O
BnO
BnO
I
40
138.530
138.428
138.313
138.042
128.463
128.421
128.406
128.341
128.042
127.919
127.892
127.672
127.645
127.533
76.435
74.198
73.472
73.245
73.120
73.073
72.736
67.760
31.626
3.095
126
2000
1500
1000
5000
0
-5000
200
150
100
50
0
ppm (t1)

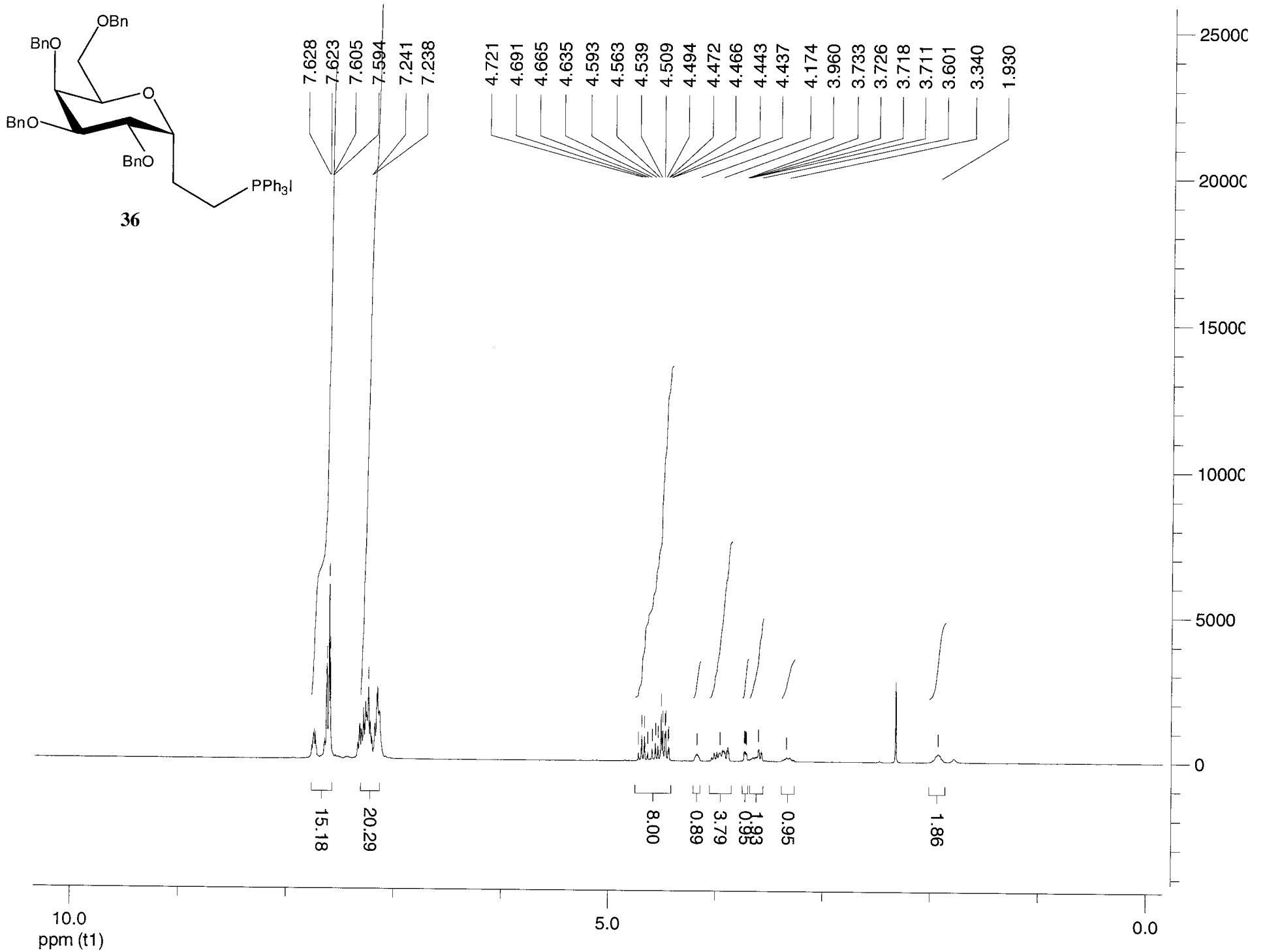
OBn
BnO
O
BnO
BnO
PPh3I
36
7.628
7.623
7.605
7.594
7.241
7.238
4.721
4.691
4.665
4.635
4.593
4.563
4.539
4.509
4.494
4.472
4.466
4.443
4.437
4.174
3.960
3.733
3.726
3.718
3.711
3.601
3.340
1.930
25000
20000
15000
10000
5000
0
15.18
20.29
8.00
0.89
3.79
0.95
1.86
10.0
ppm (t1)
5.0
0.0

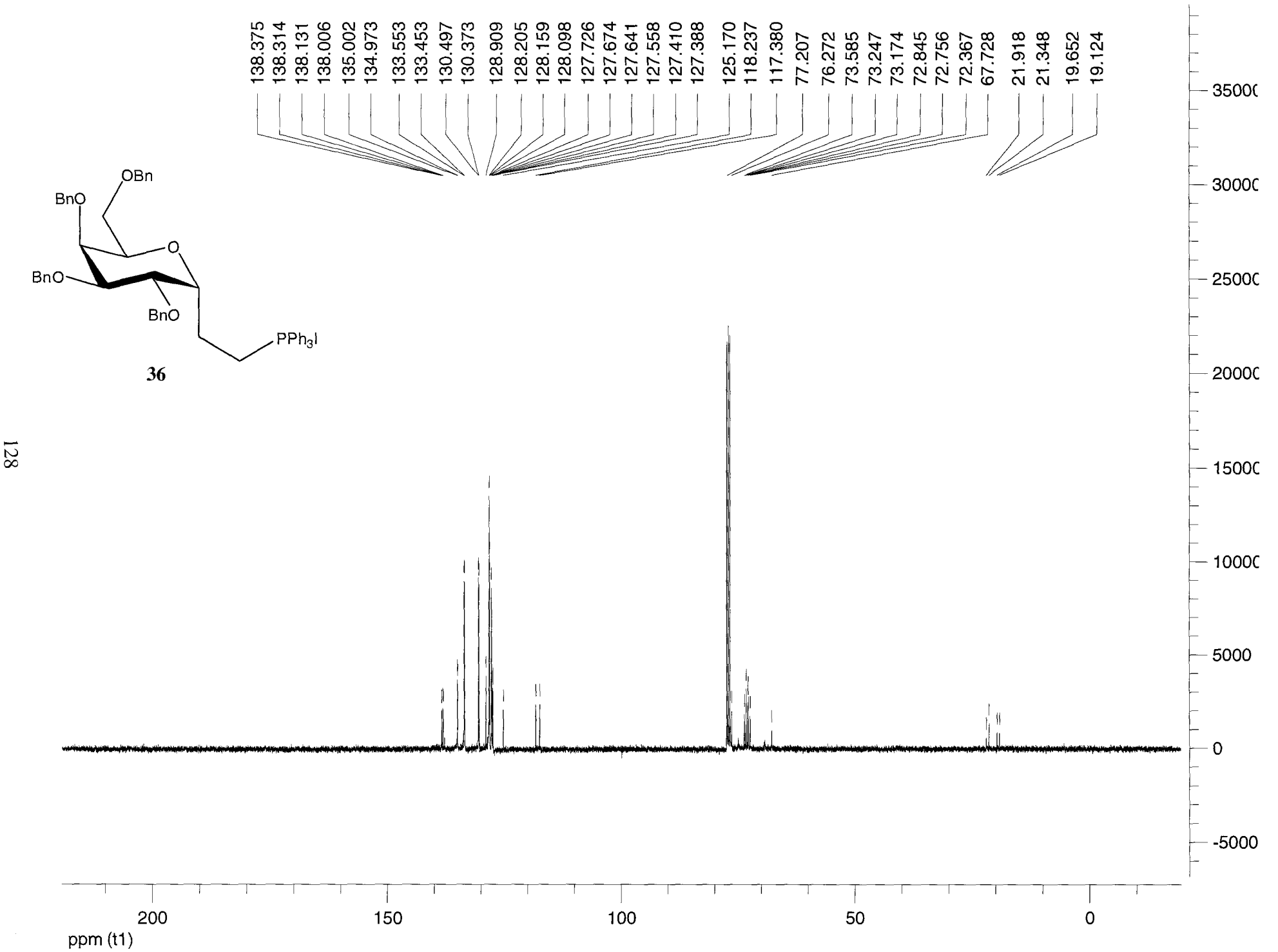
138.375
138.314
138.131
138.006
135.002
134.973
133.553
133.453
130.497
130.373
128.909
128.205
128.159
128.098
127.726
127.674
127.641
127.558
127.410
127.388
125.170
118.237
117.380
77.207
76.272
73.585
73.247
73.174
72.845
72.756
72.367
67.728
21.918
21.348
19.652
19.124
OBn
BnO
BnO
BnO
O
PPh3I
36
128
200
150
100
50
0
ppm (t1)
35000
30000
25000
20000
15000
10000
5000
0
-5000

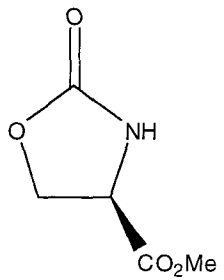
O
NH
O
CO_2Me

18

6,472
4,666
4,636
4,604
4,565
4,550
4,535
4,520
4,478
4,463
4,446
4,431
3,832
0.94
1.00
3.00
1500
1000
5000
0
10.0
5.0
0.0
ppm (f1)

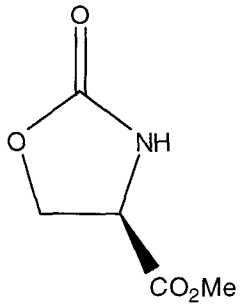
O
O
NH
CO2Me

18

170,746
159,386
66,989
53,979
53,253
130
700
600
500
400
300
200
100
0
200
150
100
50
0
ppm (t1)

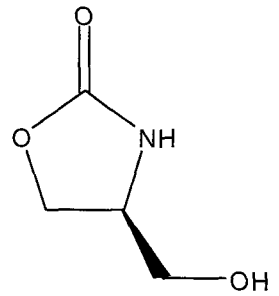
O
NH
O
OH

19

4,588
4,565
4,543
4,318
4,305
4,296
4,283
4,091
4,079
4,069
3,702
3,693
3,672
3,663
3,616
3,605
3,586
3,575
1.05
1.05
1.00
1.87
1.02
35000
30000
25000
20000
15000
10000
5000
0
-5000
10.0
5.0
0.0
ppm (t1)

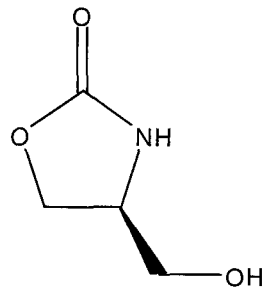
O
NH
O
OH

19

164,900
70,512
65,011
56,248
15000
10000
5000
0
200
150
100
50
0
ppm (t1)

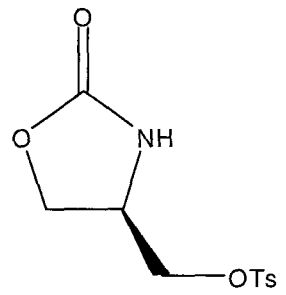
O
NH
O
OTs

20

7,801
7,780
7,389
7,368
5,802
4,489
4,469
4,449
4,066
2,464
2.00
2.00
1.00
1.00
4.00
3.00
8000
7000
6000
5000
4000
3000
2000
1000
0
-1000
10.0
5.0
0.0
ppm (t1)

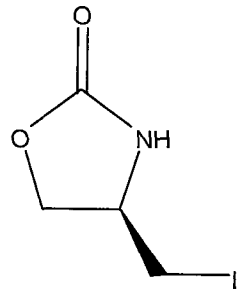
O
O
NH
I

21

6,791
4,513
4,496
4,479
4,138
4,128
4,120
4,110
4,072
3,220
1.00
1.00
2.03
3500
3000
2500
2000
1500
1000
5000
0
-5000
10.0
ppm (t1)
5.0
0.0

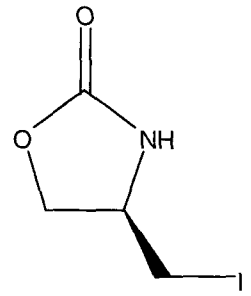
O
O
NH
I

21

159,361
70,438
53,193
8,122
15000
10000
50000
0
135
200
150
100
50
0
ppm (t1)

150
100
500
0
0.0
5.0
10.0
ppm (t1)
3,753
3,907
3,993
4,005
4,015
4,028
4,328
4,330
4,351
4,372
4,374
4,496
0.81
0.82
0.91
1.00
1.00
15.00
7,699
7,708
7,719
7,728
7,738
7,747
7,791
7,809
7,824
7,842
7,866
7,883
7,887
7,904
PPh3I
NH
O
O

22

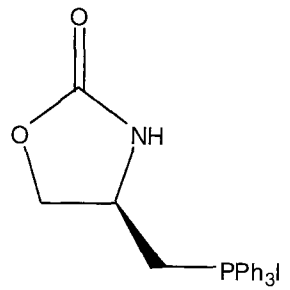
O
O
NH
PPh3I

22

157,800
132,432
132,404
130,573
130,469
127,337
127,209
114,371
113,505
67,798
67,708
44,274
50
40
30
20
10
0
200
150
100
50
0
ppm (t1)

10000
5000
0
0,052
0,898
2,277
3,635
3,652
3,669
5,025
5,799
6.17
9.25
2.13
2.16
2.10
1.03
0.0
5.0
10.0
ppm (t1)

OTBDMS

23

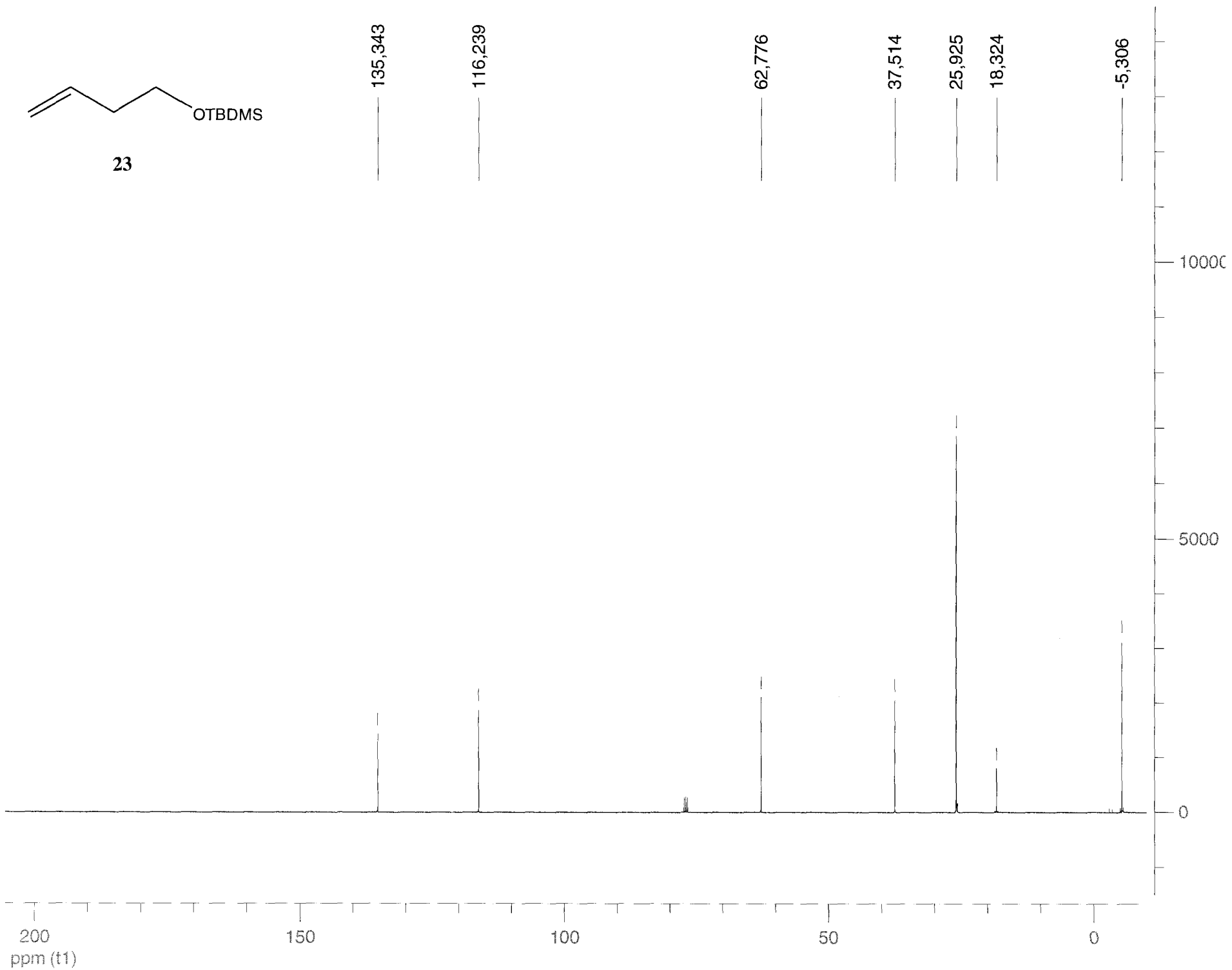
OTBDMS
23
135,343
116,239
62,776
37,514
25,925
18,324
-5,306
10000
5000
0
200
150
100
50
0
ppm (t1)
139

5000
4000
3000
2000
1000
0
0,058
0,873
2,567
2,574
2,587
2,594
2,607
2,614
3,961
3,981
4,001
9,788
9,795
9,801
6.09
9.04
2.01
2.00
0.90
0.0
5.0
10.0
ppm (t1)
OTBDMS
O

24

-5,673
17,968
25,577
46,309
57,144
201,778
OTBDMS
O
24
ppm (t1)

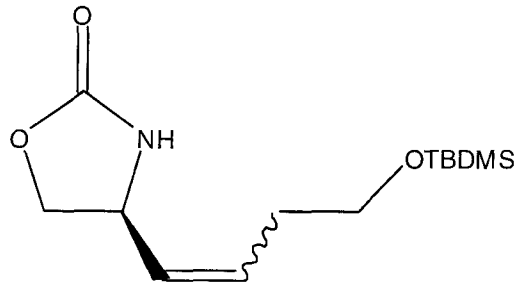
O
O
NH
OTBDMS

25

5,702
5,534
5,382
4,751
4,731
4,712
4,691
4,533
4,512
4,491
4,040
4,018
4,000
3,656
3,641
3,626
2,294
0,886
0,058
142
4000
3000
2000
10000
0
0.92
0.97
0.85
0.77
0.97
0.98
1.95
2.00
9.00
5.73
10.0
5.0
0.0
ppm (t1)

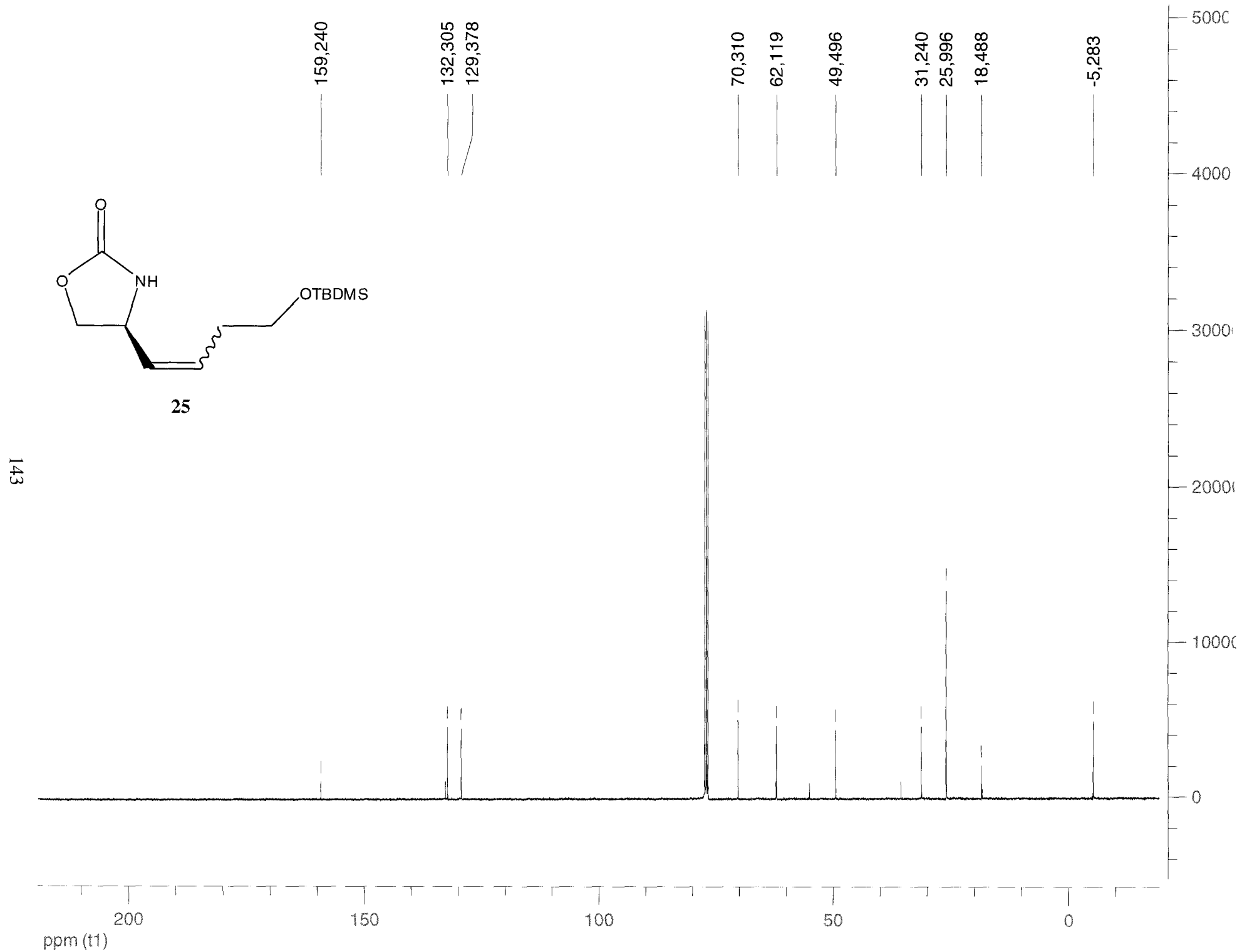
159,240
132,305
129,378
70,310
62,119
49,496
31,240
25,996
18,488
-5,283
5000
4000
3000
2000
1000
0
O
O
NH
OTBDMS
200
150
100
50
0
ppm (t1)

25

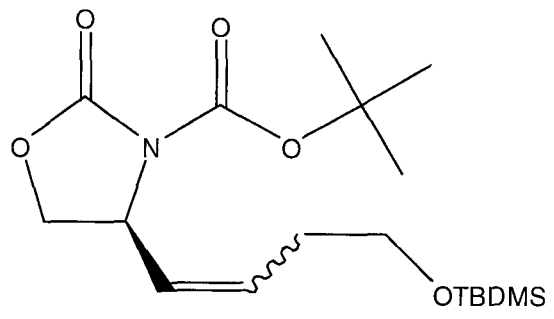
O
O
O
N
O
OTBDMS

30

5,687
5,673
5,534
5,529
5,043
5,031
5,015
5,001
4,443
4,414
4,385
3,957
3,940
3,928
3,912
3,705
3,595
2,351
1,502
0,882
0,043
1500
1000
5000
0
0.97
0.97
1.00
0.99
2.00
9.01
9.13
6.01
10.0
5.0
0.0
ppm (t1)

-5,328
18,389
25,929
27,961
31,257
52,380
62,144
67,325
83,779
128,527
130,968
149,147
152,248
OTBDMS
O
O
N
O
O
ppm (t1)

30

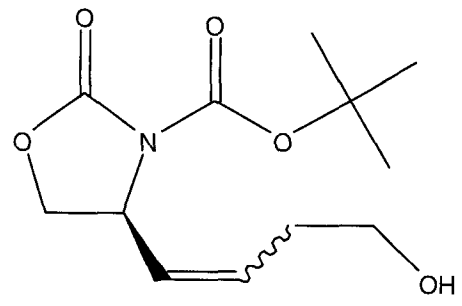

31

5,756
5,732
5,623
5,593
5,098
5,081
4,690
4,676
4,473
4,444
4,414
4,385
4,041
4,026
4,011
3,997
3,967
3,950
3,938
3,921
3,685
2,374
2,217
1,657
1,504

10000
5000
0

1.80
0.59
0.46
1.02
1.03
2.02
2.03
0.52
8.00
0.55

10.0
5.0
0.0

ppm (t1)

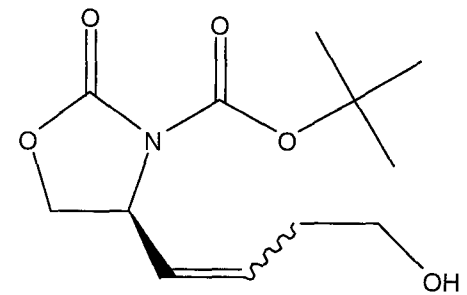
O
O
O
N
O
OH

31

152,049
149,714
132,296
129,305
84,306
67,086
61,374
56,977
35,321
27,928
4000
3000
2000
1000
0
147
200
150
100
50
0
ppm (t1)

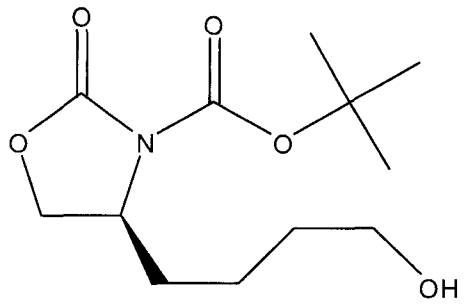
O
O
O
N
O
OH

28

4,362
4,335
4,307
4,242
4,061
4,052
4,033
4,024
3,673
3,652
3,631
1,841
1,734
1,600
1,532
1,423
5000
0
0.89
1.01
1.86
10.0
5.0
0.0
ppm (t1)

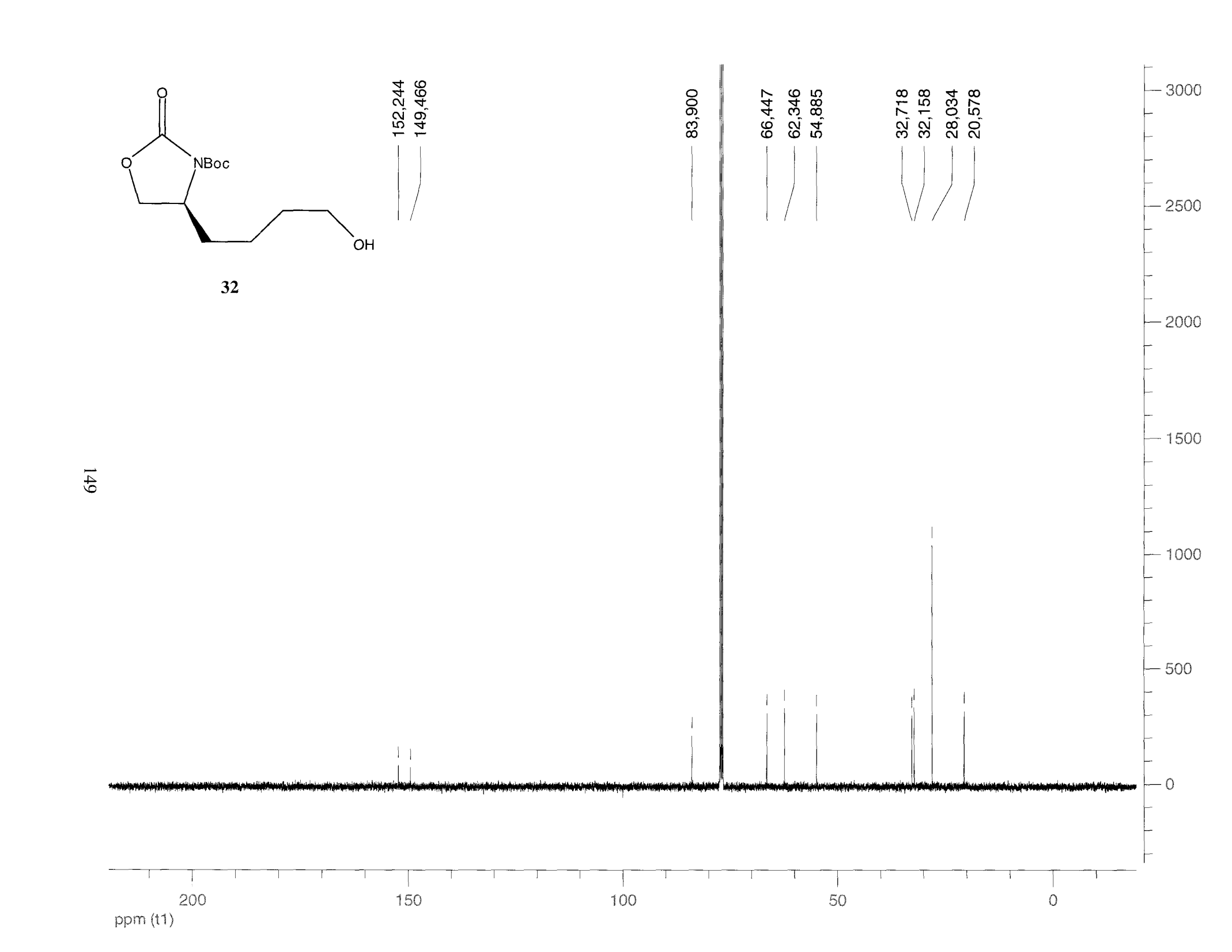
O
O
NBoc
OH
32
152,244
149,466
83,900
66,447
62,346
54,885
32,718
32,158
28,034
20,578
3000
2500
2000
1500
1000
500
0
200
150
100
50
0
ppm (t1)
149

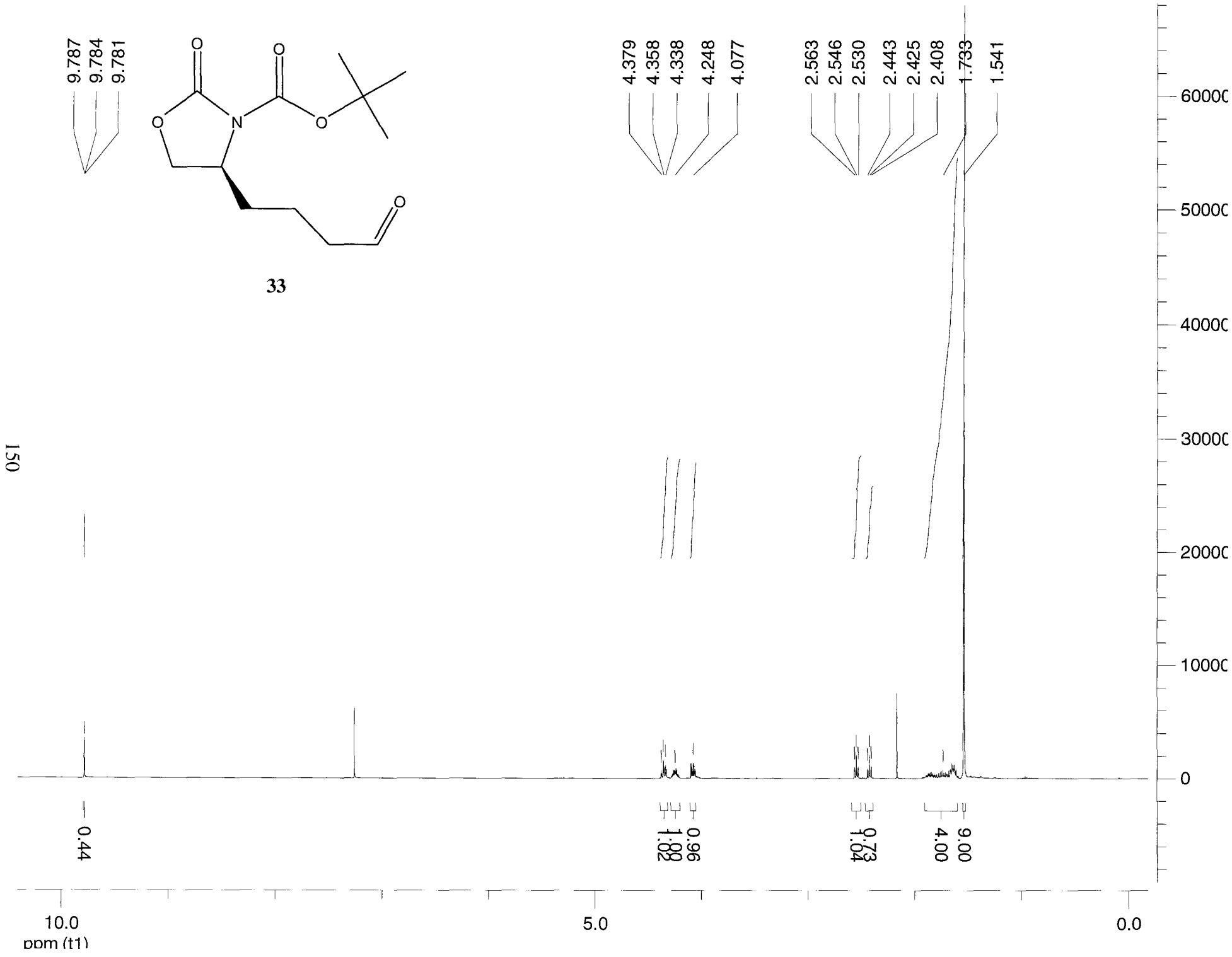
9.787
9.784
9.781
4.379
4.358
4.338
4.248
4.077
2.563
2.546
2.530
2.443
2.425
2.408
1.733
1.541
O
O
O
N
O
O
150
60000
50000
40000
30000
20000
10000
0
0.44
1.20
1.00
0.96
1.04
0.73
4.00
9.00
10.0
5.0
0.0
ppm (t1)

33

16,468
27,874
32,240
43,030
54,557
66,244
83,880
149,222
152,054
201,071
37
ppm (t1)

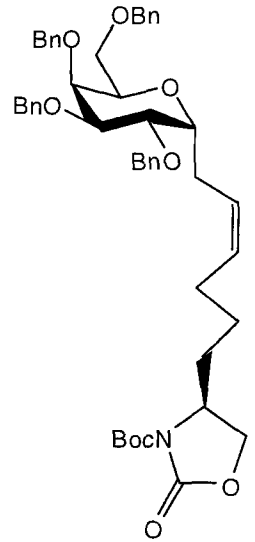
OBn
BnO
BnO
O
BnO
BocN
O
O
O

41

7.305
7.298
7.294
5.401
5.390
5.377
4.591
4.581
4.253
4.233
4.212
4.153
4.011
4.005
3.956
3.949
3.942
3.928
3.921
3.833
3.743
3.737
3.682
3.671
3.656
3.644
2.331
2.322
2.046
1.529
15000
10000
5000
0
20.14
1.89
8.00
2.00
2.17
4.01
9.00
10.0
5.0
0.0
ppm (t1)

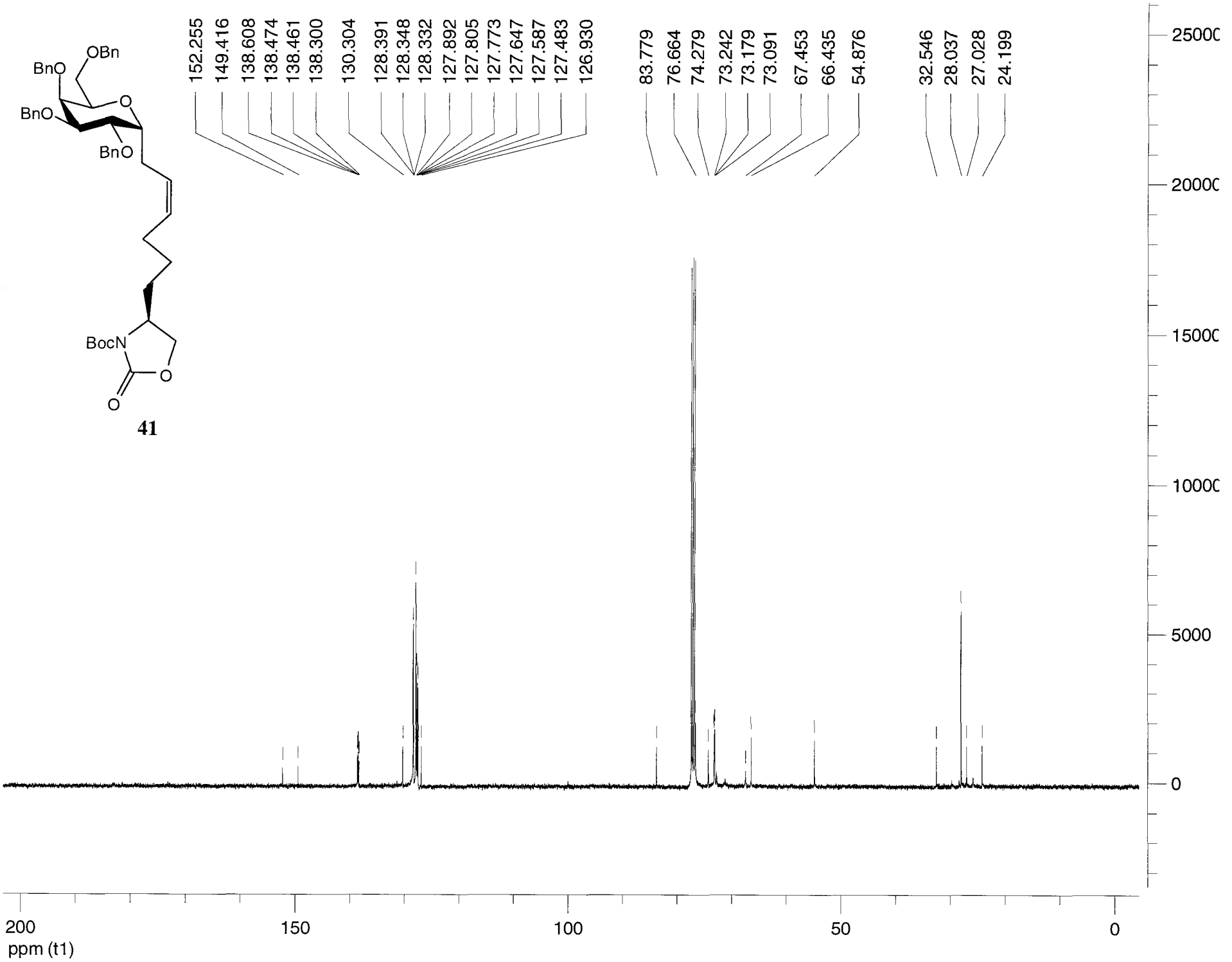
152.255
149.416
138.608
138.474
138.461
138.300
130.304
128.391
128.348
128.332
127.892
127.805
127.773
127.647
127.587
127.483
126.930
83.779
76.664
74.279
73.242
73.179
73.091
67.453
66.435
54.876
32.546
28.037
27.028
24.199
OBn
BnO
BnO
BnO
O
BocN
O
O
O
2500
2000
1500
1000
5000
0
200
150
100
50
0
ppm (t1)

41

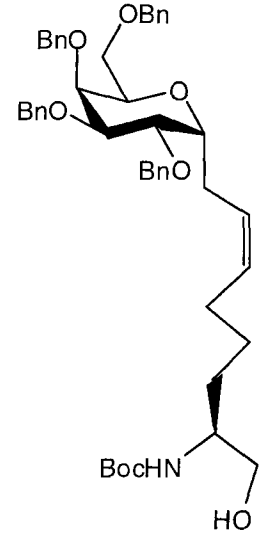

42

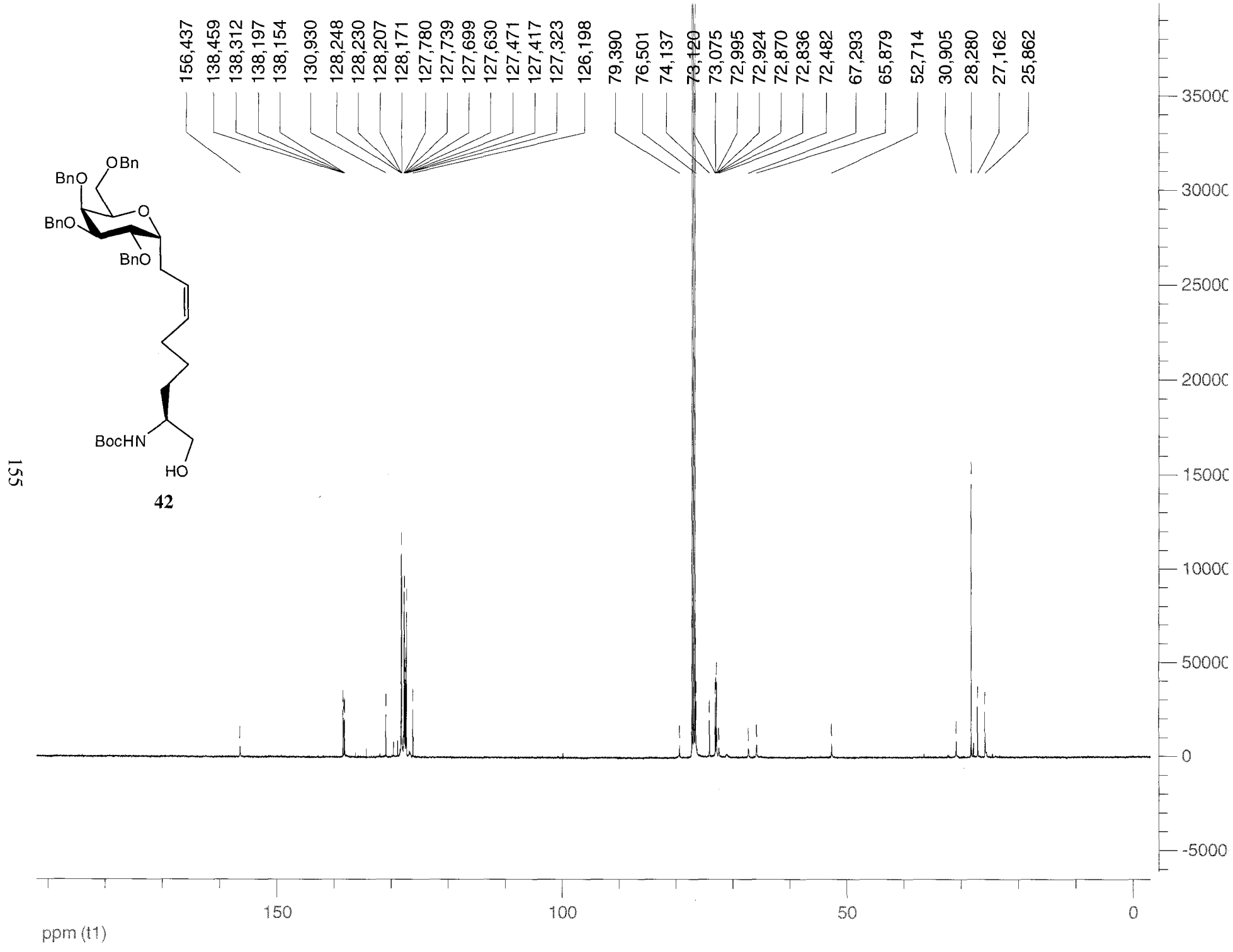
156,437
138,459
138,312
138,197
138,154
130,930
128,248
128,230
128,207
128,171
127,780
127,739
127,699
127,630
127,471
127,417
127,323
126,198
79,390
76,501
74,137
73,120
73,075
72,995
72,924
72,870
72,836
72,482
67,293
65,879
52,714
30,905
28,280
27,162
25,862
OBn
BnO
BnO
O
BnO
BocHN
HO
42
35000
30000
25000
20000
15000
10000
50000
0
-5000
150
100
50
0
ppm (t1)

10000
5000
0
3.824
3.843
3.868
3.869
3.897
3.971
3.972
3.978
4.041
4.044
4.047
4.228
4.230
4.231
4.233
4.238
4.473
4.489
4.504
4.528
4.537
4.552
4.562
4.582
4.592
4.647
4.659
4.676
4.689
5.325
5.326
5.329
5.331
5.341
5.350
5.357
5.382
5.400
5.410
5.417
5.419
5.426
7.241
7.261
7.271
7.284
9.12
4.00
2.06
1.12
1.22
1.06
1.81
0.95
1.03
0.94
8.01
0.83
2.00
20.14
0.0
5.0
10.0
ppm (t1)
OBn
BnO
BnO
BnO
O
BocHN
HO
O

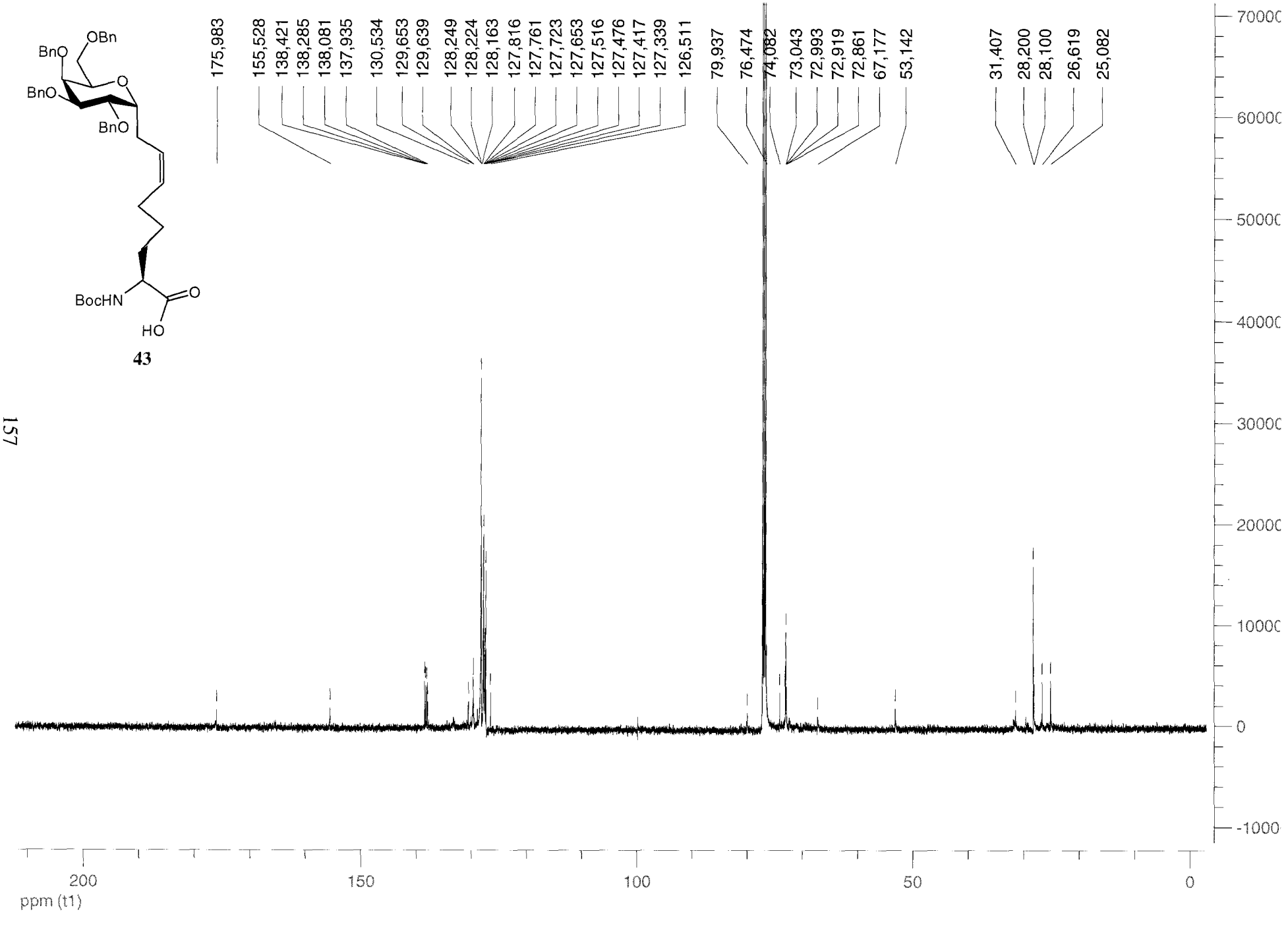
BnO
OBn
BnO
O
BnO
BocHN
O
HO
43
175,983
155,528
138,421
138,285
138,081
137,935
130,534
129,653
129,639
128,249
128,224
128,163
127,816
127,761
127,723
127,653
127,516
127,476
127,417
127,339
126,511
79,937
76,474
74,082
73,043
72,993
72,919
72,861
67,177
53,142
31,407
28,200
28,100
26,619
25,082
70000
60000
50000
40000
30000
20000
10000
0
-1000
200
150
100
50
0
ppm (t1)

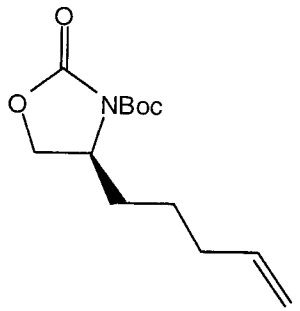
O
O
NBoc

38

5.804
5.778
5.761
5.736
5.050
5.045
5.011
5.007
5.003
4.985
4.983
4.981
4.355
4.335
4.314
4.250
4.242
4.234
4.041
4.034
4.020
4.013
2.129
2.126
2.110
2.093
2.091
2.075
2.073
1.850
1.841
1.829
1.821
1.734
1.717
1.713
1.01
2.00
1.04
2.02
1.03
1.10
8.95
2.38
10.0
ppm (t1)
5.0
0.0
30000
25000
20000
15000
10000
5000
0

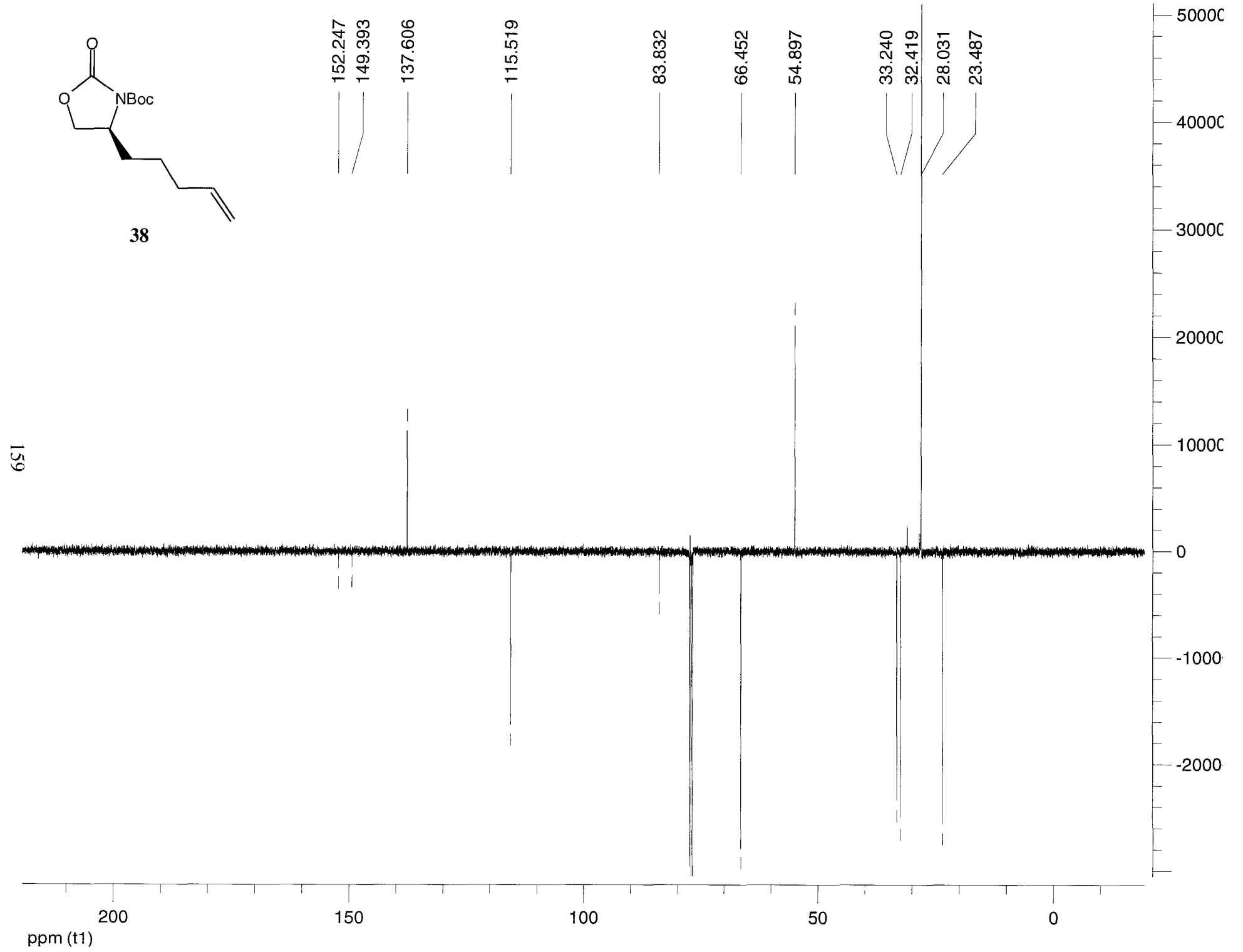
O
O
NBoc
38
152.247
149.393
137.606
115.519
83.832
66.452
54.897
33.240
32.419
28.031
23.487
159
50000
40000
30000
20000
10000
0
-1000
-2000
200
150
100
50
0
ppm (t1)

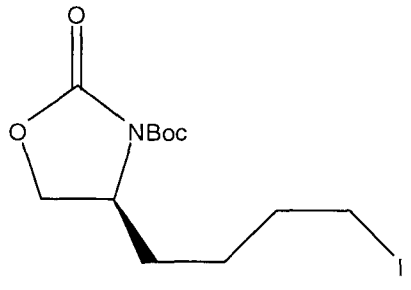
O
O
NBoc
I

33

4,374
4,353
4,332
4,270
4,250
4,241
4,061
4,053
4,039
4,032
3,214
3,208
3,197
3,191
3,180
3,174
1,738
1,719
1,704
1,699
1,548
1,477
1,457
1,446
1,438
1,425
1,418
0.99
0.97
1.00
1.97
2.16
1.07
1.96
160
10.0
ppm (t1)
5.0
0.0

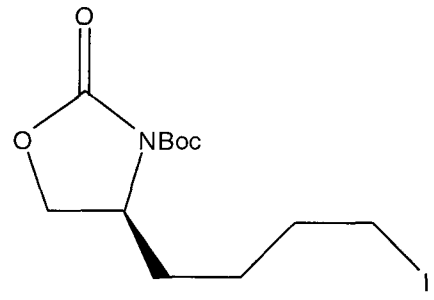
O
O
NBoc
I

33

152,080
149,426
84,009
66,425
54,693
32,675
31,850
28,055
25,115
5,989
1000
500
0
161
200
150
100
50
0
ppm (t1)

25000
20000
15000
10000
5000
0
1,463
1,710
1,756
1,763
3,607
3,785
4,269
4,286
4,338
4,361
7,702
7,710
7,720
7,729
7,777
7,796
7,809
7,828
9.03
6.03
1.03
1.03
1.79
0.95
15.00
NBoc
PPh3I
8
0.0
5.0
10.0
ppm (t1)

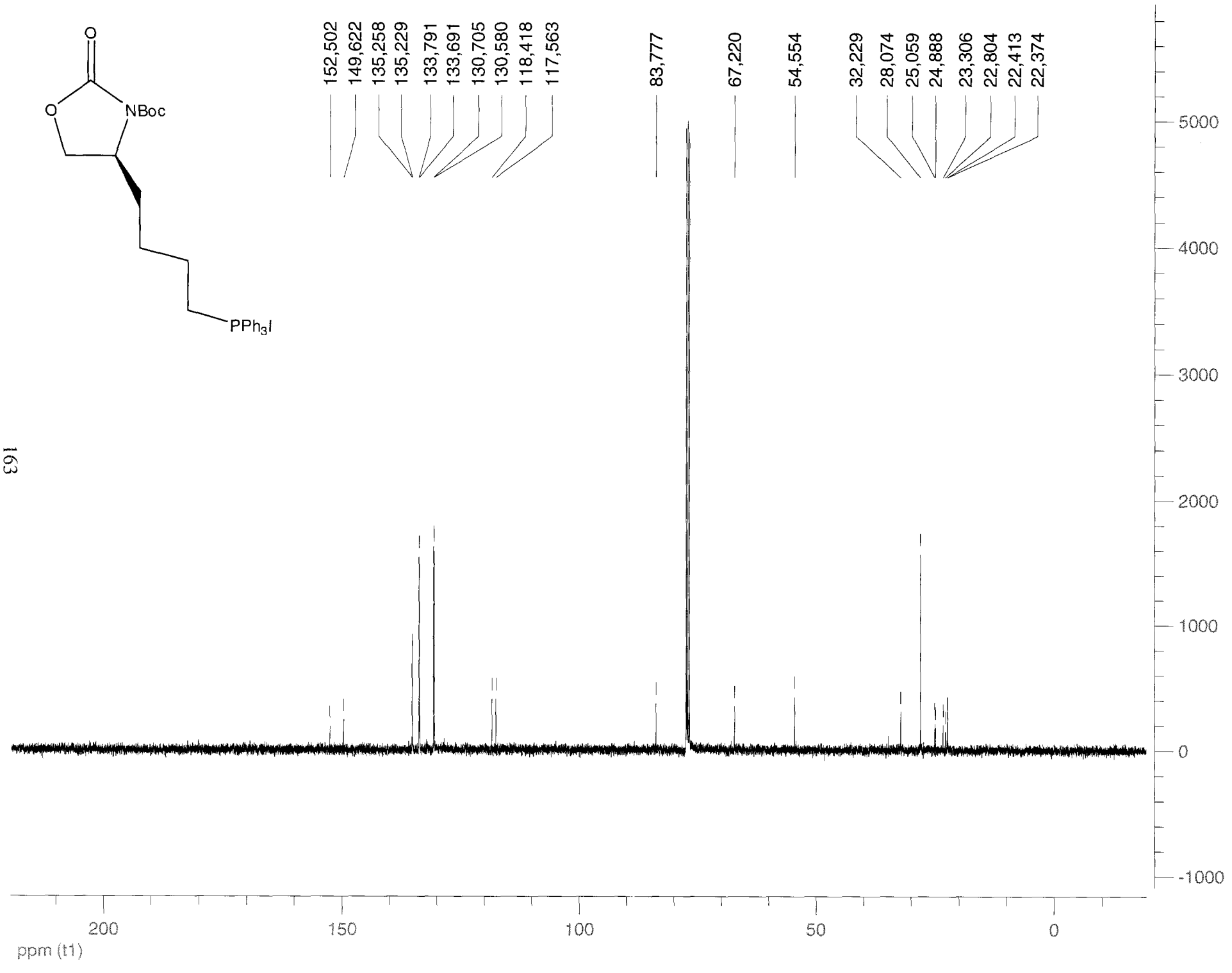
O
O
NBoc
PPh3I
152,502
149,622
135,258
135,229
133,791
133,691
130,705
130,580
118,418
117,563
83,777
67,220
54,554
32,229
28,074
25,059
24,888
23,306
22,804
22,413
22,374
5000
4000
3000
2000
1000
0
-1000
200
150
100
50
0
ppm (t1)